Faculdade de Engenharia da Universidade do Porto

Biomechanical applications of a novel simple machine

Carlos Aurelio Andreucci

Programa Doutoral em Engenharia Biomédica

March 2024

Biomechanical applications of a novel simple machine

by

Carlos Aurelio Andreucci

A thesis submitted in conformity with the requirements for the Doctoral Degree in Biomedical Engineering by the Faculty of Engineering of the University of Porto

Supervisor:

Renato Manuel Natal Jorge

Full Professor, Department of Mechanical Engineering, Faculty of Engineering,University of Porto, Porto, Portugal

Co-Supervisor:

Elza Maria Morais Fonseca

Associate Professor, Department of Mechanical Engineering, Polytechnic Institute of Porto, ISEP-IPP, Porto, Portugal

Porto, March 2024

"Mathematics in biomedical engineering is a science. It is a philosophy applied to the fundamental pillars of life in the experimental biophysical environment. There is nothing more satisfying than family, health, and the incessant search for wisdom."

Carlos Aurelio Andreucci

Agradecimentos

As palavras limitam a nossa capacidade de expressar ideias e principalmente os sentimentos de gratidão e apreço por aqueles que vieram antes de nos e inspiram a produção científica. O Professor Renato M. Natal Jorge foi aquele que acreditando na proposta de trabalho, trouxe com sua vasta experiência académica a segurança necessária na elaboração de um projeto motivando honrar sua orientação.

A professora Elza M. M. Fonseca ensinou e orientou através do exemplo e paciência como traduzir um experimento em artigos académicos de alto valor e conteúdo, de maneira objetiva e clara. As oportunidades de publicações em jornais, revistas, congressos e a confiança depositada jamais serão esquecidas.

Professor Jorge Monteiro na elegante condução do curso de doutoramento principalmente nas escolhas das aulas e condução dos seminários, assim como na orientação, condução do projeto e execução da tese, injetou força e animo em todos doutorandos.

Referir também o importante apoio de todas as instituições envolvidas, sobretudo a FEUP (Faculdade de Engenharia da Universidade do Porto) e a Universidade do Kuwait. Agradeço a inspiração e as excelentes condições de trabalho e todas as ferramentas fornecidas para o desenvolvimento desta tese de doutoramento.

Agradecer aos Professores Abdullah Alshaya (Kuwait University) por ter acreditado e apoiado o projeto desde o nosso contato inicial através do departamento de Engenharia Mecânica; Professores Carlos Alberto Andreucci e Maria Bernadete de Carvalho Andreucci pela introdução de novos pontos de vista a serem analisados durante a condução do projeto; Professor Laerte Ramos de Carvalho (in memoriam) por introduzir a filosofia e a educação no Brasil como pilares na busca da ciência; Professor Gino Emílio Lasco (in memoriam) por dar a honra de se tornar seu discípulo e Professor Assistente e pelo incessante questionamento sobre as complicações inerentes as fixações e implantes ósseos que estimularam a busca de uma alternativa apresentada nesta Tese.

Agradecer por fim aos amigos, a família, meus pais, eterna fonte de inspirações e exemplos, irmãos pelo apoio incondicional em toda minha vida, meus filhos Murillo e Ravi, *motum perpetum* para minha busca incessante por um mundo melhor, e minha esposa Elaine, amor incondicional sem a qual tamanha obrigação na conclusão desta Tese não seria possível.

Eternamente grato.

Abstract

This thesis presents a new simple machine, the Bioactive Kinetic Screw (BKS), which, when drilled into a material such as bone, allows technical simplification, preservation of the perforated material, compaction, collection, transplantation, volumetric measurement, with passive stabilization of the BKS when used as a screw, which is patented as a simple machine and as a dental implant. In addition to achieving better control and parameters for osseointegration, which motivated this initial study, other applications of BKS were identified during the research. These include bone density measurement and other materials (kinetic sand and aluminium phyllosilicates), bone harvesting for transplantation, single-stage sinus lift and bone screw fixation. The implications of the new simple machine have been studied from a biomedical engineering perspective.

Synthetic bone (polyurethane foams of varying densities), kinetic sand and aluminium phyllosilicates were used in a series of experimental tests. Digital torque wrenches (TQ8801) and precision digital scales (Taylor and Brifit) were used to record the drilling torque and counter-torque and to measure the weight before and after drilling during the BKS insertion and removal process.

Computational modelling of bone insertion includes mechanical material models to analyse the thermomechanical behaviour of bone tissue. Numerical models can predict the stress distribution during drilling, considering the bone characteristics, the geometry of the BKS and the cutting conditions, such as rotational speed, feed rate, hole depth and/or the use of a cooling system. The results of the developed numerical models and experimental results were described by the Finite Element Method (FEM).

The main outcome of this thesis is to obtain a detailed description of the biomechanical advantages and disadvantages of the new BKS in the form of a dental implant, the determination of a simplified and optimised surgical protocol, and the experimental analysis of its effects on synthetic bone, aluminium phyllosilicates, and kinetic sand. The results contribute to a comprehensive understanding of the effects of a simplified drilling technique, collection, compaction, densification effects and torque standardisation for the BKS. To optimise primary stability for osseointegration of dental implants, torque was standardised in five different bone densities of polyurethane cellular foam (PCF), PCF1O, PCF15, PCF20, PCF30, and PCF40.

The results found determined the properties of compacting and densifying material in different materials within the internal volume of the BKS 3.45 times more than the material where it was applied. It was possible to collect the compacted material inside and transport it to different areas of the same synthetic jaw, as well as to use the collected material for different applications, limited by the amount removed. Through the formula developed and applied in the studies, it was possible to determine the property of BKS for measuring the apparent density of the applied materials. The values of maximum insertion torque (MIT) and maximum removal torque (MRT), determined experimentally at different bone densities, showed that the MRT is greater than the MIT, thus increasing the load that the BKS can mechanically support. It was also observed that the maximum insertion torque of the BKS differs from that of conventional bone screws because it does not exert pressure on the bone from the metals in which it is manufactured (304 steel, Ti6Al4V), due to the properties of the drill bit. The locking of the BKS, which has been shown to increase the maximum removal torque, is due to increased friction, cohesion of the materials and compaction and densification of the internal material. When a bone screw is only used temporarily and its removal is planned, the indication for BKS should be used with caution, as a greater initial mechanical stability is achieved as a stimulating factor for osseointegration.

Resumo

Nesta tese foi apresentada uma nova máquina simples, o Parafuso Cinético Bioativo (BKS), que através da perfuração de um material como o osso, permite a simplificação técnica, a preservação do material perfurado, a compactação, a recolha, o transplante, a medição volumétrica, estabilização passiva do BKS quando utilizado como parafuso, que se encontra patenteado como máquina simples e como implante dentário. Para além da obtenção de um melhor controlo e parâmetros para a osseointegração, que motivou este estudo inicial, foram identificadas outras aplicações da BKS durante a investigação. Estas incluem a medição da densidade óssea e outros materiais (areia cinética e filossilicatos de alumínio), colheita de osso para transplante, elevação do seio maxilar numa única fase e fixação de parafusos ósseos. As implicações da nova máquina simples foram estudadas numa perspetiva de engenharia biomédica.

Numa série de testes experimentais, foram utilizados osso sintético (espumas de poliuretano de diferentes densidades), areia cinética e filossilicatos de alumínio. Foram utilizadas chaves de torque digitais (TQ8801) e balanças digitais de precisão (Taylor e Brifit) para registar o torque de perfuração e o contra torque, para medir o peso antes e depois da perfuração durante o processo de inserção e remoção do BKS.

A modelação computacional da inserção óssea inclui modelos de materiais mecânicos para analisar o comportamento termomecânico do tecido ósseo. Os modelos numéricos podem prever a distribuição de tensões durante a perfuração, tendo em conta as características do osso, a geometria da BKS e as condições de corte, tais como a velocidade de rotação, a velocidade de avanço, a profundidade do furo e a utilização ou não de um sistema de arrefecimento. Os resultados dos modelos numéricos desenvolvidos e os resultados experimentais foram descritos pela utilização do método dos elementos finitos (MEF).

O principal resultado desta tese é a obtenção de uma descrição detalhada das vantagens e desvantagens biomecânicas da nova máquina simples BKS sob a forma de um implante dentário, a determinação de um protocolo cirúrgico simplificado e otimizado e a análise experimental dos seus efeitos no osso sintético, filossilicatos de alumínio e areia cinética. Os resultados contribuem para uma compreensão abrangente dos efeitos da técnica de perfuração simplificada, recolha, compactação, efeitos de densificação e padronização do torque para a máquina simples BKS. Para otimizar a estabilidade primária para a osseointegração de implantes dentários, o torque foi padronizado em cinco densidades ósseas diferentes de espuma celular de poliuretano (PCF), PCF1O, PCF15, PCF20, PCF30 e PCF40. Os resultados encontrados determinaram as propriedades de compactação e densificação do material em diferentes materiais dentro do volume interno do BKS 3.45 vezes maior do que o material onde foi aplicado. Foi possível recolher o material compactado no seu interior e transportá-lo para diferentes zonas da mesma mandíbula sintética, bem como utilizar o material recolhido para diferentes aplicações, limitado pela quantidade retirada. Por meio da fórmula desenvolvida e aplicada nos estudos, foi possível determinar a propriedade do BKS para a medição da densidade aparente dos materiais aplicados. Os valores de torque máximo de inserção (MIT) e torque máximo de remoção (MRT) determinados experimentalmente nas diferentes densidades ósseas demonstraram a propriedade de tornar o MRT maior que o MIT, aumentando, assim, a carga que a BKS pode suportar mecanicamente comparada ao torque máximo de inserção. Observou-se também que o torque máximo de inserção do BKS difere do torque dos parafusos ósseos comuns, pois não exerce pressão dos metais em que é fabricado (aço 304, Ti6Al4V) no osso devido às suas propriedades de broca. O travamento do BKS, que demonstrou aumentar o torque máximo de remoção, deve-se ao aumento da fricção, coesão dos materiais e à compactação e densificação do material no seu interior. Se a aplicação de um parafuso ósseo for apenas temporária e estiver prevista a sua remoção, a indicação para o BKS deve ser utilizada com precaução, uma vez que se consegue uma maior estabilidade mecânica inicial como fator estimulante da osseointegração.

Table of Contents

List of Figures

CHAPTER II:

CHAPTER III:

CHAPTER IV:

CHAPTER V:

CHAPTER VI:

CHAPTER VII:

CHAPTER VIII:

List of Tables

CHAPTER II:

CHAPTER IV:

CHAPTER V:

CHAPTER VI:

List of Abbreviations

AO	Arbeitsgemeinschaft für Osteosyntheses
AP	Anteroposterior
BCE	Before Comon Era
BIC	Bone-Implant Contact
BKS	Bioactive Kinetic Screw
BMD	Bone Mass Density
BMP	Bone Morphogenetic Protein
CVM	Cervical Vertebral Maturation
CT scan	Computerized Tomography
DEXA	Dual Energy X-ray Absorptiometry
ECM	Extra cellular Matrix
EO	Endochondral Ossification
FBGCs	Foreign Body Giant Cells
FEA	Finite Element Analysis
IMA	Ideal Mechanical Advantage
IMF	Intermaxillary Fixation
IE	Insertion Energy
IO	Intramembranous Ossification
ISQ	Implant Stability Quotient
MA	Mechanical Advantage
M-CSF	Macrophage Colony-Stimulating Factor
MES	Minimum Effective Strain
MIT	Maximum Insertion Torque
MRT	Maximum Removal Torque
PCF	Polyurethane Cell Foam
RANKL	Receptor Activator of Nuclear factor κβ Ligand
RFA	Resonance Frequency Analysis

SM	Simple Machine
SFT	Static Friction Torque
ST	Standard Torque
Th1	T helper type 1
Th2	T helper type 2

List of Symbols

M	Torque	Nm
F	Force	N
d	Moment Arm	m
F_{out}	Output Force	N
F_{in}	Input Force	N
P	Pressure	Pa
A	Area	m^2
Pa	Pascals	N/m^2
N	Newton	kgm/s^2
D	Density	kg/m^3
m	Mass	kg
V	Volume	m^3
F_{in}	Force Input	N
F_{out}	Force Output	N
d_{in}	Distance Input	m
d_{out}	Distance Output	m
d_e	Effort Distance	m
d_r	Resistance Distance	m
μs	Static Friction	-
μ_k	Kinetic Friction	-
F_f	Frictional Force	N
N	Normal Force	N
F_d	External Force	N
F_{SF}	Maximum Static Friction Force	N
MRT_{BKS}	Maximum Removal Torque BKS	Nm
MIT_{BKS}	Maximum Insertion Torque BKS	Nm

CHAPTER I

General Introduction and Motivation

1.1 Background and Motivation

Developing a biomechanism that incorporates desirable biological and mechanical properties in a safe and practical way for biomechanical rehabilitation is the foundation of all the specialties involved in this field, from molecular, protein and genetic therapies to functional biomechanical restoration of limbs, oral rehabilitation, and organs, especially with the acceleration of global population ageing [1, 2]. A screw is a combination of simple machines [3, 4], an inclined plane wound around a central axis, with a sharp outer edge that acts as a wedge when driving material. Some screw threads are designed to mate with a complementary thread called a female (internal) thread, usually as a nut or something internally threaded. Other screw threads are designed to cut a helical groove in a softer material as the screw is driven into the material (bone screws and implants). The most common uses of screws are to hold objects together and to position objects. The screw was one of the last simple machines to be invented. It first appeared in Mesopotamia during the Neo-Assyrian period (911-609 BCE) and later in Ancient Egypt [3]. Archimedes developed a rigorous theory of levers and the kinematics of the screw and systematized the design of simple machines by studying their functions. The screw was used in the form of the screw press and Archimedes' screw by the first century BCE [3].

Screws were first used in orthopedic surgery in 1850 by the French surgeons Cucel and Rigaud, who used two wooden screws and a leather strap to fix an olecranon fracture [5]. At the beginning of the 20th century, William O'Neill Sherman (1880-1979) was a pioneer in the internal fixation of bone fractures, who modified conventional screw designs for orthopedic applications [6, 7]. The founding of the AO (arbeitsgemeinschaft für osteosyntheses) in Switzerland in 1958 was preceded by Robert Danis' pioneering work in internal fixation, including improved screw design and plate technology [8, 9]. The worldwide standardisation of surgical principles and techniques, and the introduction of a uniform design for orthopedic implants and instruments was one of the fundamental achievements of the AO [6]. However, in vivo axial loading forces from physiological motion are not typically experienced by orthopedic screws. As a result, there is still a significant risk of failure with standard buttress screws when they are subjected to multi-directional loading forces [10, 11]. Several studies have shown that in current dental practice, dental implants have been accepted as the standard of care for edentulous patients and have shown a good long-term success rate. [12]

A high level of performance in treatment and successful application has been claimed for the different materials and designs of each of the implant systems. The transmission of occlusal force to the surrounding bone at the bone-implant interface is the critical function of a dental implant [13]. The greater the contact area between bone and implant, the more force is distributed to the surrounding bone. Compressive, tensile and shear forces are the three main types of loads generated at the bone-implant contact (BIC) [14, 15]. Studies have shown that compression forces have a positive effect on bone density and bone strength after healing. Tensile and shear forces have been shown to lead to weaker bone, with shear forces being the least favorable. The macroscopic implant design is a factor that has influenced the stress in the surrounding bone [16, 17]. The macroscopic implant components, including body and thread geometry, directly contact the bone during implant placement [18]. Bone damage is minimized, and bone healing is enhanced by the appropriate level of stress generated during the insertion process. According to Wolff's theory, the response of the bone in terms of resorption or healing is directly related to the stress in the bone [19]. The relationship between implant geometric design and force distribution in a static condition has been reported in several studies [19, 20, 21].

Bone drilling is ubiquitous in many areas of surgery, including orthopedics, neurosurgery, plastic, and reconstructive surgery, craniomaxillofacial surgery and otolaryngology. Bone screws are used in a variety of surgical procedures, including orthopedics, trauma, plastic surgery, craniomaxillofacial surgery and ear, nose, and throat surgery, to create a cylindrical tunnel in the bone using a surgical drill to receive a screw or other threaded device for rigid fixation by incorporating bone (trabecular and/or cortical) into the screw threads. In this configuration, bone screws are resistant to axial and shear forces as well as bending moments and are therefore suitable for the load bearing function of the skeleton during locomotion. In the preparation of bony tunnels, such as in the reconstruction of the anterior cruciate ligament, drill bits are also used [22]. The environment in which a surgical drill operates is unique and differs greatly from the environment in which engineering drills used in manufacturing or traditional non-biological engineering operate. Bone is a complex, anisotropic, porous, viscoelastic composite material that is also non-homogeneous in terms of both its material properties and its geometry [13, 14, 15, 22, 23]. Bone's outer cortex can be curved, and irregular, and drilled holes are rarely perpendicular to this surface. Eriksson and Albrektsson [24] found that maintaining bone temperature above 47°C for at least one minute caused osteonecrosis. Since then, the reduction of bone temperature rise during drilling has been an important issue in bone surgery.

The effect of the drilling feed force on the temperature rise of bovine cortical bone has been discussed by some researchers [25-29], who indicated that increasing the drilling feed force reduces the friction time between the drill and the bone, thereby reducing the heat generation and the bone temperature rise during drilling. Authors [29, 30] conducted drilling experiments on bovine mandibular cortical bone using drill bits with different geometric shapes and concluded that different geometric parameters of the drill bits directly affected the bone temperature increase.

Soon after completion of my undergraduate degree in Dentistry, the interest in the specialty of Oral and Maxillofacial Surgery and Traumatology motivated the implementation and completion of this specialty in a medical residency program, directed and coordinated by one of the pioneers of this discipline in Brazil, Professor Gino Emilio Lasco, who at that time had more than fifty years of surgical, academic and research experience in Oral & Maxillofacial Trauma. One of the topics there was constantly discussed during the residency and afterwards as an assistant professor of the same specialty, was the lack of robust results on the effects of screw osseointegration in the treatment of bone fractures and other elective surgeries in which fixation screws or implants were used. The hospital complex where the emergency treatment of general and facial trauma was carried out provided a clear opportunity to monitor the results of the proposed treatments in the short, medium, and long term [31], with an abundance of cases found [32].

In his lectures, Professor Gino shared his experience of more than 50 years of work in the field, the evolution of bone fixation screws over the decades [3-12] in search of satisfactory results with lower rates of infection and implant loss. Alloys of metals, stainless steel, tantalum, vanadium, cobalt-chromium, magnesium, and niobium alloys were tested until, by chance, promising results were obtained with titanium [1,33-37]. From then on, the use of bone fixation and implants became common surgical practice, although the phenomenon of osseointegration is still not fully understood [38-41]. The orientation has always been to use screws and implants as biomaterials with care and efficiency, implementing the concept of Hippocrates *primum non nocere* [42].

During surgical procedures for dental implants, bone is removed for implant screwing and many procedures are used to reuse this particulate bone from the drill cut, called bone collectors [43, 44]. This procedure is still much questioned due to the risk of contaminants such as saliva and bacteria increasing the risk of infections and early implant loss [45]. Under ideal conditions the success of dental implants is above 90% although these conditions are the least common in clinical practice [46]. Bone fixation screws of traumatic and elective fractures are more likely to need post-surgical removal, implying a new surgery and its inherent risks [47-49]. The morbidity and mortality rate in surgeries of femoral prostheses is higher with age and complications after surgeries [50]. Cases in which under ideal conditions and the proper planning and technical execution are performed and yet osseointegration is not obtained, still instigate the need for a greater understanding on the subject [45-49].

The first report of bone tissue growing in apparent direct contact with a metallic implant was made by Branemark [33,36, 37] and later, in 1977, the term osseointegration was coined by the same author to describe this phenomenon. However, osseointegration is a concept rather than a biological term. It is not at all accepted that there should be any kind of direct bone-metal contact without any intervening soft tissue layers. However, not only did Branemark provide histological evidence for the direct bone anchorage of titanium implants and developed an oral implant that produced excellent clinical results, in sharp contrast to the fibrous tissue-anchored dental devices that had been used until then [34, 36]. To this day, osseointegration has become a familiar concept to those working in the field of biomaterials, and dental implants, surgical screws and prostheses have received recognition from scientists and the scientific community [51]. Several factors determine the interfacial response to a foreign material, including the biocompatibility, design and surface of the implant, the status of the host bed, the surgical technique used to place it, and the loading conditions to which it is subsequently subjected [52-55].

The biomechanical determinants of osseointegration phenomena are related to bone remodeling around implants (adaptation of bone structure to the presence of a biomaterial) [56]. Dental implants made of zirconia (3Y-TZP) have been subjected to more in vivo studies than those made of titanium. In animal studies, 3Y-TZP and pure titanium have similar BIC values, peri-implant bone densities and mechanical parameters of maximum removal torque (MRT) and maximum insertion torque (MIT) [57-59]. The two materials have also shown similar ability to osseointegrate. A prerequisite for the long-term success of implant-supported prostheses is bone growth on the implant surface. The composition, surface morphology and surface roughness of dental implants influence the rate of osseointegration [33-37, 51-55].

Understanding osseointegration means advancing the knowledge of the relationship between biomaterials and complex animal and human organism, bringing multidisciplinary benefits as well as better control and prediction of results [51, 52, 55]. Since the first observations by Branemark and Albrektsson, who have dedicated their lives to the study of osseointegration through laboratory and clinical research, various hypotheses have been put forward to understand this phenomenon. In the search for optimizing osseointegration results, research is mainly based on surface treatments and their bioactivation, seeking organic repair interactions and favorable remodeling with the immune and healing responses of the human body [51-55]. Changes in implant designs are characterized by the material type, size, and pitch of threads, whether cylindrical or conical, and the type of connections of their prostheses [60].

From this point of view, the idea of reusing bone from bone drilling during the installation of dental implants led to a patent for a new Bioactive Kinetic Screw (BKS) model [61], which allows simultaneous drilling and screwing, with the cut material (bone chips) being inserted into the internal volume of this new BKS device. The need to prove the concept of this new biomechanism has led to a detailed knowledge of the BKS, now defined as a new simple machine (SM) and not just a dental implant, through its various applications [62-66]. Another patent has been filed for the BKS as a simple machine.

1.2 Thesis Objectives

The main objectives of this thesis are to describe the properties of the novel SM BKS, its application as a densimeter, bone collector, bone graft and dental implant, to determine a surgical bone drilling and simultaneous screwing protocol for BKS, determining the coefficient of friction between bone and BKS to enhance primary stability for osseointegration. BKS is biomechanically experimented in distinct materials for this purpose: in aluminium phyllosilicates (clay), kinetic sand, five densities of synthetic bone polyurethane cell foam blocks (PCF) 10, 15, 20, 30, and 40 PCF, and a synthetic bone mandible (Synbones, 10 PCF):

1. To test the BKS SM property of compacting material within its internal volume mathematically proven in two different materials, human bone and in four synthetic bone densities (10, 20, 30, 40 PCF), and experimental study in aluminium phyllosilicates (clay) and kinetic sand.

   1.1 To test the BKS model as a bone graft collector, drill it into the posterior molar region of the synthetic mandible (Synbones), unscrew it and collect the material to be grafted.

1.2 To test BKS as an immediate autogenous graft, it is drilled into the retromolar region of a synthetic mandible (Synbones), removed, and reimplanted with the material collected in its internal volume in a surgical alveolus created in the same mandible.

1.3 To test the BKS model in the form of a dental implant in synthetic bone blocks (10, 15, 20, 30, 40 PCF) to obtain values of initial weight before drilling/screwing, MIT, MRT and weight after total removal. All data were analyzed to create a simplified surgical protocol for the BKS, to optimize its biomechanical insertion in four classical bone densities (Mish) and to obtain the amount and efficiency of bone collected within its internal volume, to obtain a standardization of torque in these bone densities for the BKS and to determine its coefficient of friction.

To achieve the described purpose, the following specific aims were defined in this thesis:

1. The BKS model has been experimentally tested in aluminium phyllosilicates (clay) and kinetic sand, weighed before being manually screwed and unscrewed into the materials using a standard hexagonal spanner. After collecting and compacting the material inside the BKS, another weight measurement was taken with all the material compacted. The difference between the before and after weights were determined on a Taylor and Brifit Precision Compact Digital Scale, using the calibration button prior to all weight measurements;
2. A synthetic bone mandible (Synbones) with a density of 0.16 g/cm^3 was selected to demonstrate the Dentoflex surgical protocol used in dental implant surgery and to compare it with the new simplified protocol used in the BKS, given its simultaneous drilling and screwing capability. A Techdrill Surgical Motor-1 with a power of 150 watts and a preset torque of 45 N/cm was used. In the Dentoflex Surgical Kit used, we performed the drilling protocol with 2.3 mm, 2.6 mm, 2.9 mm, 3.2 mm, 3.4 mm, and 3.7 mm drills for insertion of the 4.0 mm diameter non-BKS implant. All drills were 10.0 mm deep, the same size as the BKS and non-BKS screws used in this study. No holes were drilled in the mandible prior to BKS drilling;
3. Drill the mandibular synthetic bone (Synbones) with the BKS at low speed (60 rpm) and after inserting the entire length into the bone, reverse the direction of rotation on the motor to remove the BKS completely from the bone donor bed. With the particulate bone(chips) in its internal volume, and without direct manipulation of the

bone, it is removed from inside the BKS using a dental explorer and can be placed directly into the desired recipient site;

4. The BKS was removed (unscrewed) after insertion (drilling and screwing simultaneously) into the retromolar region of the synthetic mandible (Synbones) to harvest bone from this region and graft it (within the BKS) into a surgical alveolus previously prepared in the same mandible. The BKS was drilled, inserted and removed at low speeds (60 rpm) to retain the maximum amount of bone harvested;
5. Development of a surgical protocol for BKS dental implant using engineering materials (synthetic bone Nacional Ossos 10, 15, 20, 30, and 40 PCF) with properties similar to those of cancellous and trabecular human bone to study the inherent variation in mechanical MIT and MRT of the new dental implant drilling and screwing simultaneously protocol determining the coefficient of friction of the BKS to bone in five densities;
6. To measure the MIT and the MRT of the BKS dental implant tested in this study using a digital torque meter (LQ8800) and to determine the BKS-bone friction coefficient obtained by the novel BKS biomechanical SM used as a dental implant in five distinct densities of bone;
7. Record the amount of bone particles inside the BKS dental implant after removal by weighing the screws individually before and after insertion and removal in five bone densities;
8. Analysis of MIT and MRT obtained in five densities of synthetic bone to describe the coefficient of friction between bone-BKS surfaces to develop a standard torque (ST) achieving MIT to optimize primary stability for the novel BKS dental implant.

1.3 Thesis Structure

This thesis is divided into nine chapters and two main parts. The first part consists of chapters I and II. Chapter I contains the thesis topic with the main questions and concerns describing the new SM BKS and its applications as a dental implant, densimeter, bone graft, bone screw, and bone collector. The main motivations and overall objectives are presented. Chapter II offers the reader a literature review on the definition of SM's and their properties, the proposed innovation with the patented BKS, as well as a comprehensive review of the most relevant investigations carried out on bone properties, bone healing and applications of the BKS as a biomechanical device. The main results are described and compared. The second part consists of seven chapters with the most important papers published (or under review) and a final chapter with general conclusions and future perspectives. The order of the papers is as follows:

Chapter III. The first paper, entitled *"A New Biomechanism: A Bioactive Kinetic Screw"*, presents the simple BKS device as a bone screw, using the bone particles, cells and molecules removed during bone drilling as an autogenous homogeneous graft to create bone remodeling through the implant screw.

This paper was published in *Chapter in book: Advances and Current Trends in Biomechanics 2021*, by the authors Carlos Aurelio Andreucci, Elza Fonseca, and Renato Natal Jorge.

Chapter IV. The second paper, entitled "*Static in Bone Implants: Standard Steady-State Torque and Primary Stability in a Bioactive Kinetic Screw*", describes the relationship between the MIT, MRT, and maximum force of static friction between implant-bone and bone-to-bone, achieving a controlled and predictable standard steady-state torque that maintains equilibrium in elastic stress for the primary stability of bone implants.

This paper was submitted to the *Journal of the Brazilian Society of Mechanical Sciences and Engineering*, by the authors Carlos Aurelio Andreucci, Elza Fonseca, and Renato Natal Jorge.

Chapter V. Third paper, entitled *"Increased Material Density within a New Biomechanism"*, describes an experimental in vitro test that validates the mathematical results, describing how the same compact factor of 3.45 was determined in two different materials using the new BKS simple machine.

This paper was published in *Mathematical and Computational applications; Numerical and Symbolic Computation: Developments and Applications*, by the authors Carlos Aurelio Andreucci, Elza Fonseca and Renato Natal Jorge.

Chapter VI. The fourth paper, entitled *"3D Printing as an Efficient Way to Prototype and Develop Dental Implants"*, describes how to develop a new biomechanical model for dental implants from its conception for the patent to the final product which is ready to be manufactured using additive manufacturing.

This paper was published in *BioMedinformatics*, by the authors Carlos Aurelio Andreucci, Elza Fonseca, Renato Natal Jorge.

Chapter VII. Fifth paper, entitled *"A New Simplified Autogenous Sinus Lift Technique"*, describes an experimental study of an innovative technique for the BKS bone implant model that simplifies and effectively performs autogenous grafting, sinus augmentation, and implant fixation in a single step.

This paper was published in *Bioengineering,* by the authors Carlos Aurelio Andreucci, Elza Fonseca, Renato Natal Jorge.

Chapter VIII. Sixth paper, entitled *"A new simple machine that converts torque into steady-state pressure in solids"*, describes experimental studies in which the SM BKS converts the movement of rotation into linear movement, torque into compression, by increasing the density of the mass on which it acts, reducing its original volume under measured conditions.

This paper was published in *IEEE 7th Portuguese Meeting on Bioengineering (ENBENG) 2023,* by the authors Carlos Aurelio Andreucci, Elza Fonseca, Renato Natal Jorge.

Finally, there is the Appendix containing the consent forms signed by all authors and glossary.

References

1. Gobbi SJ, Reinke G, Gobbi VJ, Rocha Y, Sousa TP, Coutinho MM. (2020) Concepts and

Basics Properties. *European International Journal of Science and Technology*. *Biomaterial* 9(2), 23-42.

2. Lutz W, Sanderson W, Scherbov S. (2008) The coming acceleration of global population ageing. *Nature* 451(7179), 716-719.
3. Chondros TG. (2010) Archimedes life works and machines. *Mechanism and Machine Theory* 45(11), 1766-1775.
4. Wang P, Xu Q. (2018) Design and modeling of constant-force mechanisms: A survey. *Mechanism and Machine Theory* 119, 1-21.
5. Kakria HL. (2010) Evolution in fracture management. *Med J Armed Forces India* 61(4), 311–2.
6. Venable CS, Stuck WG. (1947) The internal fixation of fractures. Springfield: Charles C. Thomas.
7. Roberts TT, Prummer CM, Papliodis DN, Uhl RL, Wagner TA. (2013) History of the orthopedic screw. *Orthopedics* 36(1), 12–4.
8. Schlich T. (2002) Surgery, science and industry: a revolution in fracture care, 1950s-1990s. New York: Palgrave-MacMillan.
9. Uhthoff HK, Poitras P, Backman DS. (2006) Internal plate fixation of fractures: short history and recent developments. *J Orthop Sci* 11(2), 118–26.
10. Archdeacon MT, Anglen JO, Ostrum RF, Herscovici Jr D. (2012) Prevention and management of common fracture complications. Thorofare: Slack Inc.
11. Mosavar A, Ziaei A, Kadkhodaei M. (2015) The effect of implant thread design on stress distribution in anisotropic bone with different osseontegration conditions: a finite element analysis. *Int J Oral Maxillofac Implants* 30(6), 1317–26.
12. Fugazzotto, P. A. (2005) Success and failure rates of osseointegrated implants in function in regenerated bone for 72 to 133 months. *The International Journal of Oral & Maxillofacial Implants* 20, 77–83.
13. Abuhussein H, Pagni G, Rebaudi A, Wang H-L. (2010) The effect of thread pattern upon implant osseointegration. *Clin. Oral Impl. Res*. 21, 129–136.
14. Adell R, Lekholm U, Rockler B, Branemark P. (1981) A 15 year study of osseointegrated implants in the treatment of the edentulous jaw. *Int J Oral Surg* 10(6), 387-416.
15. Albrektsson T, Albrektsson B. (1987) Osseointegration of bone implants: A review of an alternative mode of fixation. *Acta Orthopaedica Scandinavica* 58(5), 567-577.
16. Havaldar R, Pilli SC, Putti BB. (2014) Insights into the effects of tensile and compressive

loadings on human femur bone. *Advanced Biomedical Research* 3, 101–101.

17. Oftadeh R, Perez-Viloria M, Villa-Camacho JC, Vaziri A, Nazarian A. (2015) Biomechanics and mechanobiology of trabecular bone: A review. *Journal of Biomechanical Engineering*, 137, 0108021–01080215.
18. Vandeweghe S, Cosyn J, Thevissen E, Teerlinck J, De Bruyn H. (2012). The influence of implant design on bone remodeling around surface-modified Southern Implants®. *Clinical Implant Dentistry and Related Research*, 14, 655–662.
19. Stock J.T. (2018) Wolff's law (bone functional adaptation). In The International Encyclopedia of Biological Anthropology (eds W. Trevathan, M. Cartmill, D. Dufour, C. Larsen, D. O.Rourke, K. Rosenberg and K. Strier).
20. Herekar MG, Patil VN, Mulani SS, Sethi M, Padhye O. (2014) The influence of thread geometry on biomechanical load transfer to bone: A finite element analysis comparing two implant thread designs. *Dental Research Journal* 11, 489–494.
21. Oswal MM, Amasi UN, Oswal MS, Bhagat AS. (2016) Influence of three different implant thread designs on stress distribution: A three-dimensional finite element analysis. *Journal of Indian Prosthodontic Society* 16, 359–365.
22. Bertollo N, Walsh WR. (2011) Drilling of Bone: Practicality, Limitations and Complications Associated with Surgical Drill-Bits, Biomechanics in Applications, Dr Vaclav Klika (Ed.), ISBN: 978-953-307- 969-1.
23. Eraslan O, Inan O. (2010) The effect of thread design on stress distribution in a solid screw implant: a 3D finite element analysis. *Clin Oral Investig* 14(4), 411–6.
24. Eriksson AR, Albrektsson T. (1983) Temperature threshold levels for heat-induced bone tissue injury: a vital-microscopic study in the rabbit. *J Prosthet Dent* 50, 101–7.
25. Watanabe F, Tawada Y, Komatsu S, Hata Y. (1992) Heat distribution in bone during preparation of implant sites: heat analysis by real-time thermography. *Int J Oral Maxillofac Implants* 7, 212–19.
26. Abouzgia MB, James DF. (1995) Measurements of shaft speed while drilling through bone. *J Oral Maxillofac Surg* 53, 1315–16 1308-15.
27. Abouzgia MB, Symington JM. (1996) Effect of drill speed on bone temperature. *Int J Oral Maxillofac Surg* 25, 394–9.
28. Brisman DL. (1996) The effect of speed, pressure, and time on bone temperature during the drilling of implant sites. *Int J Oral Maxillofac Implants* 11, 35–7.
29. Fernandes MGA. (2017) Analysis of Bone Damage during Drilling Processes. Doctoral

dissertation, Universidade do Porto, Porto, Portugal.

30. Benington IC, Biagioni PA, Crossey PJ, Hussey DL, Sheridan S, Lamey PJ. (1996) Temperature changes in bovine mandibular bone during implant site preparation: an assessment using infrared thermography. *J Dent* 24, 263–7.
31. Andreucci CA. (2000) Primum non nocere. Diagnostico e tratamento das fraturas faciais. *Especialização em Cirurgia e traumatologia Bucomaxilofacial em regime de residência* Universidade Brasil, São Paulo, Brasil, 114.
32. Andreucci CA. (2009) Epidemiologia dos traumatismos craniofaciais no centro hospitalar de Santo André (Brasil) no ano de 1999, na vigência do novo código de trânsito. *Mestrado em Ciências da Saúde* Centro Univ. FMABC, Santo André, Brasil, 126.
33. Branemark P I, Adell R, Breine U, Hansson BO, Lindstrom J, Ohlsson A. (1969) Intra-osseous anchorage of dental prostheses. I. Experimental studies. *Scand J Plast Reconstr Surg* 3(2), 81-100.
34. Branemark PI, Hansson BO, Adell R, Breine U, Lindstrom J. Hallen O, Ohman A. (1977) Osseointegrated implants in the treatment of the edentulous jaw. Experience from a 10 year period *Scand J Plast Reconstr Surg* (16), l-132.
35. Albrektsson T, Branemark PI, Hansson HA, Kasemo B, Larsson K, Lundstrom I, McQueen D, Skalak R. (1983) The interface zone of inorganic implants in vivo: Titanium implants in bone. *Ann Biomed Eng* 11, 1-27.
36. Branemark PI. (1985) Introduction to osseointegration. In: Tissue integrated Prostheses. Osseointegration in Clinical Dentistry (Eds. Branemark P I, Zarb G, Albrektsson T.) Quintessence, Berlin, Chicago, Tokyo 1-76.
37. Branemark PI. (1992) Osseointegration-a method of anchoring prostheses. *The Swedish Society of Medicine* 7-15.
38. Albrektsson T. (1985) The response of bone to titanium implants. *Crit Rev Biocompat* 1(1), 53-84.
39. Albrektsson T, Jacobson M. (1987) Bone metal interface in osseointegration. *J Prosthet Dent* 57(5), 597- 607.
40. Albrektsson T, Branemark PI, Hansson HA, Kasemo B, Larsson K, Lundstrom I, McQueen D, Skalak R. (1983) The interface zone of inorganic implants in vivo: Titanium implants in bone. *Ann Biomed Eng* 11, 1-27.
41. Eriksson R A. (1984) Heat induced bone tissue injury. An in vivo investigation of heat

tolerance of bone tissue and temperature rise in the drilling of cortical bone. Doctoral dissertation, University of Gothenburg, Goteborg, Sweden.

42. Smith C.M. (2005) Origin and Uses of Primum Non Nocere—Above All, Do No Harm! *The Journal of Clinical Pharmacology* 45, 371-377.
43. Jang KY, Lee JH, Oh SH, Ham BD, Chung SM, Lee JK, Ku JK. (2020) Bone graft materials for current implant dentistry. *J. Dent. Res*. 39, 1.
44. Graziani F, Cei S, Ivanovski S, Ferla F, Gabriele M. (2007) A systematic review of the effectiveness of bone collectors. *The Inter jour of oral & max imp*. 22, 729-35.
45. Zamborsky R, Svec A, Bohac M, Kilian M, Kokavec M. (2016) Infection in Bone Allograft Transplants. *Exp. Clin. Transplant*. 14, 484–490.
46. Howe MS, Keys W, Richards D. (2019) Long-term (10-year) dental implant survival: A systematic review and sensitivity meta-analysis. *J Dent*. 84, 9-21.
47. Kordbacheh CK, Finkelstein J, Papapanou PN. (2019) Peri-implantitis prevalence, incidence rate, and risk factors: a study of electronic health records at a U.S. dental school. *Clin Oral Implants Res* 30, 306–314.
48. Buser D, Janner SFM, Wittneben JG, Brägger U, Ramseier CA, Salvi GE. (2012) 10-year survival and success rates of 511 titanium implants with a sandblasted and acid-etched surface: a retrospective study in 303 partially edentulous patients. *Clin Implant Dent Relat Res* 14, 839–851.
49. Khan MS, ur Rehman S, Ali MA, Sultan B, Sultan S. (2008) Infection in orthopedic implant surgery, its risk factors and outcome. *J Ayub Med Coll Abbottabad*. 20(1), 23-25.
50. Lundin N, Huttunen TT, Enocson A, Marcano AI, Felländer-Tsai L, Berg HE. (2021) Epidemiology and mortality of pelvic and femur fractures—a nationwide register study of 417,840 fractures in Sweden across 16 years: diverging trends for potentially lethal fractures, *Acta Orthopaedica*, 92, 3, 323-328.
51. Pandey C, Rokaya D, Bhattarai BP. (2022) Contemporary Concepts in Osseointegration of Dental Implants: A Review. *Biomed Res Int*. 6170452.
52. Albrektsson T, Albrektsson B. (1987) Osseointegration of bone implants: A review of an alternative mode of fixation, *Acta Orthopaedica Scandinavica*, 58, 5, 567-577.
53. Albrektsson T, Dahlin C, Jemt T, Sennerby L, Turri A, Wennerberg A. (2014) Is marginal bone loss around oral implants the result of a provoked foreign body reaction? *Clin Implant Dent Relat Res*. 16, 155- 165.

54. Albrektsson T, Chrcanovic B, Jacobsson M, Wennerberg A. (2017) Osseointegration of implants—a biological and clinical overview. *JSM Dent Surg*. 2, 1- 6.
55. Albrektsson T, Wennerberg A. (2019) On osseointegration in relation to implant surfaces. *Clin Implant Dent Relat Res*. 21, 4– 7.
56. Mathieu V, Vayron R, Richard G, Lambert G, Nailia S, Meningaud JP, Haiat G. (2014) Biomechanical determinants of the stability of dental implants: Influence of the bone–implant interface properties. *Journal of Biomechanics* 47(1), 3-13.
57. Kohal RJ, Bächle M, Renz A, Butz F. (2016) Evaluation of alumina toughened zirconia implants with a sintered, moderately rough surface: an experiment in the rat. *Dent Mater*. 32(1), 65–72.
58. Gahlert M, Roehling S, Sprecher CM, Kniha H, Milz S, Bormann K. (2012) In vivo performance of zirconia and titanium implants: a histomorphometric study in mini pig maxillae. *Clin Oral Implants Res*. 23(3), 281–286.
59. Koch FP, Weng D, Krämer S, Biesterfeld S, Jahn-Eimermacher A, Wagner W. (2010) Osseointegration of one-piece zirconia implants compared with a titanium implant of identical design: a histomorphometric study in the dog. *Clin Oral Implants Res.* 21(3), 350–356.
60. Jiang X, Yao Y, Tang W, et al. (2020) Design of dental implants at materials level: An overview. *J Biomed Mater Res A*. 108(8), 1634-1661.
61. Andreucci CA. (2022) Disposição construtiva aplicada em parafuso para implante ósseo. São Paulo, Brasil. Internacional Patent No. WO2022036425A1. WIPO (PCT).
62. Andreucci CA, Alshaya A, Fonseca EMM, Jorge RN. (2022) Proposal for a New Bioactive Kinetic Screw in an Implant, Using a Numerical Model. *Appl. Sci*. 12, 779.
63. Andreucci CA, Fonseca EMM, Jorge RN. (2022) Increased Material Density within a New Biomechanism. Math. *Comput. Appl*. 27, 90.
64. Andreucci CA, Fonseca EMM, Jorge RN. (2022) 3D Printing as an Efficient Way to Prototype and Develop Dental Implants. *BioMedInformatics* 2, 44.
65. Andreucci CA, Fonseca EMM, Jorge RN. (2022) J. Structural analysis of the new Bioactive Kinetic Screw in titanium alloy vs. commercially pure titanium. *J. Comp. Art. Int. Mec. Biomec*. 2, 35–43.
66. Andreucci CA, Fonseca EMM, Jorge RN. (2023) Bio-lubricant Properties Analysis of Drilling an Innovative Design of Bioactive Kinetic Screw into Bone. *Designs*. 7(1), 21.

CHAPTER II

Literature Overview

2.1 Simple Machine

The innovation of the BKS, as seen in figure 1, is in using the same properties of the screw [1-5] adding angles and cutting grooves at its apex decreasing the area of contact with the perforated material thus increasing the cutting pressure of a conventional screw. In addition to this benefit, the innovation introduced was the ability to store and compact the chips from drilling and inserting the BKS, through its dual flutes, by flowing the chips that meet at a common point in the BKS's inner volume and are pressed together. After the material where the new BKS has been applied fills the entire internal volume with its chips, compaction increases the density of the material [6-11] transferring the torque exerted in the pressure area, to the entire internal volume of the BKS in all directions, acting as a fluid while there is torque, and increasing the coefficient of static friction, and self-locking in the absence of torque. The regular screws have a very low efficiency, due to the amount of friction between the materials. In BKS, these have become an advantage for self-locking the SM.

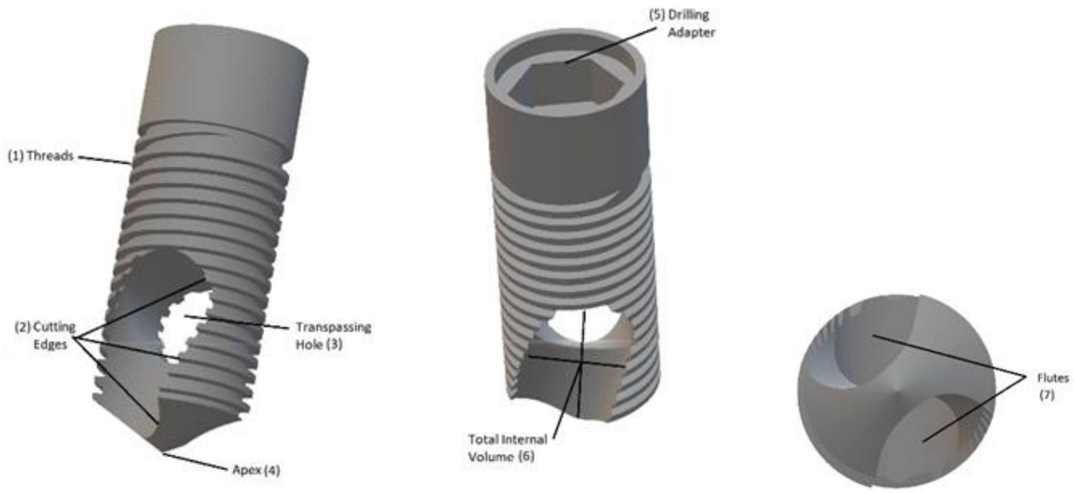

(a) (b) (c)

Figure 1. (a) BKS innovative Simple Machine: (1) Properties of the Screw; (2) adding angles and cutting grooves; (3) Transpassing hole connecting flutes; (4) Apex; (b) (5) Drilling or spanner adapter for insertion torque; (6) Inner volume; (c) Apex and (7) flutes [6-11].

2.1.1 Mechanical advantages

Torque (*M*) is the rotational equivalent of linear force. It is the force (*F*) times the moment arm (*d*) or lever arm that's equal to the perpendicular distance from the axis of rotation to the line of action, that's parallel to the *F*, as seen in equation:

$$M = F \times d \tag{1}$$

The concept of *M* is very useful for leverage to multiply a *F* by adjusting the *d* of a SM obtaining Actual Mechanical Advantage (*AMA*), that is the ratio of output (F_{out}) to input force (F_{in}), as seen equation:

$$AMA = \frac{F_{out}}{F_{in}} \tag{2}$$

All machines transmit mechanical energy, and the measure of its efficiency is the ratio obtained according to equation 2.

Pressure (*P*) is *F* per unit of area (*A*) and the standard unit of pressure is Pa, as seen in equation:

$$P = \frac{F}{A} \tag{3}$$

The *P* is directly related to the *F* but inversely related to the *A* upon which that *F* is applied. Whatever the source is, always the *F* is perpendicular which means the component of the *F* is at right angles to the surface it is colliding with.

Density (*D*) it is a measure of how much mass (*m*) a substance has per unit of its volume (*V*) or how heavy an object is for its size, based on the arrangement of the atoms and how close these atoms and molecules are packed together, as seen in equation:

$$D = \frac{m}{V} \tag{4}$$

A SM is a mechanical device that changes the direction or magnitude of a *F*, defined as the simplest mechanisms that transfer energy allowing work to be done with mechanical advantage (MA) [1, 2]. The energy transfer during the operation of a SM can be described by the work input into the SM equal to the work that is output. In operation, deflection, friction, and wear will reduce the ideal MA to the AMA defined by efficiency, a value that is determined by experimentation. The work done by a force is calculated as the product of *F* and distance (*d*) moved by the object, so the SM equation (2) can be replaced with their equivalent expressions in terms of *F* and *d* as follows:

$$F_{in}\, d_{in} = F_{out}\, d_{out} \tag{5}$$

A third expression for MA can be determined by the ratio of these two distances (d_{in} and d_{out}):

$$MA = \frac{d_{in}}{d_{out}} \tag{6}$$

The screw, one of the properties of the innovative BKS mechanical device, has a high MA because it is two associated SM's, an inclined spiral plane (MA_1) combined with a wheel and an axle (MA_2) when friction is overwhelmed by the rotational force (M) of the wheel multiplied by the MA [2-4]. It translates rotational movement into linear movement. The MA of two SMs working together is equal to the product of the MA of each SM as seen in the equation:

$$MA = MA_1 MA_2 \tag{7}$$

2.1.2 Efficiency

The ideal mechanical advantage (IMA) of the screw [5] starts with the transfer of the rotational movement of the torque being translated into linear downward movement. The expected MA produced is calculated by $IMA = d_E/d_R$, where d_E is the effort (input) distance and d_R is resistance (output) distance. Once the screw is inserted with one complete rotation, a thread penetrates a linear distance to the applied material, and it is possible to measure the IMA by the ratio of the circumference of the screw (d_E) to the Pitch (d_R) as seen in equation:

$$IMA = \frac{2\pi r}{Pitch} \tag{8}$$

In experimental application, deflection, friction, and wear will reduce the MA [4, 5]. The amount of this reduction from the IMA to AMA is defined by a factor called efficiency (%E), a quantity which is determined by experimentation, as seen equation:

$$\%E = \left(\frac{AMA}{IMA}\right) 100 \tag{9}$$

2.1.3 Coefficient of friction

Friction occurs when two materials resists moving against one another like titanium screwed into the bone [12]. The coefficient of static friction depends on the combined effects of material deformation characteristics and surface roughness, both of which originate from the chemical bonding between the atoms of the materials between their surfaces and any adsorbed material. The fractality of surfaces, a parameter that describes the integration of structural and molecular interactions across a range of scales of surface roughness, plays an important role in determining the magnitude of static friction [13]. The amount of friction generated depends primarily on the materials which are in sliding contact. The coefficient of friction (μ) is a dimensionless quantity which describes the ratio of the force of the friction between two bodies and the force of them pressing together. This coefficient can be used to help to determine the amount of force required to move a drill bit, a screw, a saw, and BKS in the bone. The amount of F required to slide a load and overcome the static friction (μs), kinetic friction (μ_k), is calculated by multiplying μ by the weight of the load for horizontal forces, where F_f is the frictional force and N is the normal force, as seeing in equation [14].

$$F_f = \mu N \tag{10}$$

If an object is on a flat surface and subjected to an external F sliding, then the N between the object and the surface is $N = mg + F_d$ only where mg is the object's weight and F_d is the component of the external F. The μ has different values for μs and μ_k. In μs, the F_f resists F that is applied to an object, and the object remains at rest, like a dental implant totally screwed into the bone, resulting from molecular interactions between the implant and the bone surface at primary stability. In μ_k, the F_f resists the motion of an object like during drilling bone. The F_f itself is directed oppositely to the motion of the object. The value of μs varies between zero and the smallest F needed to start motion. This smallest F required to start motion, or to overcome μs, is always greater than the F required to continue the motion, or to overcome μ_k, as seeing in figure 2 [14].

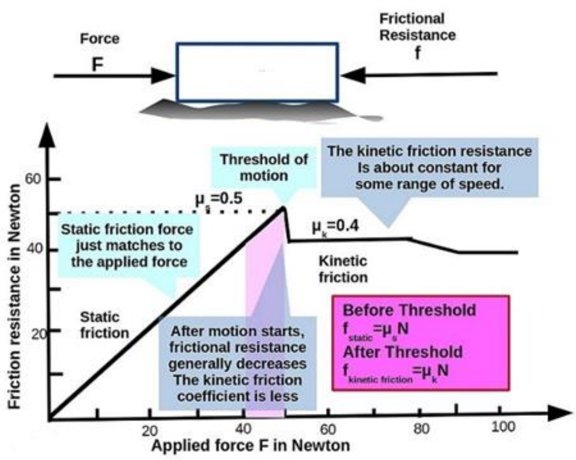

Figure 2. The amount of μ is nearly independent of the A of contact and μ is proportional to the load or mg that presses the surfaces together (adapted from [14]).

μ_k is lower than μs, and correspondingly, kinetic self-locking is less likely to occur than static self-locking. The μ_k is also affected by the BKS speed and the lubrication's behavior [11] under dynamic conditions. The μs generally depends on the materials of the two components and any lubrication between them. Other factors like condition of the surfaces or the presence of external vibrations, can lower the μs.

The amount of μ generated depends primarily on the materials which are in sliding contact, the μ is a dimensionless quantity which describes the ratio of the F of the μ between two bodies and the F of them pressing together. This coefficient can be used to help to determine the amount of F required to move BKS into the material applied. The amount of F required to slide a load and overcome the μs, μ_k, is calculated by multiplying the μ by the mg of the load for horizontal Fs, as seen in equation 10 [14].

Adhesion is the tendency of different particles or surfaces to cling to each other as it occurs between the BKS structure and the applied material. Cohesive attraction, or cohesive force, is the property of similar molecules sticking together, being mutually attracted. It is an intrinsic property of a substance that is caused by the shape and structure of its molecules, making the distribution of surrounding electrons irregular by forming electrical attraction while maintaining a microscopic structure. Cohesion allows a surface tension, creating a "solid" state, which can be observed when BKS collects and compacts the material where it is applied to its inner volume and is thus also constituted by this material inducing cohesion through its surface [15].

Since a system under P has the potential to perform work on its surroundings, P is a measure of potential energy stored per unit volume. It is therefore related to energy density and may be expressed in units such as J/m^3, which is equal to Pa. Mathematically:

$$P = \frac{Work}{Volume} \tag{11}$$

The P exerted by the BKS insertion on its inner volume makes the collected granular matter (chips) denser [8] in proportion to the size of the grains formed, and the amount of F applied. This process occurs until a limit is established between the materials (self-locking), experimentally given by the amount of F applied and the innovative MA created, without rupturing the system.

The depth where the M increases more abruptly is considered as the point of flute clogging or full-filling the BKS inner volume marked as beginning the compaction of the material, same criterion for chip-evacuation capability. This provides the means to make comparisons of the BKS performance of different tooling parameters drill geometry, substrate material, coating and cutting conditions [16].

Chips can be classified as granular solids, which are characterized as a group of particles that are of roughly the same size. Granular solids have characteristics of both fluids and solids. They occupy the shape of the container in which they fill, exert P on the container boundaries, and flow through openings like fluids. Like solids, they have cohesive strength, can have anisotropic stress distributions, and have shear stresses that are proportional to the normal stress [17].

The BKS model presented here relates to the properties of granular solids collected in its internal volume, where the chips exert P on the flute surfaces of the body and internal walls of the BKS, flow and fill the internal V, remain in contact with each other, have isotropic stress distributions due to the compaction capability of the BKS, and have the μ increased by the filling material inside it. Friction between similar materials is always higher than between different materials [16-18].

The BKS model determines two depths of interest when drilling: the depth that can be drilled before being subjected to an increasing at which compaction (chip jamming) begins to occur, and the limit based on the material's breaking point, and thus the maximum desired depth to compact material. These two critical depths can be used jointly to change the BKS design accordingly with process planning and materials applied. For a given specified depth, the BKS model can be used to determine if the hole can be drilled in one step without exceeding the chosen M limit. If the hole cannot be drilled without violating the limit, a pilot or more previous drilling (multistep) should be made.

❖ *Static friction implant to bone*

μs is required for dental implants primary stability or mechanical stability avoiding micromovements that leads to failure in osseointegration. MIT is mistakenly used as a parameter for mechanical initial stability in dental implants, clinical and experimental procedures, as observed by conflicting results in literature for decades [19-21].

Obtaining higher M in dental implants due higher μs and not by undersized drilling, increases the BIC, without over-pressuring the bone due high loads like when MIT is generated majority by the difference of the undersized drilling into the bone (smaller diameter) and the geometry of the metal bone implant (screwed under pressure). The distinct hardness of bone, and metal implant, increase the stress/strain into the bone increasing the risk of osseointegration failure with undersized drilling unpredictable protocol implant to bone pressure during the healing process [20]. Because the properties and density of the bone varies, it is impossible to precisely predict the optimized undersize of the drilled holes to each specific geometry of implants. It is being used in literature different undersized drilling protocols, related to bone densities and implants properties without clear correlation of the results [22-24].

Once totally screwed, the dental implant reaches μs. This is the parameter that will avoid micromovements of the implant within the bone, and its value will determine the load that will be supported mechanically in this stage of the healing process without compromising long-term osseointegration. If we apply immediately after obtaining MIT, an MRT to the same implant, as soon it starts to move, we precisely achieve the value of the *F* needed to overcome μ, static friction force or, static friction torque (SFT), equivalent to MRT in implants, already described robustly in literature. This is only possible in experimental studies in laboratory or in animals, otherwise the osseointegration will be compromised [25-27].

The implant site-preparation protocol should be accurately chosen to reduce implant micro-movement below the 50–150 μm threshold and provide proper stability and prosthetic support in accordance with the planned loading protocol (delayed, early, or immediate) [28-30]. This distance between implant and bone (BIC) does not consider the contact volume between these materials.

With distinct drilling parameters and protocols, its unpredictable in humans the SFT achieved until now, and distinct MIT standards are described in the literature as ideal, with differences between 15 to 150 Ncm, showing discrepancies and inconsistency in the results [19-24]. Also, different tests for primary stability analysis, shows no correlations with each other, like resonance frequency analysis (RFA) achieving implant stability quotient (ISQ), insertion energy (IE) measurements, that is the total energy needed to place the implant into its site, and screwing MIT [31-34].

The BKS presents one solution for standardization of the MIT, and its correlation with μs values in different bone densities inherent its innovative mechanical properties of drilling, screwing and bone compacting in the same surgical procedure [6-11]. Since is also a drill bit, there is no lateral load pressure from the BKS implant into the bone bed site due the bone cut by the groove flutes with the same size of the BKS. The retention and immobilization of the BKS will be done primarily by the resulting *F* applied through the implant into the bone, correlated with μ_k of the implant into the bone (μ_{KIB}), and the μ_k of the compacted bone (μ_{KBB}) inside and through the BKS to the bone bed site until the *M* is removed, becoming μs [12-18]. μs is the limit to the amount of masticatory load that can be applied to the abutment supporting the crown before micromovements occur between the bone and implant contacts that can prevent proper primary (mechanical) and secondary (biological) stability.

The depth where the *M* increases more abruptly has been considered as the point of flute clogging (bone chips) and used as a performance criterion for chip-evacuation capability [16-18]. In the BKS, the increase of the *M* indicates the beginning of the compaction of the collected material (μ_{KIB}) where the addition of more *M* continuously reaches the limit (μ_{KBB}) allowed and established by the properties of the applied materials, like BKS and bone, without breaking the integrity of the system causing rupture or ultimate load or strength.

Chips, classified as granular solids, occupy the inside geometry of the BKS. Due to the compaction effect and the simultaneous drilling and screwing properties of BKS, the threads are also produced in the denser material inside. The collected material is combined into the BKS total volume, as seeing in figure 3, in which they fill, exert *P* on the container boundaries, and flow through openings like fluids, possess cohesive strength, can have non isotropic stress distributions, and have shear stresses that are proportional to the normal stress [35].

Figure 3. BKS 3D printed filled with aluminum phyllosilicates (clay) after insertion and removal of the BKS into the material tested [8].

Bone drilled chips (bone graft) that are collected during implant site preparation can be reused as homogenous, autologous bone-grafting material and for increasing the μ values due to bone particles cohesive molecular retention into the bone bed site. It is widely known in the literature that living cells have been found in the bone chips even after drilling with twist drills [17, 36].

Implant stability decreases during early weeks of healing followed by an increase as seen on figure 4, [37] related to the repair of the bone to surgical trauma, where bone is resorbed by osteoclastic activity, reflecting a reduction in implant stability. This process is followed by new bone apposition by osteoblastic activity leading to adaptive bone remodeling around the implant [38]. An accelerated formation of BIC contributes to a faster increase in biological (secondary) stability. This biologic process provides consistency of stability overtime during the healing period.

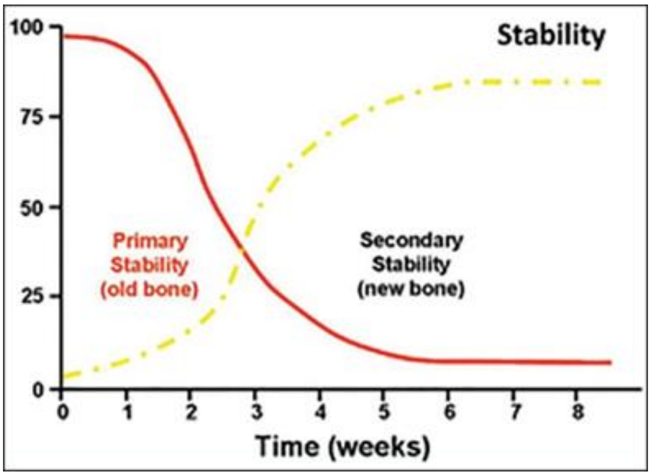

Figure 4. Primary stability comes with old bone. Secondary stability comes with new bone [38].

❖ *Static friction bone to bone*

The Fs of M (MIT and MRT), and μ analysis aims to find the required rotational moment to push (insertion) and pull (removal) a screw to impending motion [39-46]. As impending motion is the threshold between the system holding still and moving, the knowledge of the moments required at impending motion allows you to interpret what happens to the screw system in static-but-not-impending conditions as well. Since all friction is impending, we will use the μs after reaching the MIT and the related F_f to describe the maximum insertion force and or IE [47-50] associated directly to μs by the equation (10), where the N between the object and the surface is $N = mg + F_d$ applied as follows:

$$\mu_S = \frac{F_f}{m\,g+F_d} \tag{12}$$

The innovation presented through the BKS is, after totally screwed the implant (MIT), it reaches μs without lateral load pressure into the bone, due its SM properties [6-11, 51]. Applying MRT to the BKS, as soon as the implant starts to move, we can precisely measure the value of the maximum static friction force (F_{SF}) that will avoid micromovements of the implant within the bone, to accomplish primary stability [52]. Findings in literature suggest that a rough surface finish to cut bone, in a well-reduced fracture, should promote healing by stabilizing the fracture interface [53].

The tribological properties from the friction of the bone, and titanium alloys should be considered, both exhibiting friction wear. In the bone, wear is more severe than titanium and its alloys. The wear debris (chips) from the bones, should be considered influencing the micromotion by stiffness or looseness of the implants [54]. The wear form of bone is a plastic deformation with critical digs, debris, and microcracks, whereas while that of the titanium alloy (Ti-6Al-4V) is a micro-cutting with scratches, denoting adhesive, and abrasive wear [55].

Authors [56] validated testing methods to provide bone-implant friction data concluding that the rotation method, like when drilling or screwing, presented accurate friction estimates, and was less affected by N and speed, than the sled method. The testing of bone against implant surfaces produced a variety of different F displacement curves and a wide range of μ in bovines, ranging from 0.19 to 0.78. A weak positive correlation was observed between bone porosity and μ.

In the experiment to determine the F_{SF}, a new ST obtained was determined, correlated with success or failure probabilities in osseointegration. Our ST proposal is described by the MIT relationship with MRT, obtaining the amount of F_{SF} to start unscrewing the implant (BKS). This approach is only valid for individual measurements on implants that are inserted without any bone bed compression when the bone bed size is drilled same size as the implant geometry. It is not possible to obtain controlled similar values and predictions using this method, in any protocol of undersized bone drilling, and perforations with unthreaded holes, applied regularly in bone implants. The equation to determine the ST for BKS is:

$$ST_{BKS} = MIT_{BKS} \tag{13}$$

The ST will be a non-absolute value but proportional to the bone densities applied. The higher the MIT the higher the MRT, but due to the properties of BKS the measured difference between MIT and MRT remains proportional and predictable. In μs when a F_{SF} is applied and eventually the object begins to move this is defined as the μs, distinct from the μ_k. Mathematically it can be represented by an equation between the MRT for BKS (MRT_{BKS}) that is equal to F_{SF}, the F required to start moving the implant (MRT), divided by the $N + F_d$ (equation 12).

The F (MRT_{BKS} or F_{SF}) required to start moving the BKS implant divided by the N is equal to the μs of the BKS into the bone. For the BKS, the *m* includes the material collected inside, which adds to its total weight. A *D* increases constant of the material inside the BKS of 3.45 [8] has been determined for the four bone densities classified and found in clinical practice. Therefore, the μs of the BKS will always be greater than that of the conventional implant screw, considering this factor and the cohesiveness of the materials (bone to bone contact).

Applying equation (14) with the experimental results obtaining the MRT_{BKS} that is equal to F_{SF} precisely determine the μs using equations (14), and (15), correlated it in different bone densities. Measuring the MIT_{BKS} and applying its correlation with μs, we can predict the amount of force (F_{SF}) or ST (ST_{BKS}) that the mechanical primary stability will support to avoid micromotions and lead to secondary stability promoting osseointegration as seen:

$$ST_{BKS} = MIT_{BKS} - (\mu_S mg) \quad (14)$$

Knowing μs and mg we can determine F_{SF}, that is equals to MRT_{BKS}. Without applying MRT_{BKS} into the BKS implant, the ST_{BKS} proposed can be mathematically determined with precision and safety, without compromising osseointegration, allowing to have improved data collection, precise adjustments on the surgical protocols planning, and controlling the osseointegration predictable results based on mechanical primary stability. A new measure of volumetric coefficient of friction (μV) when there is full contact between the walls of a volume of material that is inserted into another material, with one of the surfaces being subjected to the insertion force was determined.

2.2 Innovative simple machine BKS

The BKS is a mechanism that converts the movement of rotation into linear movement, *M* into compression by increasing the density of the *m* on which it acts decreasing its original *V* under measured conditions. The BKS material must be more resistant than the material on which it will be applied, making it possible to drilling it. To do this, it makes the collected *m* smaller than the original by cutting and breaking its original structure, forming granular solids, moving them like fluids into the internal *V* of the BKS due to the insertion *M* applied, increasing μ between these materials. This is an innovative SM that can compact particles within its internal *V*, making the material collected denser under mechanical *P*. Experimental studies have shown that the BKS modifies its original surface, incorporating inside its *V* the same material on which it's applied, standardizing inner's *V* measurement under given precise conditions. With the introduction of this new SM, we expand the possibility to create and develop new mechanical and biomechanical devices applying the MA determined in this work [6-11].

2.2.1 Multiple applications

Bone drilling is an ancient medical procedure, yet the penetration of a sharp tool into bone tissue remains a clinical and surgical challenge, with many pertinent questions still unanswered. As a manual procedure, drilling requires a high degree of dexterity and extensive training due to the difficulties caused by vibration and the risk of drill bit breakage during perforation [64]. In addition to material removal, drilling causes damage to the bone tissue. This damage can be broadly classified as mechanical and thermal. Improvements are constantly being made and new methods need to be defined to analyse and minimise the damage. Bone is considered a hard biological material, but excessive force from a cutting tool can physically damage bone. This can result in cracks, surface roughness and volume changes which can lead to post-operative complications [65-67].

In addition, the drilling action can produce different surface finishes on the bone tissue depending on the drill bit geometry and cutting parameters. Research shows that surface roughness affects the mechanical properties of bone and bone healing [68, 69]. Although V removal is a necessary part of the drilling process, other secondary effects are also detrimental. Another important factor in these procedures is that the drilling is carried out with handheld drills, which means that the drilling F and the feed rate of the bone drill are controlled manually by the surgeon. The drilling F felt by the surgeon is therefore personal and dependent on the feed rate of the tool, the quality of the bone and the type of cutting tool. In order to improve the drilling process, it is essential to develop methods for predicting drilling forces and correlating them with mechanical damage.

The use of uncontrolled forces can result in drill breakthrough, drill breakage, excessive heat generation and mechanical damage to the bone, which can cause irreversible damage to surrounding tissues and promote crack formation that may lead to prosthesis or bone failure [67, 70-73]. A review of drill bit geometry studies has shown a strong relationship between geometry type and bone drilling forces [74-76], observing that the smaller tip angles produced lower forces but also increased unwanted drill breakthrough. The twist drills with larger (fast) helix angles produced lower forces, more effective chip removal, and may cause breakthrough increasing bone trauma [76]. Regardless of the type of bone drilled, the parameters chosen also to play a key role in determining the overall success achieved. The main parameters reported in the literature fall into two categories, drill bit specifications and drilling parameters. It's worth noting that these parameters did not influence drilling efficiency by themselves, they are related [77]. It is generally accepted that the applied force should not exceed the safe material thermomechanical limit [78].

The new SM BKS can be used as a drill to simultaneously drill and tap the recipient bed and holds the bone *V* to be removed internally. The size of the BKS and the ratio of its internal *V* determine the drilling capacity of its use as a drill. The same procedure used as a drill can also be used to collect the volume of material drilled from the BKS, such as bone, and transplant it to another site [6-11]. It can also be used as a modified screw to obtain a higher *M* in precise conditions according to the material used, mainly in cases where the material to be drilled and screwed does not have the adequate strength for the required fixation like low density bones [6-11].

Thanks to the precise measurements obtained in the design of its geometry and the accurate confection by additive manufacturing (3D print), it is possible to measure the density of the material collected and by the proportion established in the materials studied in experimental research. With the BKS it is possible to determine by the applied *M* the beginning of material compaction (kinetic torque increase during insertion) and the moment of self-locking before material or BKS breakage occurs. The desired depth can be determined by the precise geometry of the BKS and its internal *V* ratio when drilling the desired material to be applied.

Because it is an innovative, SM, it enables the understanding of new mechanical properties through the application of physics, mathematics, and engineering, and opens new possibilities for applications in chemistry and biology research.

❖ *Combined mechanical advantages*

The innovative BKS MA's (MA_{BKS}) combines the MA of the screw, which are the inclined spiral plane (*MA1*) and the wheel and axle (*MA2*), adding the compaction of material in its inner *V* under mechanical *P* (*MA3*) through the resistance movement of the material being drained by double cutting grooves like a drill, densifying the material in which it is applied. The ability to in the same movement of simultaneous insertion and screwing create *P* in its inner *V* determines a new MA and therefore becomes an innovative SM as seen equation:

$$MA_{BKS} = MA_1 MA_2 MA_3 \tag{18}$$

Experimental studies in synthetic bones were conducted to demonstrate these properties, pointing out the benefits and disadvantages of the new BKS [79]. The smaller granules the chips created, the greater the efficiency of the BKS.

❖ *Increased Coefficient of friction*

Due to the innovative properties of the BKS to collect and densify the material where it is applied within its internal *V*, this material becomes part of the total *V* of the BKS, incorporating its properties, making it possible to have cohesion between the BKS and the applied material, such as bone. In addition, due to the increase in the *M* required for insertion and self-locking of the BKS, an increase in the μ between the materials has been noted [51], without an increase in the *P* on the sidewalls due to a smaller predrilling, the protocol normally used in traditional bone drilling operations.

The increase in the μ present in the BKS does not increase the lateral pressure in the bone due to the metal implant material, but due to the condensation and compaction of the material in its internal *V*, which is desired to obtain mechanical stability (primary) and long-term osseointegration.

2.2.2 Increased material density

The new SM BKS studies [7, 8] observed that at all five different synthetic bones densities the bone inside the BKS are 3.45 times denser. Even after a pilot drill in cases where a guide hole or multistep drilling is needed, the increased ratio of the material collected is equal to 2.7 times inside and around the BKS.

With BKS, it is possible to directly access the bone mass density (BMD) [8] in cases where more reliable data are needed, during surgery treatments in patients with osteopenia to help confirm the diagnosis and improve treatment, and when the clinical findings do not match the imaging tests by dual energy X-ray absorptiometry (DEXA), becoming a powerful tool in diagnosis and a tool for improving the treatment of natural bone conditions, and different types of bone disease.

❖ *Densimeter*

The characteristics and properties of the BKS, when cutting, perforating, and collecting the material applied, make it possible to homogenise the *V* inside, compacting the particles of this material by rotating them along their longitudinal axis [8]. This allows the absolute volumetric density of this area to be determined within the total *V* compacted, even in the case of composite materials or materials with differing densities. As the BKS has precise measurements of the compacted *V* inside, it is possible to use a simple equation to determine the exact density of the materials tested [8].

❖ *Measure unit for volumetric density*

Since the BKS can be manufactured with micrometric precision using additive manufacturing (3D printing), the geometry of its internal *V* can be determined in advance according to the needs of its application. This allows us to standardise the measurement of the internal *V* and even establish a measurement standard to be used in materials where it's necessary to determine the density or use the same partial measurement to approximate that of the total *V* of the measured body.

2.2.3 Bone tissue

Bone is a dynamic organ, changing throughout life from embryologic formation until adulthood remodeling (25% of trabecular bone and 3% of cortical bone are removed and replaced every year) [80]. Composed by osseous tissue (mineralized connective tissue) aggregating cells and calcified extracellular matrix. Bone is a complex anisotropic porous viscoelastic composite that is also non-homogenous both in material properties as well as geometry [81].

The extracellular matrix (ECM) composition is organic and inorganic, (mostly collagen fibers, mucopolysaccharides and non-collagen proteins) giving tensile strength to the bone, and inorganic calcified minerals (calcium and Phosphorus) in a form of carbon-hydroxyapatite (hardness of the bone) respectively [82, 83]. Other minerals in the bone (magnesium, fluoride, and manganese) play smaller roles in strengthening or forming ECM.

Bone cells are osteoprogenitor, osteocyte, osteoblast, and osteoclast. Periosteum is a dense connective tissue surrounding the entirety of the bone's outer surface except where articular cartilage is located [84]. It is attached to the bone by specific fibers (Sharpey's) protecting (fibrous layer) and promoting bone grow (cellular layer) [85, 86]. Endosteum is a thin membrane of cells (osteoblast, osteoclast, and osteogenic cell) and small amount of connective tissue lining medullary cavity and trabeculae bone.

Bone marrow will be held within bone tissue found in hollow spaces of the bone presenting two major types, red marrow, and yellow marrow. Red marrow is hemopoietic tissue (blood elements are formed) and yellow marrow is a network of connective tissue that supports a numerous blood vessels and cells (mostly adipocytes) [82-86]. Almost the entirety of the skeleton system has an extremely robust neurovasculature supply (arteries, veins, and nerves) except for cartilage.

The bone formation starts around 6th week of embryonic development in utero, composed of mesenchymal cells (connective tissue) following one or two patterns of ossification, intramembranous ossification (IO) and endochondral ossification (EO) [87]. The first occurs within the membrane of mesenchymal "skeleton" cells and the second within the cartilage. Ossification occurs in initial formation of bone, during juvenile and adult grow, and when remodeling and bone repair. Osteoblasts will lay down the organic material at the ECM which will initiate calcification process within ossification for bone tissue hardening [81-83].

In IO the bone directly replaces the mesenchymal "skeleton". In the EO, mesenchymal cells will be replaced by a hyalin cartilage model first and eventually will be replaced by bone [83, 87]. A minority of bones forms through IO initially, including flat bones of the skull, most of facial bones, mandible, and medial part of clavicle. IO is also important role in bone remodeling (repair, widening and thickening) throughout life.

Most bone formation occurs initially by EO and this process stops with skeletal maturity. In the cartilage model ossification development (under more direct genetic control), chemical messages will cause the mesenchymal cells to crowd together and form the general shape of the future bone. The cells will differentiate into chondroblasts (hyaline cartilage). This cartilage will grow interstitial (cartilage grow within, in length) and appositional (cartilage and bone growth of the outer surface, in width) [83, 87].

Appositional growth once initiated only occurs at the bone surface, deep at the periosteum. The periosteum osteoblasts begin to secrete the organic materials at the bone ECM initiating calcification surrounding itself by concentric bone tissue (Lamellae), becoming an osteocyte forming a few or numerous osteons [85, 88]. Moreover, osteoblast will deposit new circumferential lamellae surrounding the entirety of the outer bone. This process will maintain if the stimulus who initiate it continues. To keep the balance of the bone structure and function, osteoclasts from the inner surface (endosteum) begins to compensate the compact bone being formed by breaking down the inner surface, balancing the spongy bone and medullary cavity size, remodeling.

In the primary ossification center [89] development bone will begin to replace the cartilage model in the diaphyseal region then in the epiphyseal region, leaving an epiphyseal plate of cartilage (metaphyseal region) to allow bone grow in length, initiating the secondary ossification center development. After that, the cartilage model will be fully replaced by bone except in the end or articular region, as seeing in figure 5:

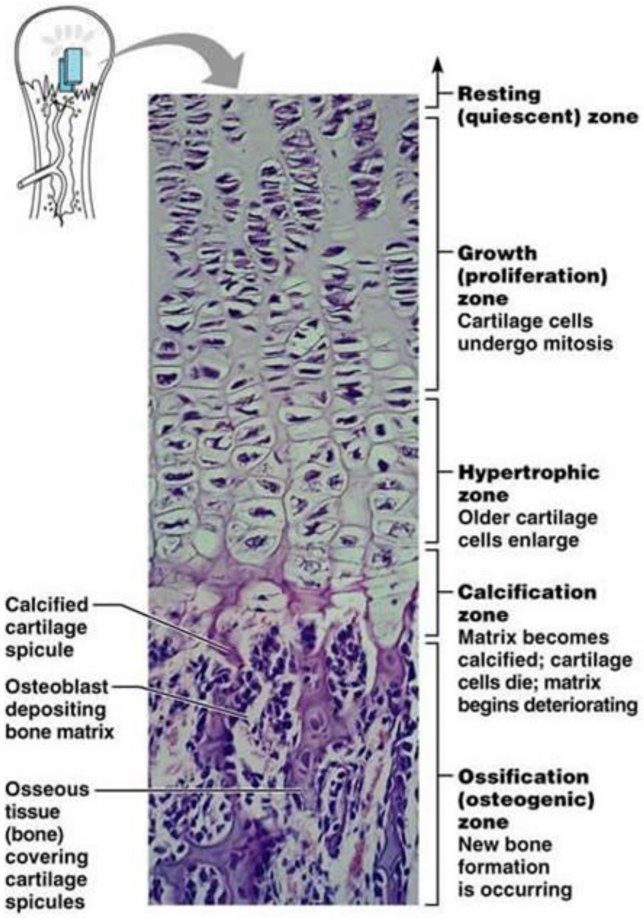

Figure 5. EO in a microscopical description in an epiphyseal plate of the bone [89].

The facial bones, flat bones of the skull, and medial part of clavicle, are the only ones that initially are formed by intramembranous ossification and are unique in their continuous remodeling throughout life by the same kind of ossification, differently of all other bones in the skeletal system that are formed by osteochondral ossification and remodeled by IO.

The critical period for face and palate development is between week 6 to 12. Development of the face begins by week four of development from three main structures: the frontonasal process, maxillary process, and mandibular process. The frontonasal process gives rise to the medial and lateral nasal processes with the two medial processes merging in the midline forming the intermaxillary segment, which gives rise to the philtrum of the lip. The fusion of the maxillary processes with the intermaxillary segment on both sides completes the formation of the upper lip and the mandibular processes gives rise to the lower jaw [90-92].

By the 7^{th} week of human embryonic development most of the facial structures can be observed and in the next 5 weeks of development the mesenchymal skeleton of the face is directly replaced by bone and there is an overall increase in shape and size of the different structures of the face [93, 94]. From childhood to adulthood the face continues to develop through further growth and remodeling.

There are four major bone cells. Osteogenic cells (osteoprogenitor stem cells) derived from mesenchyme, only one capable of cell division. Once these cells are ready to begin to secrete ECM, they will become osteoblasts. They are in the deep side of the periosteum, endosteum, and neurovascular canals [81, 82].

Osteoblasts are the bone-building cells, synthesize and secrete organic components called osteoid (collagen fibers, chondroitin sulfate and osteocalcin) and initiates calcification transitioning to osteocytes [83].

Osteocytes have the main function maintain daily metabolism of the bone, passing nutrients, chemicals signals, metabolic waste to the nearest blood vessel to disposal. Recent studies shown that they can also work as strain sensors acting like a mechano-sensor, adapting responses to mechanical loading on bone [81-83].

Osteoclasts are derived from the fusion of numerous monocytes (type of white blood cell). It has a distinct ruffled border which will be always bone facing. With specific signals, start releasing lysosomal enzymes and acids to break down extracellular matrix of bone, causing resorption of the bone tissue. Also helps to increase blood calcium when its needed [82].

ECM is the material that is going to be located between widely separated cells in the bone tissue. Composed by water (15%), organic material (30% collagen fibers) and inorganic material (55% crystallized mineral salts in a form of carbon hydroxyapatite) [95].

There are two major structural types of bone tissue, compact bone (cortical, dense), and spongy bone (trabecular, cancellous). Compact bone is denser, presents strength in bending, and forms external layer of all bones and bulk of diaphysis. Spongy bone forms the bulk of regular bones, majority of short, flat, irregular bones and within articular epiphyses. Contains larger spaces and present stronger strength in compression [81-86].

Microscopically compact bone is organized by repeating structures named osteons (haversian systems). They are aligned in the same direction and parallel to the diaphyseal length, along of stress lines, resisting bending forces. These lines of stresses are dynamic and will change throughout life as seen in figure 6:

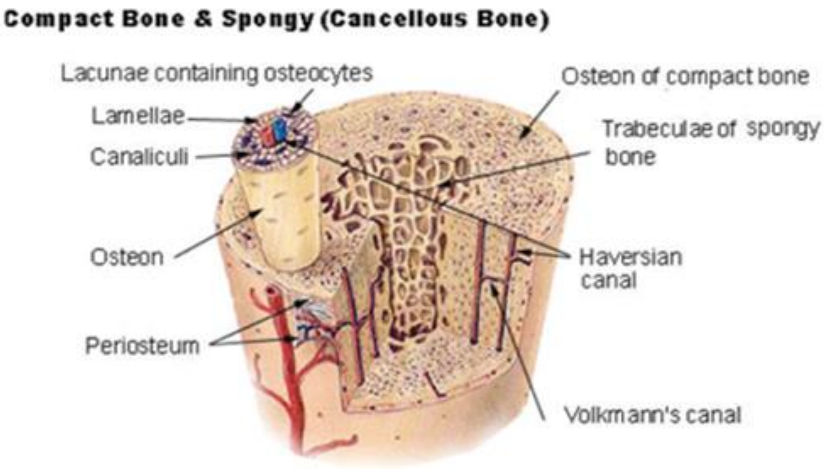

Figure 6. Cortical (compact) and trabecular (cancellous) bone and characteristics [88].

Each individual osteon consists of concentric lamellae that are circular plates of mineralized (calcified) bone EMC, and this will increase in diameter the further you get away from the central canal [96]. The small spaces between concentric lamellae are named lacunae and in situ within are the osteocytes (mature bone cells). Several extensions of the osteocyte cell body are situated in canaliculi (small channels), also known as extensions of the lacunae, allowing communication and exchanges between them with other osteocytes, also providing nutrients and oxygen for the osteocytes and waste removal [97]. Interstitial lamellae are fragments of partially destroyed (by bone growth or bone remodeling) osteons, observed in areas in between neighboring osteons with the same structures but less organized.

Neurovasculature from the periosteum get inside of the bone through transverse perforating canals (Volkmann's) to the central canal of the osteon and even to the large medullary cavity [96, 97].

Circumferential lamellae (important in appositional growth) surround the entirety outer space (external) of the bone, attached to periosteum via perforating sharpey's fibers and the inner space of the bone, surrounding the endosteum region. The sharpey's fibers are important because muscle tendons will often interline in some areas in bone and periosteum to form close connection to achieve the muscle contractions lead to bone movement [98].

Spongy bone has the same structures described for the compact bone, but they are not arranged in osteons, containing same components. They have very distinct trabeculae (small beams of bone) separated by macroscopic spaces filled by red bone marrow or yellow bone marrow. The trabeculae are organized on the long lines of stress and help to reduce the weight of the bone [85, 86].

Bone functions are, support serving as structural framework providing attachment for tendons of skeleton muscle, protection (internal organs), assistance in movement, mineral storage, and release (primarily calcium), blood cell production (red blood cells, white blood cells and platelets), and triglyceride storage (adipose cells) [81-86].

During the timeframe of birth to adolescence more bone tissue is produced than it is lost through natural processes of bone formation or remodeling. In younger adults (20 years old) the rate of bone resorption and apposition are balanced. However, with increasing age the rates change due numerous factors, increasing of level of sexual hormones, and osteoclast activity can outpace osteoblasts. These leads to two main effects on osseous tissues on aging adults,' loss of bone mass (demineralization on women starts at 30 years old) and brittleness (slowing production of collagen) [99, 100].

Osteopenia is when you have low bone mass compared a healthy bone mass increasing the risk of osteoporosis (overly poor bone) occurring bone resorption at higher pace than bone deposition with depletion of calcium of the body [101]. With osteoporosis abnormal findings which includes fewer trabeculae in the spongy bone and thinning of cortical bone as well the widening of haversian canals. These bone changes increase the risk of fracture (fragility or pathologic fractures).

Factors that accelerate bone mass loss and increase the risk of osteoporosis are low estrogen (like after menopause) and low serum calcium. Others key factors are alcohol consumption, smoking, drugs (glucocorticoids, heparin, and L-thyroxine), physical inactivity and diseases like diabetes mellitus [101].

With aging bone mass loss is a natural process to happen that you can slow down in terms of aging effects on the skeletal system. One of the main ways is through weight-bearing even with small weights, anything done to have muscles contracting affecting and altering the strength due to the mechanical stress in this region. Any time you have a contraction of muscle that is going to pull on the bone and affect the bone, it increases the osteoblastic activity keeping the relationship with osteoclasts more even, incrementing the ECM levels, allowing mineral salts calcify and have the structural strong integrity of the bone [102].

BMD is regulated by both mechanical and biochemical stimuli. Like muscles, bones add mass when they are loaded (physical activity or implants) and will lose mass if they are not (immobilization or time spent at low or zero gravity) [88]. It will change throughout life based on the strain it experiences by mechanical stresses caused by pulling skeletal muscles, fractures, osteotomies, and gravity.

Magnitudes of strain collected by bone from muscular contraction and gravitational load structure the fundamental thesis and most dominant element of bone adaptation [88, 102]. The mechanostat theory is a qualitatively described dose-response sequence of strain magnitudes that can promote resorptive, regenerative or formative feedback into the bone, [61, 103, 104] meeting mechanical requirements, and maintaining bone mass in a minimum effective strain (MES). If the strain magnitude remains under the MES point, bone resorption occurs, and if the strain magnitude outpaces the MES threshold, bone formation occurs [105].

In fractures, bone callus formation can be stimulated, and healing is accelerated by appropriate relative motion between fracture fragments [106]. Authors have suggested that relatively stable secondary fracture healing can be achieved by the maintenance of 2%-10% strain between fracture ends [107, 108]. On the other hand, too much or too little stress interferes with this process, preventing or delaying the union [109, 110]. This hypothesis has been supported by both experimental and clinical studies [111, 112, 113].

❖ *Bone growth and development*

Growth and development can be related as two sides of the same object, even being distinct processes, because they work in harmony towards the same goal. Bone growth is related to an increase in size or number; an increase in the size of cells is called hypertrophy; an increase the number of cells is called hyperplasia, associated with height, weight, length, and width (quantitative numbers). Development is an increase in complexity or specialization of functions being more physiological or behavioral (qualitative) [114-119]. To analyze bone growth and development, the skull and specially the face, the most complex skeletal system in the body due to its inherent multiple functions (protection of the brain, visual system, olfactory system, upper respiratory system, upper digestive system, and speech) will be described.

Development follows three basic laws, there's a pattern, predictable changes in how a body will grow over time, general timing, and variability. The cephalocaudal growth gradient is one pattern. Body parts closer to the cranium, growth faster early on, while body parts further from the cranium growth more later. In a 2 months fetus, the head comprises 50% of its body with total length decreasing after 1 to 2 months in utero to 30%. At birth, the head is 25% and as an adult the head is about 12% of the total human body height [120-123]. The same can be said for the upper limbs (growth first) versus the lower limbs, and the maxilla and mandible. The maxilla will fully mature earlier than the mandible because is closer to the cranium.

One visual depiction of a typical growth of pattern and timing is the Scammon's growth curves as seeing in figure 7. These curves show age on the x-axis in years, and tissue size on the y-axis. From top to bottom we have the lymphoid growth curve (immune tissues), neural growth curve (brain), maxilla, mandible, general body tissues (bones, muscles), and genital tissues [124].

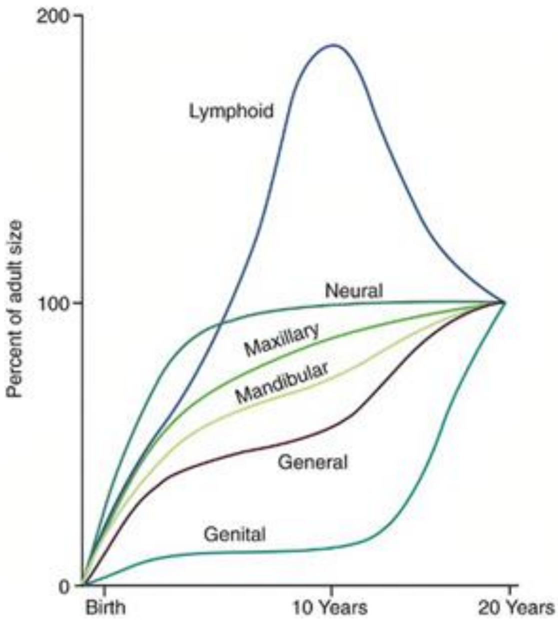

Figure 7. Scammon's growth curves [124].

Each of these has a unique pattern to it, and neural tissues including the brain growth rapidly after birth, presents the steepest of these curves and then reach near adult size by the age 6 or 7 and levels out. Lymphoid tissues also growth rapidly reaching twice their adult sizes by age 10 and then they shrink during the pubertal growth spurt to reach their final adult size [125]. The general body tissues, including majority of the bones, grow rapidly after birth slowing down in childhood and increasing during the period growth spurt.

The maxilla follows a bit closer to the neural growth curve because is closer to the brain and the mandible follows more closer to the general growth curve. The lymphoid and genital curves after age 10 act opposite to each other like mirror images because as the concentration of sex hormones (estrogen and testosterone) increases, they drive the growth spurt, and this inhibits further growth of lymphoid tissue [126].

Growing timing can be determined by chronologic age, dental age, skeletal age, and biologic age. The skeletal age can be measured by two methods: CVM staging which is the cervical vertebral maturation, where you take a cephalometric x-ray and analyses the shape of the cervical vertebrae; and hand wrist method [127]. Biologic development is based on certain markers of maturation like menarche which occurs just after the peak velocity of growth and secondary markers like facial hair, these being the best indicators of an individual’s growth status and maturity.

Growth happens through growth sites, any area where growth is occurring, and growth centers, a site of growth with the ability to control their own growth independently and control other growth sites. As far as craniofacial structures go, most of the growth happens in growth sites, the only true growth center is a synchondrosis (primary cartilaginous joint, where hyaline cartilage completely fuse two bones); sutures surfaces, and the mandibular condyle are all growth sites [120-123].

There are three different mechanisms that have been proposed for growth and no one theory explains all craniofacial growth control, they are consider working in concert. Harry Sicher [128] proposed the suture theory where direct genetic control determines how bone is going to grow and bone will determine its own growth, having sutures acting as growth centers, that push bone structures apart. James Scott [129, 130] described the cartilage theory, saying that epigenetic birth control has cartilage pushing and pulling bone structures apart acting as growth centers and bone simply follows along.

Melvin Moss [131] produced the functional matrix theory governed by environmental growth control (chewing, speaking, and other functions) caused the nasal and oral cavities to growth, which serve as the primary determinants of growth for the maxilla and the mandible. So here the soft tissue matrix determines growth and bone and cartilage follow that pattern. The five main regions of the cranium and face are the cranial vault, cranial base, nasomaxillary complex, mandible, and two dentoalveolar processes supporting the teeth [132].

The cranial vault is the top part of the skull that encases the brain. At birth, the cranial bones are widely separated by this loose connective tissue called fontanelles. These wide spaces enable delivery of the baby through the birth canal. The bone tissue laid down along the membranes of these bones, shrinking down these spaces at which point they are called sutures, thinner spaces that separate the cranial bones in childhood, adolescence, and they eventually fuse later in adult life [133].

As the brain growth, these cranial bones are being pushed apart, so to keep the space from opening wider and wider, new bone is being laid down along these membranes (Intramembranous Ossification) growing in length, as seeing in figure 8 [134-136]:

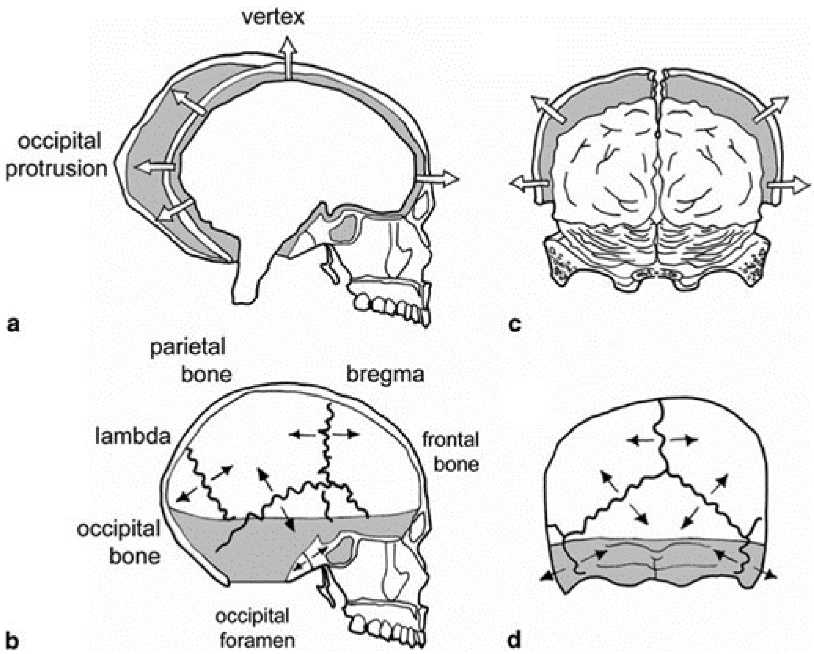

Figure 8. Illustration of a growth model of neurobasicranium complex (NBC). Intra-sutural and synchondral growth reacts to tension in the basi cranium and below the circum-cranial reverse line by drift, areas shaded gray. [137].

Outside of the skull we have direct apposition of bone in addition to what is happening at the sutures, new bone is being laid down at the outer surface (periosteum) of the bone and being resorbed from the inner surface (endosteum), growing in width [138, 139].

The cranial base consists of the ethmoid, sphenoid, and occipital bones at the base of the skull. These three bones are initially cartilage part of the chondro-cranium in the fetus, and they later transform into bone. Three bands of cartilage that stick around that bones are important growth centers called synchondrosis. Each synchondrosis acts like a two-sided epiphyseal plate, splitting these bones apart from each other, which continues to grow and increases the length of this structure (EO) [140].

In the maxilla, growth occurs at the sutures posterior and superior to the nasomaxillary complex and its connections to the cranial vault and the cranial base. There is appositional bone growth at the sutures because soft tissue, that is the nasal and oral cavities which are expanding, are pulling this maxilla downward and forward away from the cranial base. Simultaneously there is also surface remodeling, which includes resorption of bone anteriorly and apposition of bone inferiorly at the palate and at the alveolar ridges as the teeth erupt down. There's also additional bone at the tuberosity posteriorly to make room for the second and third molars. The ultimate result of all of this is a downward and forward translation of the maxilla away from the cranial base (figure 9) [141].

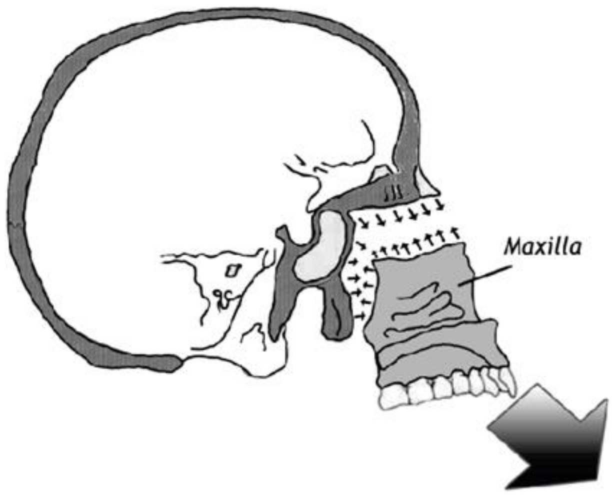

Figure 9. Growth of the soft tissues moves the maxilla downward and forward, creating space at the superior and posterior region, allowing bone formation on both sides of the sutures [137].

The mandible has interesting steps, it develops in the embryo just lateral to the cartilage of the first pharyngeal arch which is called Meckel's cartilage [142]. But this is not endochondral growth, so Meckel's cartilage is not being replaced by bone. The mandible just happens to be created by IO right next to it. Meckel's cartilage will disintegrate and contribute to the malleus, incus (ossicles of the inner ear) and sphenomandibular ligament.

The mandibular condylar cartilage which develops independently and later fuses with the developing mandibular ramus at about four months in utero. The cone shape cartilage is replaced by bone and its upper end will persist as a site for growth [143]. This cartilage proliferates and is transformed into bone as the mandible grows downward and forward again away from the cranial base but in a different mode or mechanism comparing with the maxilla. This creates a gap between the two jaws into the teeth can erupt.

In addition to this EO occurring at the condylar cartilage, there's outer surface apposition which occurs along the posterior surface of the ramus, at the coronoid process as well as to chin, balancing the condyle growth [142, 143]. Surface resorption occurs along the anterior surface of the ramus which makes room for the second and third molars to erupt, which is opposite what was happening at the maxilla where we have bone apposition to give room for these teeth in the upper jaw. Alveolar bone growth vertically as the teeth erupt into position as seeing in figure 10 [144]. In the mandible there is a mix of EO and IO.

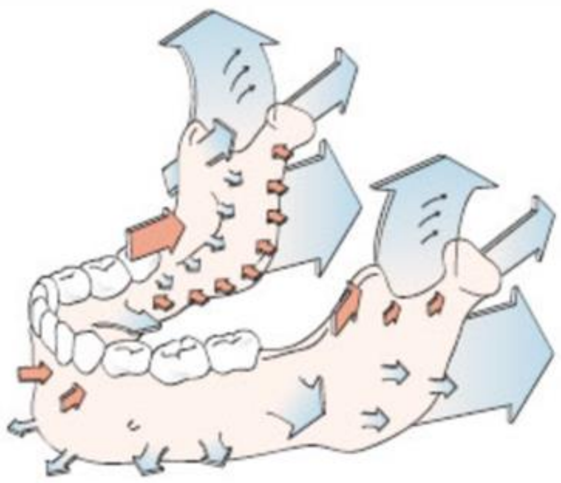

Figure 10. The mandible surface remodeling during growth. Blue arrows indicate sites of resorption and red arrows indicate sites of deposition [144].

As the mandible grows it can stay at the same angle or it can tend to rotate because it has this axis at the condyle, so it can either open increasing the angle with the base of the cranium or closing, decreasing the same angle.

An average growth rotation is where the condylar growth is equal to the amount of molar eruption, so the mandible truly just grows downward and forward at roughly the same orientation [142-144]. If we have closer rotation (counterclockwise growth) that means that the growth of the condyle is exceeding the amount of molar eruption, leading to a shorter lower anterior face height and a skeletal deep bite tendency.

The opposite is opening rotation or clockwise growth, this is where the condylar growth is less than the amount of molar eruption, leading to a long anterior face height and skeletal anterior open bite tendency [143]. There are three planes of growth for skull and facial bones, width, length, and height or more commonly referred to as transverse, anteroposterior (AP) and vertical, respectively. Generally transverse dimension stops growing first at around age 10 to 12 years old, then AP at 14 to 16 years old, and finally vertical at 18 to 20 years old or even further on into later adult life [137, 140, 145].

❖ *Bone repair*

Bone repairs start when you have loss of bone continuity by trauma that can happens by accident (motorized vehicles, sports, and falls), surgical procedures (osteotomies, bone distraction, bone implants, bone drilling, and bone fixation devices), and clinical procedures like teeth movement in the alveolar bone in orthodontics [146-148].

With the initial stimuli, the bone repair immediately begins, having four major steps in a typical process as seen in figure 11. The first stage is formation of hematoma, by the disruption of blood vessels, which will be completed after 6 hours.

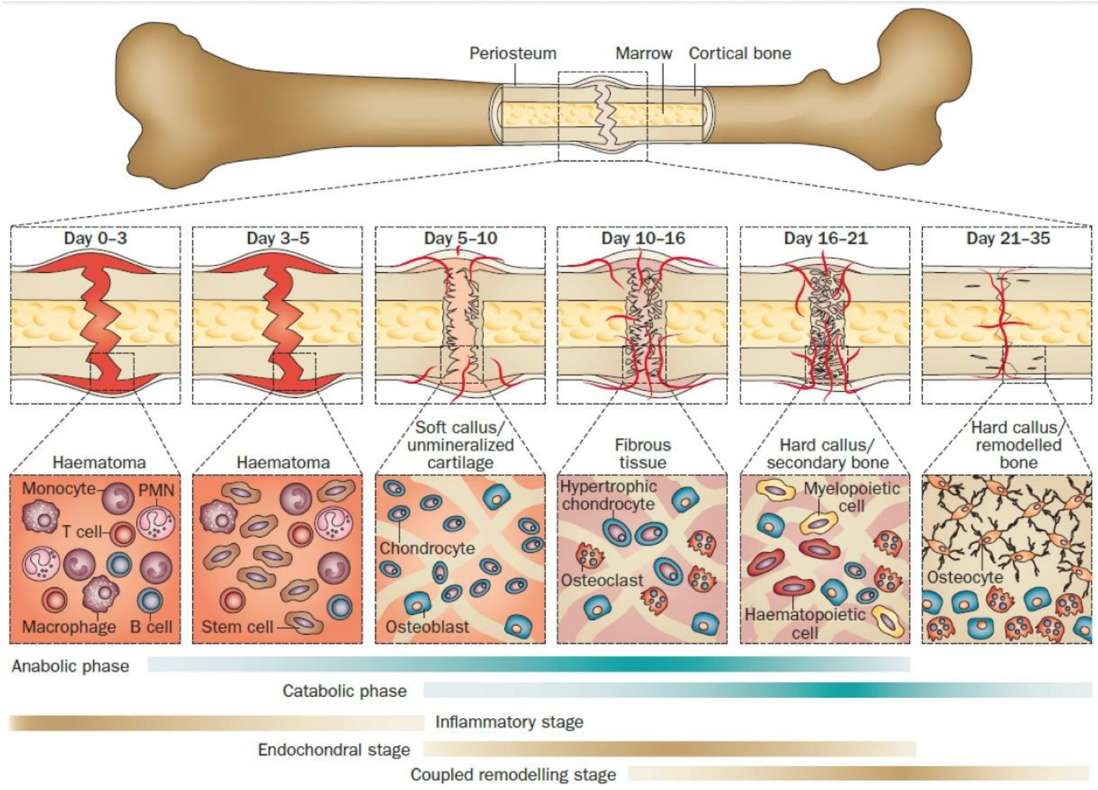

Figure 11. Illustration of a typical fracture healing process, biological events, and cellular activities at distinct phases [149].

Cells from the periosteum region (fibroblasts) will move into the repair site creating the fibrocartilaginous callus (soft callus) completing the second stage of the process after 2 weeks. In the third stage, fibrocartilaginous callus will be replaced by a relatively large bony callus, which will be remodeled over time to repair the bone as close as possible to the original shape and size if all factors of the process are under normal circumstances [146-150].

Factors that affect bone growth and repair are varying levels of minerals (calcium, phosphorous, magnesium, fluoride, and manganese); vitamin C (important in collagen synthesis); vitamin D (calcitriol increases absorption of calcium to the blood); hormone calcitonin inhibits bone resorption and parathyroid hormone promotes bone resorption; sex hormones promotes bone length growth and bone remodeling; human growth hormone in general growth of all body tissues; and exercises stimulates osteoblasts. Bone healing is observed to be a version of the existential events that occurs during embryonic development of the skeleton, enabling the wounded organ to by fully repaired to its pre-injury composition, structure, and function [151].

Bone healing can be divided into two categories: primary and secondary bone repair. Direct bone repair (primary) occurs when the gap between bones is less than 0.1 mm, and the borders of the bones are immobilized with inter-fragmentary strain less than 2% [152, 153]. It is hypothesized that the bone gap in this repair is filled directly by continuous ossification and subsequent haversian remodeling, like IO, without formation of fibrocartilaginous tissue and callus, as seeing in biomaterials with successful osseointegration [150]. This concept of primary bone healing is still discussed due to the shortage of histological evidence and clinical cases [154].

Indirect bone repair (secondary) occurs when the space between bones is less than twice the diameter of the injured bone, being the most usual form of bone healing [153]. Secondary bone repair occurs through IO and EO, and bone remodeling. Anabolism is activated initially expanding bone volume by assigning stem cells differentiation and retardation with chondrocyte apoptosis followed by long stage of catabolic activities reducing the callus volume [152]. With the return of normal and regular vascular flow to preinjury levels, the catabolic phase ends.

Bone remodeling is when old, brittle bone tissue is removed or resorbed and replaced by new tissue. It also occurs when reshaping bones after a fracture, osteotomy and repairing micro-cracks which form during ordinary activities specially when the bone is under stress. The surface of the bone is covered by periosteum consisted by outer fibrous layer which protects the bones and provides attachment for tendons and ligaments, and an inner cellular layer which houses progenitor stem cells. These progenitor stem cells develop into both osteoblasts secreting the bone matrix, and chondroblasts which produce cartilage [155].

In the bone marrow we find the hematopoietic stem cells (blood-making cells of the bone) which give rise to the lymphoid progenitor cells, maturing and differentiating into lymphocytes T and B cells, the main cells involved in the adaptative immunity, and the myeloid progenitor cells, which differentiate into red blood cells, platelets, and myeloblasts, progenitors of basophils, neutrophils, eosinophils, and monocytes [156]. There are several growth factors that help these cells to develop. Osteoblasts release a substance called M-CSF (macrophage colony-stimulating factor), which helps stimulate myeloid cells like monocytes.

In bone remodeling the process begins when osteoblasts sense micro cracks at their location, like when the bones are bearing weight or being fractured. They produce a substance called RANKL (receptor activator of nuclear factor κβ ligand), binding to RANK receptors on the surface of nearby monocytes inducing them to fuse together to form a multinucleated osteoclast cell. RANKL also helps the osteoclasts mature and activate starting resorption process [157].

The osteoclasts start secreting lysosomal enzymes (mostly collagenase), which digests the collagen protein in the organic matrix. This drills pit on the bone surface known as the Howship's lacunae. Osteoclasts also start producing hydrochloric acid (HCl), which dissolves hydroxyapatite into soluble calcium (Ca+2) and phosphate (PO43-) ions, and these ions get released into the bloodstream [158]. There is also a scattering of osteocytes which are trapped within the bony matrix. When these get freed up by the dissolving of bone, they get eaten up or phagocytosed by the osteoclasts.

To keep bone resorption under control, osteoblasts also secrete osteoprotegerin, which binds to RANKL and prevents it from activating RANK receptors slowing down the activation of osteoclasts. Once osteoclasts complete their functions, they commit suicide by means of apoptosis [157]. Following bone resorption, osteoblasts start secreting osteoid seam, a substance made of collagen, to fill the lacunae created by the osteoclasts. Calcium and phosphate begin to deposit on the seam, forming carbon-hydroxyapatite. As osteoblasts keep producing new bony material, many get trapped within tiny lacunae within the bone matrix and turn into osteocytes [158].

The parathyroid hormone travels to the bones and stimulates the osteoblasts to release RANKL, which triggers bone resorption. This allows calcium ions (Ca+2) to be released into the bloodstream, and that corrects the deficiency. When the blood calcium level is higher than normal, the parathyroid gland releases less parathyroid hormone to have less bone resorption. In addition, parafollicular cells in the thyroid gland produces a hormone called calcitonin. High calcitonin levels inhibit bone resorption which results in lower blood calcium levels [157]. Another factor on bone remodeling is mechanical stress. That is why bones that bear weight remodel at such a high rate, a phenomenon called Wolff's law [118].

Vitamin D stimulates intestinal absorption of calcium, which then causes calcitonin levels to increase and that inhibits bone resorption. Bone remodeling is a continuous process which bone are resorbed by osteoclasts and remade by osteoblasts. Osteoblasts release RANKL to initiate remodeling, and osteoprotegerin to help turn it off [157].

Bone remodeling engages in repairing those tiny cracks into the bones due to normal activities, and in helping bones heal after a fracture or surgical osteotomy like a drill perforation into the bone. In the table 1 we have the mechanical properties of the bone and the new device BKS (Titanium alloy Ti6Al4V, Grade 5) adopted as reference [8].

Table 1. Mechanical properties of human bone and the BKS [8]

Properties	**Cortical bone**	**Trabecular bone**	**BKS***
Density (kg/m3)	1.850	1.000	7.850
Young's modulus (GPa)	17	0.4	104
Poisson's ratio	0.3	0.3	0.3
Initial yield stress (MPa)	125	10	880
Tangent modulus (MPa)	1000	25	
Hardening parameter	0.1	0.1	
Cowper-Symonds model			
C	360.7	360.7	
P	4.605	4.605	
Failure strain	0.016	0.134	
Specific mass [kg/m³]	1640	640	
Specific heat [J/kg.K]	1640	1477	
Condutivicty [W/m.K]	0.452	0.087	

** Titanium alloy (Ti6Al4V, Grade5—UNS R56400).*

❖ *Osseointegration*

Biocompatibility is defined as the ability of a material to perform with an appropriate host response in a specific application. Biomaterials must be biochemically compatible, non-toxic, non-irritable, non-allergenic and non-carcinogenic, biomechanically compatible with surrounding tissues (elastic modulus), and a bio-adhesive contact must be established between the materials and living tissue [159].

There are two types of material to tissue interaction. The first one, used in intraocular lenses, heads and cups of joint prostheses and blood-contacting devices, is to create an inert surface not allowing the adsorption of proteins and adhesion of cells, and thus preventing activation of the immune system, blood coagulation, thrombosis, EMC deposition and other interactions between material and surrounding environments [160]. The second type of material interaction, used In bone implants and scaffolds, is more general and advanced strategy aims at creation of materials promoting attachment, migration, proliferation, differentiation, long term viability and cell functioning in a controllable manner [161].

The inflammatory response towards biomaterial implantation, as seeing in figure 12, initiate with the contact of different blood elements and the material interface. First, plasma proteins adhere to the biomaterial's surface and there is a rapid and considerable infiltration of neutrophils, followed by an infiltration of circulating monocytes. These monocytes differentiate toward proinflammatory macrophages when interacting with materials, causing a foreign body reaction that finally provokes biomaterial rejection, macrophage fusion (foreign body giant cells) and fibrosis, fostered by a T helper type 1 (Th1) response. However, biomaterial integration can be achieved by promoting pro-reparative macrophage phenotypes and tissue resident macrophages, promoting angiogenesis and integration, fostered through a Th2(T helper type 2) response [162].

The temporal variation in the acute inflammatory response, chronic inflammatory response, granulation tissue development, and foreign body response depends on the extent of injury created during implantation and the size, shape, topography, and chemical and physical properties of the biomaterial [162, 163]. The inflammatory response is a normal physiological reaction of vascularized living tissue to trauma and the invasion of foreign substance.

The foreign body response is indicated by the presence of foreign body giant cells (FBGCs) and the components of granulations tissue (macrophages, fibroblasts, and capillaries in varying amounts) [163, 164]. The final stage of the foreign body response and healing process is the development of a fibrous encapsulation. This involves two separate processes, replacement of tissue by mesenchymal cells of the same type like in osseointegration, or replacement by connective tissue that constitute the fibrous capsule. These processes are controlled by growth capacity of the cells in the tissue receiving the implant, the persistence of the tissue framework and degree of injury [165, 166].

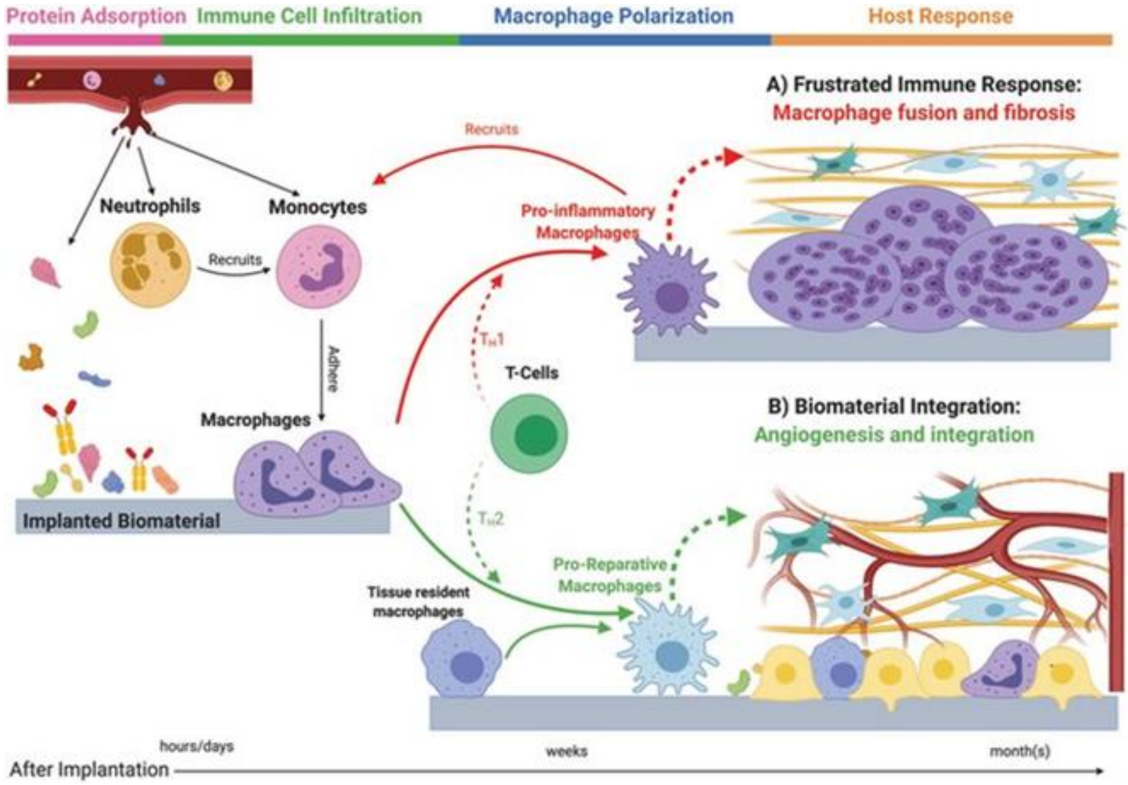

Figure 12. Illustration of a schematic diagram representing the inflammatory response that occurs after biomaterial implantation [162].

The term osseointegration derives from “osteon” which is the Greek word for bone, and the Latin word “integrate” to make whole. It refers to the process that will take place between living bone tissue and the surface of biomaterial. It is considered the most key factor in maintaining implant stability. The genesis of osseointegration as a concept was introduced by Branemark [167] first to report of bone tissue growing in what was direct contact with a metallic implant. Later in 1977, Branemark [168] coined the term osseointegration to describe this phenomenon. However, osseointegration it is more a concept than a precisely defined biological term. The idea of any type of direct bone-metal contact without intervening soft-tissue layers it is not at all accepted [63, 169, 170].

Osseointegration was, by his words at that time “a direct connection between living bone and a load-carrying endosseous implant at the light microscopic level.” American Academy of Implant Dentistry in 1986 defined osseointegration as “contact established without interposition of nonbone tissue between normal remodeled bone and an implant entailing a sustained transfer and distribution of load from the implant to and within the bone tissue." Also defined as "the apparent direct attachment or connection of osseous tissue to an inert, alloplastic material without intervening connective tissue [171-175].

The successful implant surgery is determined by the biomechanical quality of bone tissue located at a distance less than around 100 to 200 microns from the implant surface [176, 177]. This distance is an important parameter for surgical success, observed that BIC surface ratio in successful oral implants varied between 60% and 99%. BIC is correlated with biomechanical properties of the bone-implant interface, which increases during bone healing [178, 179].

The integration between bone and dental implant can occurs in diverse ways, either can be an intimate contact with gingival tissues which results in a fibro-osseointegration (pseudo ligament or peri-implant ligament) wherein connective tissue is present between the implant and bone. The second type is contact osteogenesis wherein mature bone ingrowth form around the dental implant resulting in mechanical interlocking [180].

Other related terms are adaptive osseointegration, which is osseous tissue approximating the surface of the implant without apparent soft tissue interface as seen at the light microscopic level, and biointegration, which is a direct biomechanical bone surface attachment confirmed at electron microscopic level [181].

The mechanism of osseointegration belongs to the category of direct or primary bone repair. It can be compared to direct fracture healing in which the bone fracture fragment ends become united by bone without intermediate fibrous tissue or fibrocartilage formation. Osseointegration unites bone to an implant surface, a foreign material who plays a decisive role for the achievement of microscopic contact level between them [178-182].

Blood is invariably the first tissue in contact with the implant when introduced into the bone resulting in a series of biological processes like protein deposition, coagulation, inflammation, and tissue formation. On the first day after implantation, blood clot is formed adjacent to the implant surface and neovascularization begins within 24 hours. Along with the blood clot, dead and living bone tissue, bone debris, are also present around the implant surface [11].

Therefore, the first cells to appear are erythrocytes (red blood cells) along with neutrophils and macrophages. New bone formation and calcification from the host bone onto the implant surface is observed in five to seven days. This newly formed bone fills the gap between mature bone tissue and implant, which takes about 3 to 6 weeks. At the microscopic level, the infiltrating macrophages and monocytes begin to migrate into the bone by day four and replace the blood clot that is gradually replaced by differentiating mesenchymal cells which are recruited from the bone marrow around the newly developing blood vessels. These mesenchymal cells differentiate into osteoblasts [183, 184]. After 8 to 12 weeks, the peri-implant surface interface is completely replaced by mature lamellar bone in direct contact with implant thus completing the initial phase of osseointegration. Gradually after 8 to 12 weeks after the implant surgery this newly formed bone tissue is replaced by mature bone tissue around the implant. Bone remodeling is the last stage of osseointegration which initiates in normal conditions after 12 weeks and after 6 to 12 months of increasingly high activity it slows down and continues throughout life. In the jaw bones the coronal part of the dental implants become firmly anchored within compact bone, whereas the apical segment is exposed to spongy bone and bone marrow as seen in figure 13 [183].

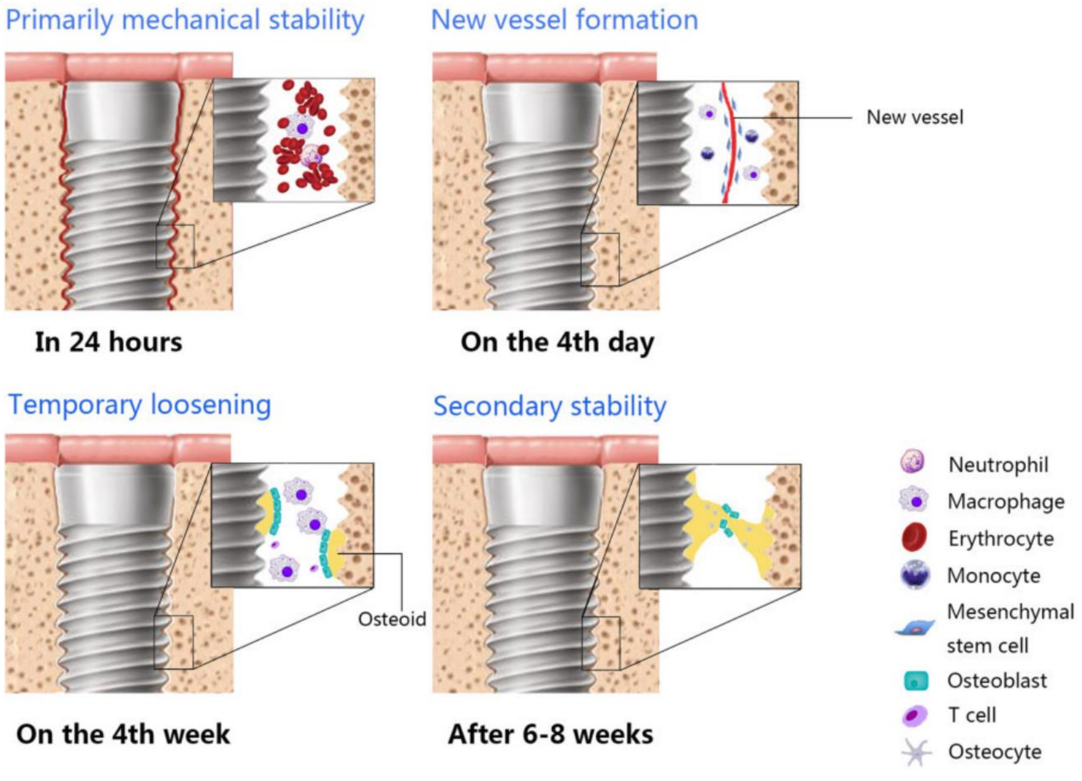

Figure 13. Illustration of a schematic diagram representing the timeline for osseointegration of dental implants with respect to changes over time [183].

Primary stability is obtained by congruency and press fitting, which leads to direct bone implant contact, with absence of mobility in the bone bed after the implant has been placed, depending on the mechanical engagement of an implant within the fresh bone socket [180, 181]. A key factor for the implant primary stability is BIC including factors such as implant size, length and diameter which can cause an increase in the BIC area, therefore increasing the mechanical stability.

During the initial stages of healing in the first week, mechanical stability (primary) decreases while biological stability (secondary) increases. Other factors which influence primary stability are implant geometry, bone density and quality, surgical protocol (osteotomy preparation), and skills of the surgeon [178-183]. Primary stability comes with the regular bone mechanical properties at the moment of the implant surgical procedure, and secondary stability appears with the new bone formation and remodeling.

Implant related factors that enhance osseointegration are design, press fit implant, chemical composition, surface topography that can be made by electropolishing, mechanical polishing, blasting and coatings by additive processes like hydroxyapatite, titanium plasma spray surfaces, ion depositions [184, 185]. The factors related to the state of the bone host bed that increase osseointegration are minimal surgical trauma preserving vascularity and cellularity on the implant bed site and mechanical stability (primary), no micromovement. Factors that can inhibit osseointegration are inappropriate porosity, uncontrolled surgical trauma, bone defects, osteoporosis, smoking, and rheumatoid arthritis. Excessive implant mobility affects the secondary stability leading to implant failure.

Adjunctive therapies like bone grafting, osteogenic coatings, biophysical stimulation, systemic administration of ibandronate and human parathyroid hormone enhance osseointegration due to their indirect effect on the formation of bone. Irradiation, pharmacological agents like cyclosporine A, cisplatin, warfarin are therapies that inhibit osseointegration [186, 187].

Available bone is particularly important in implant dentistry and describes the external architecture or volume of the bone bed site considered for implants. Bone *D* and its relation to oral implantology existed for more than 35 years [188]. In 1985, Lekholm and Zarb listed bone qualities in the anterior regions of maxilla and mandible which were, quality 1 composed of homogenous compact bone, quality 2 with a thick layer of compact bone surrounding a core of dense spongy bone, quality 3 a thin layer of cortical bone surrounding a dense spongy bone of favorable strength, and quality 4 a thin layer of cortical bone surrounding a core of low-density spongy bone. Irrespective of the distinct bone qualities, all bone was treated with the same implant design and standard surgical and prosthetic protocol [189, 190]. Following this protocol was observed a 10% difference in implant success between quality 2 and 3 bone, and 23% lower success in the poorest bone *D* quality 4.

In 1988 Misch [191-192] proposed four bone *D* groups independent of the regions of the jaws based on macroscopic cortical and spongy bone characteristics. It is described as D1, D2, D3 and D4, located in the edentulous areas of the maxilla and mandible, as seen in figure 14.

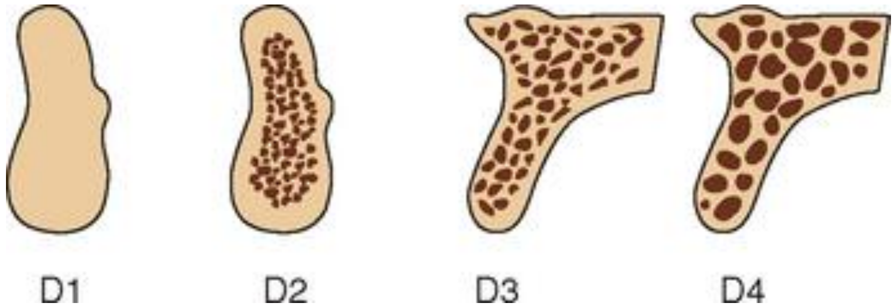

Figure 14. Illustration of a schematic diagram representing Misch bone *D* groups [192].

D1 bone is primarily dense cortical bone, and it is typical anatomical location is in the anterior region of the mandible. D2 bone presents dense to porous cortical bone on the crest, and within, coarse spongy bone, and it is found in the anterior and posterior mandible, and anterior maxilla. D3 bone types have a thinner porous cortical crest and fine spongy bone in the region next to the implant, and it is found in the anterior and posterior maxilla, and posterior mandible. D4 bone has almost no crestal cortical bone and the fine spongy bone composes the total volume of bone next to the implant, and it is found in the posterior maxilla.

There is also a soft bone with incomplete mineralization and large intra-trabecular spaces addressed as D5 bone, composed of immature bone as seen in the developing maxillary sinus graft [193]. The bone *D* is determined by tactile sense during surgery, and computerized tomography (CT scan).

Misch also proposed a tactile analog of the corresponding bone densities such as D1 bone tactile perception feels like oak or maple wood, D2 it is tactile analog is white pine wood, D3 it is tactile analog is balsa wood, and D4 it is tactile analog to Styrofoam [193, 194].

Bone *D* is more precisely determined by CT scan, that produces axial images of the patient's anatomy perpendicular to the long axis of the body. Each CT axial image has 260.000 pixels, and each pixel has a CT number which is measured in Hounsfield unit related to the *D* of the tissues within the pixel. In general, the higher the CT number, the denser the tissue. Based on the CT determination of bone *D*, Misch also proposed a relationship of bone *D* and its CT number in the Hounsfield unit [193]. D1 bone *D* corresponds to more than 1250 Hounsfield units, D2 bone *D* between 850 to 1250 Hounsfield units, D3 bone *D* corresponding to 350 to 850 hounsfield units, and D4 bone *D* 150 to 350 Hounsfield units. D5 equals to less than 150 Hounsfield units, as seen in immature bones.

2.2.4 BKS biomechanical properties

The new BKS transforms the μ generated with the applied material into energy %E. This ensures greater adhesion and creates cohesion between the materials. In the case of application in bone tissue, it is stimulated by the chemical cohesion (osteoinduction) of the bone chips compacted in the inner *V* of the BKS with the bone of the receptor bed [195, 196] in addition to the adhesion without excessive *P* exerted by the previous drilling of smaller size due to the characteristic of the BKS drill, which drills its own geometry [197]. The double flutes, which do not discard the material from the simultaneous drilling and screwing system, compact the material in a longitudinal centre in the internal *V* of the BKS, progressively increasing the adhesion and cohesion of the BKS with increasing *M*, respecting the fatigue and fracture limits of the materials. With these characteristics, it is possible to redirect the applied *M*, collect, compress, measure, self-lock, and transport directly and indirectly the inserted material in a linear movement perpendicular to the direction of insertion to the BKS and in the opposite direction to the material.

The BKS transforms the lack of %E due to friction present in the traditional screw into a MA intended for the adhesion and cohesiveness of the materials. In addition, it introduces other new MA's such as collecting, compacting, condensing and self-locking with increased %E of the controlled applied *M* [57, 197, 198]. Another advantage of BKS is that the compactness and densification of the trabecular bone is a desirable factor in bone fixation and implants, given the greater success of denser bone (cortical) in osseointegration compared to less dense bone (trabecular) [198-200]. A wide range of mechanical testing techniques have been defined to measure bone properties, with different test methods used depending on the type of bone. For cortical bone, mechanical properties are measured using uniaxial tensile, compression and three-point or four-point bending tests [201]. From these mechanical tests, it is possible to quantify several properties including stiffness (S), ultimate load which is the load at failure, energy, or work at failure (U) and ultimate displacement (Figure 15).

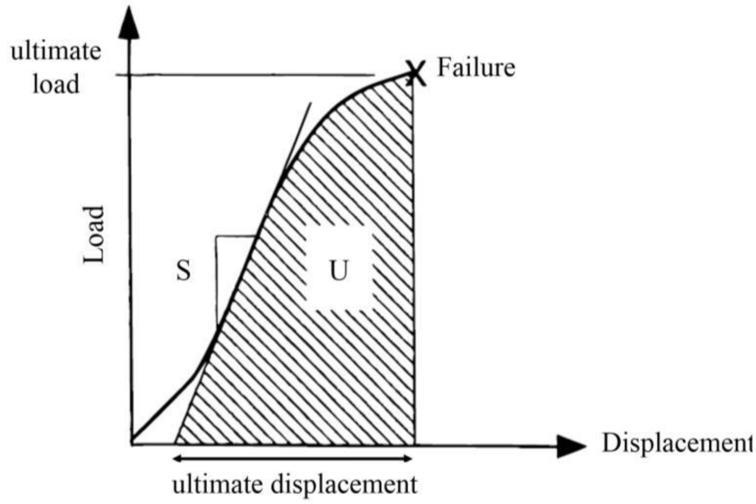

Figure 15. Bone specimen load-displacement curve illustration [202].

The curve of bone mechanical behavior is called the stress-strain curve when load is converted to stress and displacement is converted to strain [203]. Important mechanical properties such as Young modulus, yield stress and ultimate stress can be identified in this curve. The stress-strain curve is characterized by an initial linear region before yielding, the elastic region, and a non-linear region after yielding, the plastic region, which contains the ultimate stress and failure point. The Young modulus, or material stiffness, is represented by the slope of the stress-strain curve within the elastic region. The maximum stress and strain that the bone can withstand are called the ultimate stress or strength and the ultimate strain, respectively [203, 204]. These properties define the mechanical response of bone tissue to drilling [204, 205]. The properties of human cortical bone from long bones such as the tibia, femur and humerus have been found to vary between individuals despite identical densities [206]. As a heterogeneous anisotropic material, cortical bone exhibits different mechanical properties depending on the loading direction of the test method.

Bone is also a viscoelastic material, exhibiting both creep and stress relaxation. Bone's ultimate strength, energy to failure, and fracture toughness are rate dependent [207]. *D* is another highly variable bone property, making accurate determination difficult. The *D* of cortical bone is a function of the porosity and mineralization of the bone materials and is the wet *mg* divided by sample *V* [208]. There are, however, two concepts of *D* (apparent and material). The ratio of wet mineralized *m* to the *V* occupied by the tissue is known as apparent *D*. Material *D* is known as the mineralized *m* over the *V* occupied by the material itself. For cortical bone, because there is no marrow space in compact bone, apparent and material are essentially the same [208]. An average apparent *D* of approximately 1.9 g/cm^3 was found in a study of the mechanical properties of mammalian, avian and antler cortical bone [209].

Trabecular bone has a more porous structure than cortical bone, allowing mechanical description by structural and material properties. Due to the extremely small size of individual trabeculae, the mechanical properties of trabecular bone tissue are much more difficult to measure and test than those of cortical bone [210]. These include structural, trabecular connectivity, location, and role. The most common tests used to measure trabecular bone properties are compression, tensile, or bending tests. Mechanical testing has demonstrated a close correlation between trabecular bone mechanical properties, both strength and rigidity, and density.

Drill bit geometry, another BKS feature, is a very important aspect of drilling material. Its main function is the removal of material in the desired direction during drilling and the creation of a uniform and regular insertion. As drilling progresses, chips are formed that tend to follow the spiral path formed by the drill flutes, stopping, and compacting inside the BKS inner *V*. There are several types of surgical drills available in a wide range of configurations and sizes with a variety of diameters. However, BKS is mainly characterized by its diameter, cutting surface, helix angle and drill point, 3D design for precise material compaction and the possibility of modifications and adaptations according to purpose. Figure 16 shows the characteristics of drills and BKS modifications.

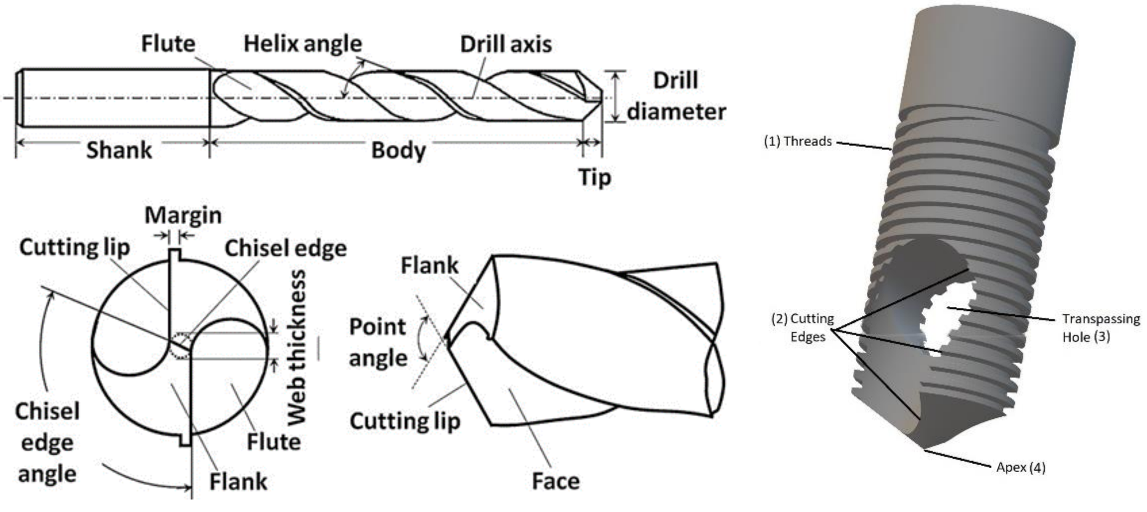

(a) **(b)**

Figure 16. (a) Twist drill geometry and its cutting tip [98]; (b) and BKS innovative properties.

Selecting the optimum BKS drill characteristics requires knowledge of the material to be drilled as well as cutting parameters, applied force, feed rate and drill speed to match these to the physical characteristics of the BKS [3].

Higher drill diameters means that the contact surface between the cutting tool and bone tissue will increase, which in turn increases the friction and the bone temperature. The authors evaluated the temperature changes during implant osteotomies with surgical drills from 2 to 5 mm diameter at various drilling depths. They verified significant differences in the temperature increase with different drill diameters [211, 212]. There is an advantage a in larger drill due to its larger flutes, which contribute to better elimination of heated bone fragments resulting in a more efficient drilling with lesser increase in bone temperature [77, 213], and drill bit deflection interferes directly with the precision. The precision is decreased when using small diameter and longer drill bits.

Drill points are defined as angles of projection of flutes on a plane passing through a tool's longitudinal axis, allowing an operator to locate drilling with minimal variation. Drill bits with a larger (> 90°) tip angle allow full contact of the cutting lip with the material as soon as drilling starts [214]. Larger drill bit point angles are better for hard materials and smaller point angles for soft materials, such as bone. For the design of orthopedic drills, a range of 110º-118º tip angle is recommended. The axial drilling force is significantly influenced by the drill tip angle. Sharper drill point angles reduce axial drilling forces. The rake angle is defined as the angle between the cutting edge and the plane perpendicular to the workpiece. This drill bit specification plays an important role in the cutting forces when drilling soft materials similar to cortical bone tissue, which are in the range of 12º-15º [215].

Most studies suggest that bit wear and heat generated during bone drilling increase with the number of times the drill is used. However, there is no evidence to suggest a specific number of uses before it becomes blunt and ineffective, causing a significant increase in temperature [211]. Flutes are helical or straight grooves that usually revolve around the bit to provide cutting lips, remove chips and allow coolant to reach the cutting lip. Drill bits can be designed with two or three flutes of different sizes and angles and the most common tool used is a twist drill with two helical flutes [77]. For BKS drilling quality and precision, cutting parameters play a fundamental role. Cutting parameters such as drill speed, feed rate, drill depth and bone D are associated with the setup of hand drills. The improvement of these parameters and all the variables involved is essential for the improvement of the drilling process. There is limited data available, but most agree that drilling axial force combined with feed can greatly reduce drilling time and subsequent heat generation [211].

Drilling of BKS can be performed in either single step or multi-step. In single-step drilling, only BKS of the required diameter is used to produce the desired function, whereas in multistep drilling, the drill diameter is gradually increased using an additional drill for pre-drilling hard materials. However, predrilling is controversial and in multistep, the total drilling time is increased. This means that the bone tissue is exposed for a longer time [8].

❖ *Standard steady-state torque*

Determine a ST measure for drilling and screwing bone implants in distinct quantities and qualities of bone tissue in a simple and suitable way controlling and predicting results, is the gold standard to achieve a successful primary stability and long-term osseointegration. Until now, the MIT has been used as a parameter to achieve success in primary stability and osseointegration, although presents conflicting results in the literature for more than four decades [216-221]. Basically, the experience of the surgeon guides the planning and execution of the surgical procedure, adapting in each case according to their tactile experience, guided by x-ray analysis and patient bone and general conditions [218]. Applying BKS as a dental implant, was mathematically and experimentally described [8] as a new method that standardizes the load *P* limit through the *M* into the BIC, in four classical distinct bone densities (Mish) during the achievement of the mechanical primary stability. The results described the relationship between MIT, MRT, μ between implant-bone and bone-to-bone, allowing the achievement of a controlled and predictable standard steady-state torque for bone implants. The measured value obtained in experiments standardized the torque (ST) values for four different synthetic bone densities, PCF 10, 20, 30, and 40, simulating Misch bone densities D4, D3, D2, and D1 respectively, and PCF 15 [8,9].

The results can be mathematically transferred for human application through the similar and proportional ratio observed in this and other experimental tests [222] even in distinct bone densities when the same protocol is applied [223].

❖ *Bone transplant*

When drilling into bone, the BKS implant can collect and compact the drilling chips in its internal *V* like particulate bone, as described in previous works [8,11, 224-226]. The BKS technique allows bone to be harvested from a variety of donors and recipients, depending on the surgeon's plans and the patient's needs. The described technique is characterised by simplicity of the procedure, reduced contact of harvested material with the external environment, and faster surgical procedure requiring basic skills necessary for any dental surgeon. The control of mechanical factors during bone drilling with the safe management of the bone graft and maintenance of its stability with quality and viability during drilling and implant screwing increases the chances of successful bone transplantation [226].

Restoration of osseous defects is accomplished by bone grafts and bone substitutes also called biomaterials. Bone grafts can be divided in four types, autograft or autogenous transplant which are derived from the same individual, allograft or allogenous transplant which is derived from the same species but different individuals, xenograft is derived from different species mainly the porcine or bovine origin, and alloplast synthetic materials [227-229].

The mechanism of action of bone graft can be either through osteogenesis, osteoinduction, osteoconduction, or a combination of these three processes. Osteogenesis refers to the formation or development of new bone by cells contained in the graft. Osteoinduction is a chemical process by which bone morphogenetic proteins (BMP) contained in the graft converting the neighboring cells into osteoblasts, which in turn form bone. Osteoconduction is a physical effect by which the matrix of the graft forms a scaffold that favors outside cells to penetrate the graft and form new bone [230]. Autogenous grafts can retain viability of the cells mainly the osteoblasts and osteoprogenitor stem cells, and does not lead to immunologic response, it is called the gold standard for bone grafts meeting the tissue engineering triad of signaling molecules, cells, and Scaffold [231]. Autogenous bone grafts can be obtained either by intra-oral or extra-oral sources. Among the intra-oral sources are healing dental extraction wounds, bone from edentulous ridges, bone trephined from within the jaw using trephine burs, bone formed in the wounds, and bone obtained from the maxillary tuberosity, ramus, and mandibular symphysis. The extra-oral sources are iliac crest which provides cancellous bone marrow, tibia and calvaria. Extra-oral sources can cause postoperative infection, increased patient expense, and difficulty finding donor material [232]. Autogenous bone grafts help in probing depth reduction, clinical attachment gain, bone fill of the osseous defect, and regeneration of new bone, cementum, and periodontal ligament in teeth. There are different techniques and devices to obtain bone grafts accordingly with the patient’s needs, location, and size of the bone defect. These are the bone scraper where the bone is removed by scraping action, rotary instruments like burs or trephine, bone chisels, rongeur pliers, and piezoelectric devices [231, 232].

The types of autogenous bone grafts are cortical bone chips, osseous coagulum and bone blend, intraoral cancellous bone and marrow, extraoral cancellous bone and marrow, bone swagging, and autogenous bone blocks [230]. The healing process after autogenous graft in the bone bed site leaves a gap between them, which is bridged by the proliferating osteoprogenitor cells or the pre-osteoblasts cells, that will become the newly formed bone around the graft area. The osteocytes in the graft due to anoxia and surgical site trauma are death, followed by micro anastomoses and restoration of circulation. The newly bone formed is initially by the surviving cells in the graft and later by the osteoinduction of the cells of the surrounding host bone [228]. Incorporation of the graft occurs after six months and continuous for two years [229].

❖ *Bone collector*

Autogenous bone grafting aids in probing depth reduction, clinical attachment gain, bone filling of the osseous defect and regeneration of new bone, cementum, and periodontal ligament in teeth. BKS can be used as an autogenous bone collector that can fill defects of 96.91 mm^3 (by the size of 4mm diameter and 10 mm length) with bone particulates or for use in bioengineered scaffolds. Experimental studies on synthetic bone [224, 225] have demonstrated the feasibility and applicability of the amount of bone obtained.

Bone defects can either be the consequence of congenital and developmental malformations or originate from tumor surgery, trauma, or infections. Functional and aesthetic bone defects are often a challenge to be overcome, mainly related to the donor source and the size of the graft needed, as well as possible complications related to the procedures, whether they are autogenous transplant (same individual), allograft or allogenous transplant (same species but different individuals), xenograft (different species), and alloplast (synthetic materials) [233-237]. The complications are mainly associated with the manipulation of the grafts and the increased risk of contamination of the material collected or to be implanted, adverse reactions when material from the same individual is not used (allografts, xenografts, and alloplast), and the need for multiple surgical procedures, especially in cases of removal of bone material individual in-dividual (autogenous). In these cases, many times the removal of the bone graft becomes a surgery of greater trauma than the procedure of bone implantation. The bio-logical qualities of bone transplantation with fresh autogenous bone still represent the gold standard for bone grafts [234-240].

Developing a bone collector device in which autogenous bone is removed with a simpler and less traumatic procedure are some of the desirable characteristics for surgeons and for patients when choosing the source and/or donor region of the bone graft. The surgery for dental implants has proven over the decades to be a safe procedure and well accepted by patients in relation to surgical trauma and its results. The use of a bone collector device in which the same procedures are applied in dental implantation, makes the act itself like the surgeon's routine, as well as the prediction of the expected results related to the patient's acceptance [233, 235]. The BKS is a simple multifunctional SM able to simultaneously drill and screw, measure the volume density of the material where it is applied, compact the material inside [241-245], and another application, which the material collected in its interior volume can be used to be transplanted to other regions for bone filling, or to be used as a stimulus of osteogenesis, osteoinduction, and osteoconduction in bone scaffolds (figure 17).

Figure 17. BKS as a bone collector with a contra-angle hand piece connector adapted.

The BKS can be manufactured in a variety of sizes to suit specific requirements and applications. The sizes can be modified internally (flute length and width, diameter, and position in relation to the longitudinal axis of the through hole) as well as the length and overall diameter of the screw. The larger the internal *V* measurements of the BKS, the greater the bone collection capacity will be in proportion to the size of the total *V* of BKS applied [246]. The choice of the amount of bone to be harvested, and therefore the size of the BKS, depends on the patient's needs, the surgeon's choice of donor site, and the purpose of the graft (bone defect filling, vertical or horizontal bone augmentation).

In addition, the larger the width of the BKS flutes, the larger the size of the particles harvested [239, 240]. To make it easier to correlate the results obtained and to describe the capacity of bone grafting for different purposes, the same model that has been studied in previous studies in another application is used as a bone collector [241-244].

The technique consists of drilling into the bone with the BKS at low speed (60 rpm) as seen in figure 1(b), and, after inserting the entire length into the bone, reversing the direction of rotation on the motor to remove the BKS completely from the bone donor bed. With the particulate bone in its internal volume, without directly manipulating the bone, the bone is removed from inside the BKS using tweezers or a dental explorer and place it directly into the desired recipient bed as seen in figure 18.

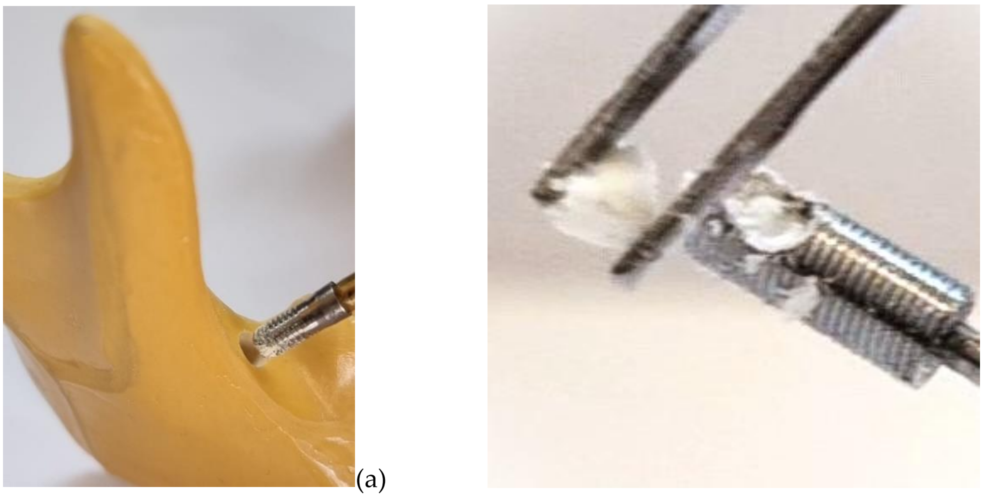
(a) (b)

Figure 18. (a) BKS bone collector removed after collecting bone from retromolar region of mandible; (b) BKS bone collector after removing bone chips from its interior volume.

The described technique presents a difference observed in the results of the experimental procedures in which the surgeon's familiarity of the applied method compared with other bone grafting techniques, made the predictability and execution like what the professional performs in his surgical implant routine [234, 235]. The innovation is mainly due to the unique characteristics of the new BKS model, which in the same drilling procedure collects and compacts the bone in its internal volume, adding only the removal procedure, which is facilitated by the presence of square threads that maintain the desired stability for removal without wasting the collected material.

The use of the new BKS device as a bone collector for autologous transplantation proved feasible and the proposed technique simple and efficient. The amount of bone harvested is limited to the *V* of the BKS, so proper planning should be done to correctly indicate this technique. The minimal manipulation of the bone graft reduces its exposure time, especially to the oral environment, and with less chance of contamination that occurs with most other devices available in surgical practice. The proposed technique is like the routine used by dental surgeons and is therefore efficient to be adopted.

❖ *Maxillaris sinus Lift*

The main objective in implant dentistry is to integrate an implant completely and firmly into the local bone. Treating the severely atrophic alveolar ridge remains a challenge and lateral and vertical bone grafting techniques have been used to increase local bone *V* [247]. For all types of horizontal and vertical bone augmentation, autogenous bone grafts are still considered the gold standard. The majority of augmentation procedures in the atrophic posterior maxilla are in combination with elevation of the maxillary sinus membrane. The basal lining of the sinus membrane is not considered pure periosteum, but studies have shown new bone formation under the sinus membrane after elevation without the use of bone graft [248]. The lateral window technique for maxillary sinus augmentation in the posterior maxilla is a well-established and documented surgical procedure allowing simultaneous or staged implant placement [236, 249]. Donor site morbidity following autogenous bone harvesting and the use of any bone grafting material can be avoided by graftless sinus membrane elevation for subsequent implant placement and less discomfort for the patient during sinusoplasty [250].

The already tested BKS innovation [224, 225] offers a new solution to the problem of the complexity and morbidity of sinus lift, because it uses the patient's own bone from the maxillary implant site to fill in the area where the alveolar bone is to be augmented, without the need for a further surgical procedure and using autogenous bone, the gold standard in bone grafting. Simultaneously with the BKS insertion, the bone is harvested, compacted, and transplanted.

❖ *Bone screw*

The treatment of bone fractures, bone tumours, hearing impairments, facial deformities, neurosurgery, etc. uses screws and/or plates for bone fixation and immobilisation. As the innovative features of the BKS can be applied to a common screw, all these specialties can benefit from the use of this new biomechanism, depending on the purpose of use. In cases where screw removal is required, BKS is not the best option because of the increased initial stability of fixation, a necessary factor for long-term osseointegration of bone screws and implants. Further research is needed in all areas to analyse the pros and cons of the use of BKS and the advantages provided by the greater initial stability and simplicity of the technology [225].

2.2.5 BKS dental implant

The original conception of the BKS was through its application as a dental implant [251]. The name Bioactive Kinetic Screw (BKS) was derived from this initial proposal. It was designed to allow the connection of a screwed or cemented prosthesis through a screwed abutment in its longitudinal axis (Figure 19). Using the properties of a drill bit, the simple innovative design reduced the number of steps and materials required to drill and screw dental implants into bone. Because it drills and screws simultaneously, it uses an innovative technique called drill and seal [252], which reduces exposure to the oral environment during the surgical procedure, reducing the risk of contamination from saliva and other materials.

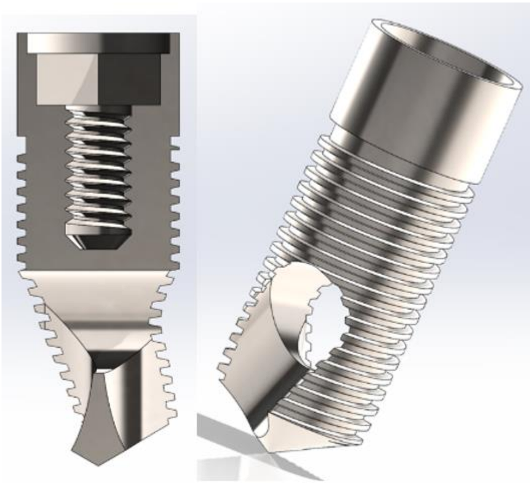

Figure 19. BKS design as a dental implant. Sagittal cut showing the internal threads for prothesis connection.

❖ *Finite element method*

FEM is used to evaluate tissue biomechanics, design, and manufacture medical devices, and simulate surgery. In bone drilling, FEM is an essential tool for reproducing the factors that influence the output variables, thus contributing to a better understanding of the drilling processes. During bone drilling, chipping occurs because the shear force exceeds the fracture strength of the material. In addition to shear, these forces can be decomposed into different components such as gravitational, normal, and shear. The development of 3D FE approaches with element removal is required to reproduce the hole formation during drilling with all the dynamic features involved in this process. The main drawback of 3D models is the high computational cost, as these simulations require many small elements to reproduce accurate results [253].

From a thermal and mechanical point of view, numerical models based on the drilling approach were discussed. The literature review showed that modelling bone drilling is difficult, and few papers presented complete material removal models capable of predicting drilling forces, temperature, and mechanical damage. Most studies only developed thermal models focusing on temperature prediction but not mechanical damage prediction. Implementing bone drilling models is challenging, probably due to the complexity of the simulation tools and the computational time required. However, numerical modelling could help to determine the appropriate drilling parameters to perform the drilling in the most efficient and least damaging way [254]. Developing accurate models and integrating them into surgical procedures requires active collaboration between medical and engineering professionals.

❖ *BKS Surgical protocol*

The effectiveness of drilling the BKS directly into the recipient bone bed without the need for pre-drilling has been proven by the simplified surgical protocol established in the BKS experiments. Pre-drilling is indicated in those cases in which the surgeon considers it necessary according to his personal experience, considering the planning and the needs of each individual case. A guide hole with a 1.6 mm diameter drill is the ideal indication to facilitate drilling in the desired position in cases where the cortical bone does not have a minimum base to start drilling.

2.2.6 BKS anchor bone screw

The use of screws for orthodontic anchorage and maxillomandibular fixation in craniofacial surgery expands the possibilities of using BKS, bringing technical and functional advantages to patients who require these therapies. Faster and safer healing, as well as a higher torque application to the fixation screw, are the most desirable characteristics in the search for better results of bone anchorage screws [255]. In vitro, both in the mandible and in the maxilla, larger diameter (2.5 mm) monocortical screws provide greater anchorage force resistance than smaller diameter (1.5 mm) monocortical screws. Bicortical screws with a smaller diameter (1.5 mm) provide an anchorage F resistance that is at least equal to that of monocortical screws with a larger diameter (2.5 mm). An alternative to the placement of a larger diameter mini screw for additional anchorage is a narrower bicortical screw and BKS [256].

Many case reports have successfully used titanium miniscrews and variations of surgical screws for rigid fixation to provide orthodontic anchorage without patient compliance [257, 258]. Miniature screws offer distinct advantages over conventional endosseous implants for anchoring: reduced size, flexibility of placement, ease of placement, less patient trauma, and lower cost. Furthermore, because the primary stability of miniscrews is thought to result from mechanical interlocking, waiting for osseointegration before orthodontic loading is unnecessary, as is a second surgical procedure (trephination) to remove. On the other hand, as miniscrews do not osseointegrate, their anchoring potential is most likely influenced by the quality and quantity of the bone into which they are placed [259]. In both the mandible and maxilla, larger-diameter (2.5 mm) monocortical screws provide greater resistance to anchorage forces than smaller-diameter (1.5 mm) monocortical screws. Bicortical screws with a smaller diameter (1.5 mm) provide at least the same resistance to anchoring forces as monocortical screws with a larger diameter (2.5 mm) and benefit from the higher coefficient of friction properties of BKS [260].

Temporary skeletal anchors have evolved from retromolar implants and interradicular miniscrews to extra-alveolar bone screws placed in the basilar bone buccal to the first molars: mandibular buccal shelf and infrazygomatic crest. The teeth, segments and arches can be moved with extra-alveolar anchorage [261]. Because bone anchored mechanics are complementary, fixed appliances and clear aligners can be used individually or together to correct a wide variety of malocclusions [262].

The cornerstone of fracture reduction and immobilisation in the treatment of maxillofacial trauma is the use of intermaxillary fixation (IMF). Recently, IMF screws have been introduced into clinical practice, but hardware failure may arise. It is a safe and time-saving procedure, but it is not without limitations or potential consequences [263]. Today, screws are commonly used for IMF. They are quick, easy, and inexpensive and reduce the risk of needlestick injury. They do not injure gingival margins and maintain gingival health better than using archwires or eyelets. Minimal hardware is required for IMF, with one screw in each quadrant usually sufficient, but more can be used if required [264].

References

1. Chondros TG. (2010) Archimedes life works and machines. *Mechanism and Machine Theory* 45(11), 1766-1775.

2. Wang P, Xu Q. (2018) Design and modeling of constant-force mechanisms: A survey. *Mechanism and Machine Theory* 119:1-21.
3. Wang C, Wang B, Liu M, Xing Z. (2022) A Review of Recent Research and Application Progress in Screw Machines. *Machines*. 10(1), 62.
4. Kerle H, Klaus M. (2010) "From Archimedean spirals to screw mechanisms - A short historical overview". The Genius of Archimedes -- 23 Centuries of Influence on Mathematics, Science and Engineering: Proceedings of an International Conference Held at Syracuse, Italy, June 8–10, 2010. Springer. pp. 163–179.
5. Chondros TG. (2009) "The Development of Machine Design as a Science from Classical Times to Modern Era". International Symposium on History of Machines and Mechanisms: Proceedings of HMM 2008. USA: Springer. p. 63.
6. Andreucci CA. (2022) Disposição construtiva aplicada em parafuso para implante ósseo. São Paulo, Brasil. Internacional Patent No. WO2022036425A1. WIPO (PCT).
7. Andreucci CA, Alshaya A, Fonseca EMM, Jorge RN. (2022) Proposal for a New Bioactive Kinetic Screw in an Implant, Using a Numerical Model. *Appl. Sci*. 12, 779.
8. Andreucci CA, Fonseca EMM, Jorge RN. (2022) Increased Material Density within a New Biomechanism. *Math. Comput*. Appl. 27, 90.
9. Andreucci CA, Fonseca EMM, Jorge RN. (2022) 3D Printing as an Efficient Way to Prototype and Develop Dental Implants. *BioMedInformatics* 2, 44.
10. Andreucci CA, Fonseca EMM, Jorge RN. (2022) J. Structural analysis of the new Bioactive Kinetic Screw in titanium alloy vs. commercially pure titanium. *J. Comp. Art. Int. Mec. Biomec.* 2, 35–43.
11. Andreucci CA, Fonseca EMM, Jorge RN. (2023) Bio-lubricant Properties Analysis of Drilling an Innovative Design of Bioactive Kinetic Screw into Bone. *Designs*. 7(1), 21.
12. Stahel PF, Alfonso NA, Henderson C. (2017) Introducing the "Bone-Screw-Fastener" for improved screw fixation in orthopedic surgery: a revolutionary paradigm shift? *Patient Saf Surg* 11, 6.
13. Hanaor DAH, Gan Y, Einav I. (2016). Static friction at fractal interfaces. *Tribology International*, 93, 229–238.
14. Moebs W, Ling SJLJ, Sanny JS. (2016). University Physics Volume 1. *OpenStax*. https://openstax.org/books/university-physics-volume-1/pages/6-2-friction.
15. Rosenholm, JB, Peiponen KE, Gornov E. (2008) Materials cohesion and interaction forces. *Advances in Colloid and Interface Science* 141, 1–2, 48-65.

16. Mellinger JC, Burak Ozdoganlar O, DeVor RE, Kapoor SG. (2002). Modeling Chip-Evacuation Forces and Prediction of Chip-Clogging in Drilling. *ASME. J. Manuf. Sci. Eng*. 124(3), 605–614.
17. Mandal R, Casert C, Sollich P. (2022) Robust prediction of force chains in jammed solids using graph neural networks. *Nat Commun* 13, 4424.
18. Ameur DK. (2021) Tribological Study of the Friction between the Same Two Materials (RAD Steel). *Tribology in Materials and Manufacturing - Wear, Friction and Lubrication*. doi: 10.5772/intechopen.93478.
19. Lemos CAA, Verri FR, de Oliveira Neto OB, Cruz RS, Gomes JML, Casado BGS, Pellizzer EP. (2021) Clinical effect of the high insertion torque on dental implants: A systematic review and meta-analysis. *J Prosthet Dent*. 126(4), 490-496.
20. Roca-Millan E, González-Navarro B, Domínguez-Mínger J, Marí-Roig A, Jané-Salas E, López-López J. (2020) Implant insertion torque and marginal bone loss: A systematic review and meta-analysis. *Int J Oral Implantol (Berl).* 13(4), 345-353.
21. Berardini M, Trisi P, Sinjari B, Rutjes AW, Caputi S. (2016) The Effects of High Insertion Torque Versus Low Insertion Torque on Marginal Bone Resorption and Implant Failure Rates: A Systematic Review With Meta-Analyses. *Implant Dent*. 25(4), 532-540.
22. Inchingolo AD, Inchingolo AM, Bordea IR, et al. (2021) The Effectiveness of Osseodensification Drilling Protocol for Implant Site Osteotomy: A Systematic Review of the Literature and Meta-Analysis. *Materials (Basel*). 14(5), 1147.
23. Gaikwad AM, Joshi AA, Nadgere JB. (2022) Biomechanical and histomorphometric analysis of endosteal implants placed by using the osseodensification technique in animal models: A systematic review and meta-analysis. *J Prosthet Dent*. 127(1), 61-70.
24. Coelho PG, Marin C, Teixeira HS, Campos FE, Gomes JB, Guastaldi F, Anchieta RB, Silveira L, Bonfante EA. (2013) Biomechanical Evaluation of Undersized Drilling on Implant Biomechanical Stability at Early Implantation Times. *J. of Oral and Max. Surg*. 71, 2, e69-e75.
25. Romeo D, Chochlidakis K, Barmak AB, Agliardi E, Lo Russo L, Ercoli C. (2022) Insertion and removal torque of dental implants placed using different drilling protocols: An experimental study on artificial bone substitutes. *J Prosthodont*. 1– 6.
26. Wang YS, Lee CT, Kandaswamy E, Theodorou K, Chien HH. (2022) Accuracy of mechanical torque-limiting devices for implant screw tightening: A systematic review and meta-analysis. The J. of Prosth. Dent.

https://doi.org/10.1016/j.prosdent.2022.08.013.

27. Gehrke SA, Júnior JA, Treichel TLE. do Prado TD, Dedavid BA, Aza PN. (2022) Effects of insertion torque values on the marginal bone loss of dental implants installed in sheep mandibles. *Sci Rep* 12, 538.
28. Gallucci GO, Hamilton A, Zhou W, Buser D, Chen S. (2018) Implant placement and loading protocols in partially edentulous patients: A systematic review. *Clin Oral Implants Res*. 29 Suppl 16, 106-134.
29. Gallardo YNR, da Silva-Olivio IR, Gonzaga L, Sesma N, Martin W. (2019) A Systematic Review of Clinical Outcomes on Patients Rehabilitated with Complete-Arch Fixed Implant-Supported Prostheses According to the Time of Loading. *J Prosthodont*. 28(9), 958-968.
30. Huynh-Ba G, Oates TW, Williams MAH. (2018) Immediate loading vs. early/conventional loading of immediately placed implants in partially edentulous patients from the patients' perspective: A systematic review. *Clin Oral Implants Res*. 29 Suppl 16, 255-269.
31. Yu X, Chang C, Guo W, Wu Y, Zhou W, Yu D. (2022) Primary implant stability based on alternative site preparation techniques: A systematic review and meta-analysis. *Clin Implant Dent Relat Res*. 24(5), 580- 590.
32. Raz P, Meir H, Levartovsky S, Sebaoun A, Beitlitum I. (2022) Primary Implant Stability Analysis of Different Dental Implant Connections and Designs—An In Vitro Comparative Study. *Materials*. 15(9), 3072.
33. Pammer D. (2019) Evaluation of postoperative dental implant primary stability using 3D finite element analysis. *Comput Methods Biomech Biomed Engin*. 22(3), 280-287.
34. Hsu JT, Huang HL, Tsai MT, Wu AY, Tu MG, Fuh LJ. (2013) Effects of the 3D bone-to-implant contact and bone stiffness on the initial stability of a dental implant: micro-CT and resonance frequency analyses. *Int J Oral Maxillofac Surg*. 42(2), 276-280.
35. Ozdoganlar O, DeVor R, Kapoor S. (2002) Modeling Chip-Evacuation Forces and Prediction of Chip-Clogging in Drilling. *Urbana*. 51, 61801.
36. Ben Achour A, Petto C, Meißner H, Hipp D, Nestler A, Lauer G, Teicher U. (2019) The Influence of Thrust Force on the Vitality of Bone Chips Harvested for Autologous Augmentation during Dental Implantation. *Materials*. 12(22), 3695.
37. Hao CP, Cao NJ, Zhu YH, Wang W. (2021) The osseointegration and stability of dental implants with different surface treatments in animal models: a network meta-analysis. *Sci*

Rep 11, 13849.

38. Albrektsson T, Branemark PI, Hansson HA, Lindstrom J. (1981) Osseointegrated titanium implants. Requirements for ensuring a long-lasting, direct bone-to-implant anchorage in man. *Acta Orthop. Scand*. 52, 155–170.
39. Gómez-Polo M, Ortega R, Gómez-Polo C, Martín C, Celemín A, Del Río J. (2016) Does Length, Diameter, or Bone Quality Affect Primary and Secondary Stability in Self-Tapping Dental Implants? *J Oral Maxillofac Surg*., 74(7), 1344-1353.
40. Huang H, Wu G, Hunziker E. (2020) The clinical significance of implant stability quotient (ISQ) measurements: A literature review. *J Oral Biol Craniofac Res*., 10(4), 629-638.
41. Nelissen RC, Wigren S, Flynn MC, Meijer GJ, Mylanus EA, Hol MK. (2015) Application and Interpretation of Resonance Frequency Analysis in Auditory Osseointegrated Implants: A Review of Literature and Establishment of Practical Recommendations. *Otol Neurotol*. 36(9), 1518-1524.
42. Gehrke SA, Cortellari GC, de Oliveira Fernandes GV, Scarano A, Martins RG, Cançado RM, Alfredo Mikail Melo Mesquita AMM. (2023) Randomized Clinical Trial Comparing Insertion Torque and Implant Stability of Two Different Implant Macrogeometries in the Initial Periods of Osseointegration. *Medicina (Kaunas)*. 59(1), 168.
43. Malchiodi L, Balzani L, Cucchi A, Ghensi P, Nocini PF. (2016) Primary and Secondary Stability of Implants in Postextraction and Healed Sites: A Randomized Controlled Clinical Trial. *Int J Oral Maxillofac Implants*. 31(6), 1435-1443.
44. Jolic M, Sharma S, Palmquist A, Shah FA. (2022) The impact of medication on osseointegration and implant anchorage in bone determined using removal torque-A review. *Heliyon*, 8(10), e10844.
45. Shah FA, Johansson ML, Omar O, Simonsson H, Palmquist A, Thomsen P. (2016) Laser-Modified Surface Enhances Osseointegration and Biomechanical Anchorage of Commercially Pure Titanium Implants for Bone-Anchored Hearing Systems. *PLoS One*, 11(6), e0157504.
46. Karazisis D, Rasmusson L, Petronis S, Palmquist A, Shah FA, Agheli H, Emanuelsson L, Johansson A, Omar O, Thomsen P. (2021) The effects of controlled nanotopography, machined topography and their combination on molecular activities, bone formation and biomechanical stability during osseointegration. *Acta Biomater*. 136, 279-290.

47. Grobecker-Karl T, Dickinson A, Heckmann S, Karl M, Steiner C. (2020) Evaluation of Insertion Energy as Novel Parameter for Dental Implant Stability. J *Clin Med*, 9(9), 2977.
48. Yang B, Irastorza-Landa A, Heuberger P, Ploeg HL. (2020) Effect of insertion factors on dental implant insertion torque/energy-experimental results. *J Mech Behav Biomed Mater*, 112, 103995.
49. Steiner C, Karl M, Grobecker-Karl T. (2020) Insertion and Loading Characteristics of Three Different Bone-Level Implants. *Int J Oral Maxillofac Implants*, 35(3), 560-565.
50. Yang B, Irastorza-Landa A, Heuberger P, Ploeg HL. (2022) Analytical model for dental implant insertion torque. *J Mech Behav Biomed Mater*, 131:105223.
51. Andreucci CA, Fonseca EMM, Jorge RN. (2023) A new simple machine that converts torque into steady-state pressure in solids. *IEEE 7th Portuguese Meeting on Bioengineering (ENBENG)* 148-150, doi: 10.1109/ENBENG58165.2023.10175336.
52. Kohli N, Stoddart JC, van Arkel RJ. (2021) The limit of tolerable micromotion for implant osseointegration: a systematic review. *Sci Rep* 11, 10797.
53. Shockey JS, von Fraunhofer JA, Seligson D. (1985) A measurement of the coefficient of static friction of human long bones. *Surface Technology*, 25, 2, 167-173.
54. Zhu B, He X, Zhao T. (2015) Friction and wear characteristics of natural bovine bone lubricated with water, *Wear*, 322–323.
55. Wang C, Zhang G, Li Z, Zeng X, Xu Y, Zhao S, Hu H, Zhang Y, Ren T. (2019) Tribological behavior of Ti-6Al-4V against cortical bone in different biolubricants. *J. of the Mech. Behav. of Biomed. Mater.*, 90, 460-471.
56. Dannaway J, Dabirrahmani D, Sonnabend D, Martin AJ, Appleyard R. (2015) An investigation into the frictional properties between bone and various orthopedic implant surfaces - implant stability. *J. Musculoskelet*, 18, 1550015.
57. Bozkaya D, Müftü S. Efficiency considerations for the purely tapered interference fit (TIF) abutments used in dental implants. J Biomech Eng. 2004;126(4):393-401. doi:10.1115/1.1784473.
58. Irandoust S, Müftü S. (2020) The interplay between bone healing and remodeling around dental implants. *Sci Rep* 10, 4335.
59. Brunski JB. (1999) In vivo bone response to biomechanical loading at the bone/dental-implant interface. *Advances in dental research* 13, 99–119.
60. Frost H. M. (1989). The biology of fracture healing. An overview for clinicians. Part I. *Clinic. Orthop. and relat. Res.* (248), 283–293.

61. Frost H. (1987) Bone “mass” and the “mechanostat”: a proposal. The Anatomical Record 219, 1–9.
62. Mavčič B, Antolič V. (2012) Optimal mechanical environment of the healing bone fracture/osteotomy. *Int Orthop*, 36(4), 689-695.
63. Branemark PI. (1983) Osseointegration and its experimental background. *Journal of Prosthetic Dentistry* 50, 399–410.
64. Tsai MD, Hsieh MS, Tsai CH (2007) Bone drilling haptic interaction for orthopedic surgical simulator. *Comput Biol Med* 37(12), 1709-18.
65. Li S, Wahab AA, Demirci E, Silberschmidt VV (2014) Penetration of cutting tool into cortical bone: Experimental and numerical investigation of anisotropic mechanical behaviour. *J Biomech* 47, 1117-1126.
66. Ebacher V, Guy P, Oxland TR, Wang R (2012) Sub-lamellar microcraking and roles of canaliculi in human cortical bone. *Acta Biomater* 8:1093-1100.
67. Kasiri S, Reilly G, Taylor D (2010) Wedge indentation fracture of cortical bone: experimental data and predictions. *J Biomech Eng* 132(8):081009.
68. Boyan BD, Sylvia VL, Liu Y, Sagun R, Cochran DL, Lohmann CH, Dean DD, Schwartz Z (1999) Surface roughness mediates its effects on osteoblasts via protein kinase A and phospholipase A2. *Biomaterials* 20(23-24), 2305-10.
69. Donnelly E, Baker SP, Boskey AL, van der Meulen MC (2006) Effects of surface roughness and maximum load on the mechanical properties of cancellous bone measured by nanoindentation. *J Biomed Mater Res A* 77(2), 426-35.
70. Lee J, Gozen BA, Ozdoganlar OB (2012) Modeling and experimentation of bone drilling forces. *J Biomech* 45(6), 1076-83.
71. Ong FR, Bouazza-Marouf K (1999) The detection of drill-bit break-through for the enhancement of safety in mechatronic assisted orthopaedic drilling. *Mechatronics* 9(6), 565–588.
72. Brett PN, Baker DA, Taylor R, Griffiths MV (2004) Controlling the penetration of flexible bone tissue using the stapedotomy microdrill. *Proc IMechE Part I: J Systems and Control Engineering* 218(5), 343-351.
73. Kendoff D, Citak M, Gardner MJ, Stübig T, Krettek C, Hüfner T (2007) Improved accuracy of navigated drilling using a drill alignment device. *J Orthop Res* 25(7), 951- 7.
74. Karmani S, Lam F (2004) The design and function of surgical drills and K-wires. *Current Orthopaedics* 18(6), 484-490.

75. Franssen BB, van Diest PJ, Schuurman AH, Kon M (2008) Keeping osteocytes alive: a comparison of drilling and hammering k-wires into bone. *J Hand Surg Eur* 33(3), 363-8.
76. Hobkirk JA, Rusiniak K (1977) Investigation of variable factors in drilling bone. *J Oral Surg* 35(12), 968-73.
77. Augustin G, Zigman T, Davila S, Udilljak T, Brezak D, Babic S (2012) Cortical bone drilling and thermal osteonecrosis. *Clin Biomech* 27, 3313-325.
78. Dahotre N, Joshi S (2016) Machining of bone and hard tissues. Springer International Publishing, Switzerland, pag.12. ISBN: 978-3-319-39158-8 (e-Book).
79. Andreucci CA, Fonseca EMM, Jorge RN. (2023) A New Collector Device for the Immediate Use of Particulate Autogenous Bone Grafts. *Applied Sciences*. 13(20), 11334. https://doi.org/10.3390/app132011334.
80. Owen R, Reilly GC. (2018) In vitro Models of Bone Remodelling and Associated Disorders. *Front Bioeng Biotechnol*. 6:134.
81. Bilgiç E, Boyacıoğlu O, Gizer M, Korkusuz P, Korkusuz P. (2020) Chapter 6 - Architecture of bone tissue and its adaptation to pathological conditions, Editor(s): Salih Angin, Ibrahim Engin Şimşek, Comparative Kinesiology of the Human Body, *Academic Press*, 71-90.
82. Stavnichuk M, Mikolajewicz N, Corlett T, Morris M, Komarova SV. (2020) A systematic review and meta-analysis of bone loss in space travelers. *npj Microgravity* 6, 13.
83. Pivonka, P, Park A, Forwood MR. (2018) Functional adaptation of bone: the mechanostat and beyond. In Multiscale Mechanobiology of Bone Remodeling and Adaptation, Springer International Publishing, Cham.
84. Duan ZW, Lu H. (2021) Effect of Mechanical Strain on Cells Involved in Fracture Healing. *Orthop Surg*. 13(2), 369-375.
85. Dwek JR. (2010) The periosteum: what is it, where is it, and what mimics it in its absence? *Skeletal Radiol*, 39, 319–323.
86. Bahney CS, Zondervan RL, Allison P, Alekos Theologis A, Ashley JW, Ahn J, Miclau T, Marcucio RS, Hankenson KD. (2019) Cellular biology of fracture healing. *J Orthop Res*, 37: 35–50.
87. Frost H. M. (1989). The biology of fracture healing. An overview for clinicians. Part II. *Clinic. Orthop. and related res*. (248), 294–309.
88. Groothuis A, Duda GN, Wilson CJ, Thompson MS, Hunter MR, Simon P, Bail HJ, van Scherpenzeel KM, Kasper G. (2010) Mechanical stimulation of the pro-angiogenic

capacity of human fracture haematoma: involvement of VEGF mechano-regulation. *Bone*, 47, 438–444.

89. Chen H, Ghori-Javed FY, Rashid H, Adhami MD, Serra R, Gutierrez SE, Javed A. (2014) Runx2 regulates endochondral ossification through control of chondrocyte proliferation and differentiation. *J Bone Miner Res*, 29: 2653–2665.
90. Aro HT, Chao EY. (1993) Bone-healing patterns affected by loading, fracture fragment stability, fracture type, and fracture site compression. *Clin Orthop Relat Res*, (293), 8-17.
91. Standring, S. (2016). Gray's Anatomy (41tst ed.). Edinburgh: Elsevier Churchill Livingstone.
92. Mellion ZJ, Behrents RG, Johnston LE Jr. (2013) The pattern of facial skeletal growth and its relationship to various common indexes of maturation. *Am J Orthod Dentofacial Orthop*. 143(6), 845-854.
93. Chvatal BA, Behrents RG, Ceen RF, Buschang PH. (2005) Development and testing of multilevel models for longitudinal craniofacial growth prediction. *Am J Orthod Dentofacial Orthop*. 128(1):45-56.
94. Jiménez-Silva A, Carnevali-Arellano R, Vivanco-Coke S, Tobar-Reyes J, Araya-Díaz P, Palomino-Montenegro H. (2021) Craniofacial growth predictors for class II and III malocclusions: A systematic review. *Clin Exp Dent Res*. 7(2), 242-262.
95. McKee TJ, Perlman G, Morris M, Komarova SV. (2019) Extracellular matrix composition of connective tissues: a systematic review and meta-analysis. *Sci Rep*. 9(1), 10542.
96. Chang B, Liu X. (2022) Osteon: Structure, Turnover, and Regeneration. *Tissue Eng Part B Rev*. 28(2), 261-278.
97. Chen H, Senda T, Kubo KY. (2015) The osteocyte plays multiple roles in bone remodeling and mineral homeostasis. *Med Mol Morphol*. 48(2), 61-68.
98. Aaron JE. (2012) Periosteal Sharpey's fibers: a novel bone matrix regulatory system? *Front Endocrinol (Lausanne).* 3, 98.
99. D'Andrea CR, Alfraihat A, Singh A, Anari JB, Cahill PJ, Schaer T, Snyder BD, Elliott D, Balasubramanian S. (2021) Part 1. Review and meta-analysis of studies on modulation of longitudinal bone growth and growth plate activity: A macro-scale perspective. *J Orthop Res*. 39, 907– 918.
100. D'Andrea CR, Alfraihat A, Singh A, Anari JB, Cahill PJ, Schaer T, Snyder BD, Elliott D, Balasubramanian. (2021) Part 2. Review and meta-analysis of studies on modulation

of longitudinal bone growth and growth plate activity: A micro-scale perspective. *J Orthop Res*. 39(5), 919-928.

101. Varacallo M, Seaman TJ, Jandu JS, et al. (2022) Osteopenia. [Updated 2022 Oct 24]. In: StatPearls [Internet]. Treasure Island (FL): StatPearls Publishing; 2022 Jan-. Available from: https://www.ncbi.nlm.nih.gov/books/NBK499878/
102. Kitsuda Y, Wada T, Noma H, Osaki M, Hagino H. (2021) Impact of high-load resistance training on bone mineral density in osteoporosis and osteopenia: a meta-analysis. *J Bone Miner Metab*. 39(5), 787-803.
103. Lerebours C, Buenzli PR. (2016) Towards a cell-based mechanostat theory of bone: the need to account for osteocyte desensitisation and osteocyte replacement. Journal of Biomechanics, 49, 13, 2600-2606.
104. Owen R, Reilly GC. (2018) In vitro Models of Bone Remodelling and Associated Disorders. *Front. Bioeng. Biotechnol*. 6, 134.
105. Hart NH, Nimphius S, Rantalainen T, Ireland A, Siafarikas A, Newton RU. (2017) Mechanical basis of bone strength: influence of bone material, bone structure and muscle action. *J Musculoskelet Neuronal Interact*. 17(3), 114-139.
106. Claes LE, Heigele CA, Neidlinger-Wilke C, Kaspar D, Seidl W, Margevicius KJ, Augatet P. (1998) Effects of mechanical factors on the fracture healing process. *Clin Orthop Relat Res*, 355S, S132–S147.
107. Egol KA, Kubiak EN, Fulkerson E, Kummer FJ, Koval KJ. (2004) Biomechanics of locked plates and screws. *J Orthop Trauma*, 18, 488–493.
108. Perren SM. (1979) Physical and biological aspects of fracture healing with special reference to internal fixation. *Clin Orthop Relat Res*, 138, 175–196.
109. Aro HT, Chao EY. (1993) Biomechanics and biology of fracture repair under external fixation. *Hand Clin*, 9, 531–542.
110. Saunders MM, Lee JS. (2008) The influence of mechanical environment on bone healing and distraction osteogenesis. *Atlas Oral Maxillofac Surg Clin North Am*, 16, 147–158.
111. Cheal EJ, Hayes WC, White AA 3rd, Perren SM. (1985) Stress analysis of compression plate fixation and its effects on long bone remodeling. *J Biomech*, 18, 141–150.
112. Lewallen DG, Chao EY, Kasman RA, Kelly PJ. (1984) Comparison of the effects of compression plates and external fixators on early bone-healing. *J Bone Joint Surg Am*, 66, 1084–1091.
113. Holmstrom T, Paavolainen P, Slatis P, Karaharju E. (1986) Effect of compression on

fracture healing. Plate fixation studied in rabbits. *Acta Orthop Scand*, 57, 368–372.
114. Salhotra A, Shah HN, Levi B, Longaker MT. (2020) Mechanisms of bone development and repair. *Nat Rev Mol Cell Biol* 21, 696–711.
115. Yang G, Zhu L, Hou N, Lan Y, Wu XM, Zhou B, Teng Y, Yanget X. (2014) Osteogenic fate of hypertrophic chondrocytes. *Cell Res* 24, 1266–1269.
116. Eyckmans J, Chen CS. (2017) Making bone via nanoscale kicks. *Nat Biomed Eng* 1, 689–690.
117. Wolf J. (1979) Das Gesetz der Transformation der Knochen. A. Hirschwald, Berlin, cited from Veldhuijzen JP, Bourret LA, Rodan GA-In vitro studies of the effect of intermittent compressive forces on cartilage cell proliferation. *J. Cell. Physiol*. 98, 299-306.
118. Wolf J. (2010) Das Gesetz der Transformation der Knochen—1892. Reprint: Pro Business, Berlin.
119. Levi G, Gitton Y. (2014) Dlx genes and the maintenance of bone homeostasis and skeletal integrity. *Cell Death Differ* 21, 1345–1346.
120. Costello BJ, Rivera RD, Shand J, Mooney M. (2012) Growth and development considerations for craniomaxillofacial surgery. *Oral Maxillofac Surg Clin North Am.* 24(3), 377-396.
121. Kaucka M, Adameyko I. (2019) Evolution and development of the cartilaginous skull: From a lancelet towards a human face. *Semin Cell Dev Biol*. 91, 2-12.
122. Ang PS, Matrongolo MJ, Zietowski ML, Nathan SL, Reid RR, Tischfield MA. (2022) Cranium growth, patterning and homeostasis. *Development*. 149(22), dev201017.
123. Ranly DM. (2000) Craniofacial growth. *Dent Clin North Am*. 44(3), 457-v.
124. Miller, EM. (2018) The first Seriatum study of growth by R. E. Scammon. *Am J Phys Anthropol*. 165, 415– 420.
125. Miller EM. (2018) The first Seriatum study of growth by R. E. Scammon. *Am J Phys Anthropol*. 165(3), 415-420.
126. Ziegler EE. (2015) 4.2 The CDC and Euro Growth Charts. *World Rev Nutr Diet*. 113, 295-307.
127. McNamara JA Jr, Franchi L. (2018) The cervical vertebral maturation method: A user's guide. *Angle Orthod.* 88(2),133-143.
128. Christen AG, Christen JA. (2003) Harry Sicher, MD, DSc.: pioneer dental anatomist. *J Hist Dent*. 51(3), 93-100.
129. Scott JH. (1954) The Growth of the Human Face. *Proceedings of the Royal Society of*

Medicine. 47(2), 91-100.

130. Nischal N, Iyengar KP, Herlekar D, Botchu R. (2023) Imaging of Cartilage and Chondral Defects: An Overview. *Life (Basel).* 13(2), 363.
131. Moss-Salentijn L. (1997) Melvin L. Moss and the functional matrix. J Dent Res. 76(12), 1814-1817.
132. Kyrkanides S, Moore T, Miller JH, Tallents RH. (2011) Melvin Moss' function matrix theory—Revisited, *Orthodontic Waves*, 70, 1, 1-7.
133. Jin SW, Sim KB, Kim SD. (2016) Development and Growth of the Normal Cranial Vault: An Embryologic Review. *J Korean Neurosurg Soc*. 59(3), 192-196.
134. Salzmann, J.A. (1977). Handbook of facial growth. *Am. J. of Orthod.* 71, 340-341.
135. Jacobson, A. (2009). Essentials of facial growth. *Am. J. of Orthod. and Dentof. Orthop*. 136, 471.
136. Ricqlès, A.J. (2007). Fifty years after Enlow and Brown's Comparative histological study of fossil and recent bone tissues (1956–1958): A review of Professor Donald H. Enlow's contribution to palaeohistology and comparative histology of bone. *Comptes Rendus Palevol*, 6, 591-601.
137. Enlow DH. (1990) Facial growth. Saunders (English), 3rd ed. Philadelphia.
138. Nahian A, Chauhan PR. (2022) Histology, Periosteum and Endosteum. In: StatPearls. Treasure Island (FL): StatPearls Publishing.
139. Li N, Song J, Zhu G, Li X, Liu L, Shi X, Wang Y. (2016) Periosteum tissue engineering-a review. *Biomaterials science*, 4(11), 1554–1561.
140. Funato N. (2020) New Insights Into Cranial Synchondrosis Development: A Mini Review. *Front. in cell and develop. Biol.*, 8, 706.
141. Schneider-Moser UEM, Moser L. (2022) Very early orthodontic treatment: when, why and how? *Dent. press j. of orthod*. 27(2), e22spe2.
142. Svandova E, Anthwal N, Tucker AS, Matalova E. (2020) Diverse Fate of an Enigmatic Structure: 200 Years of Meckel's Cartilage. *Front. in cell and develop. biol.* 8, 821.
143. Kuroda S, Tanimoto K, Izawa T, Fujihara S, Koolstra JH, Tanaka E. (2009) Biomechanical and biochemical characteristics of the mandibular condylar cartilage. *Osteoarth. and cartil*. 17(11), 1408–1415.
144. Themes, U. (2015) 5 Growth and development of the mandible. Pocket Dentistry. https://pocketdentistry.com/5-growth-and-development-of-the-mandible/.
145. Kaucka M, Adameyko I. (2019) Evolution and development of the cartilaginous skull:

From a lancelet towards a human face. *Semin. in cell & develop. biol*. 91, 2–12.
146. Salhotra A, Shah HN, Levi B, Longaker MT. (2020) Mechanisms of bone development and repair. *Nat Rev Mol Cell Biol* 21, 696–711.
147. Murphy MP, Irizarry D, Lopez M, Moore AL, Ransom RC, Longaker, MT, Wan D C, Chan CKF. (2017) The Role of Skeletal Stem Cells in the Reconstruction of Bone Defects. *The J. of cran. Surg*. 28(5), 1136–1141.
148. Long F. (2012) Building strong bones: molecular regulation of the osteoblast lineage. *Nat. Rev. Mol. Cell Biol*. 13, 27–38.
149. Einhorn T, Gerstenfeld L. (2015) Fracture healing: mechanisms and interventions. *Nat Rev Rheumatol* 11, 45–54. Springer Nature, lic. number 5515271061183, Mar 24, 2023.
150. Wang W, Yeung K. (2017). Bone grafts and biomaterials substitutes for bone defect repair: A review. *Bioac. Mat*. 2.
151. Gkiatas I, Lykissas M, Kostas-Agnantis I, Korompilias A, Batistatou A, Beris A. (2015) Factors affecting bone growth. *Am. j. of orthop. (Belle Mead, N.J.)* 44(2), 61–67.
152. Ghiasi MS, Chen J, Vaziri A, Rodriguez EK, Nazarian A. (2017) Bone fracture healing in mechanobiological modeling: A review of principles and methods. *Bone Rep.* 6, 87-100.
153. Marsell R, Einhorn TA. (2011) The biology of fracture healing. *Injury* 42(6), 551-555.
154. ElHawary H, Baradaran A, Abi-Rafeh J, Vorstenbosch J, Xu L, Efanov JI. (2021). Bone Healing and Inflammation: Principles of Fracture and Repair. *Seminars in plastic surgery*, 35(3), 198–203.
155. Kenkre JS, Bassett J. (2018). The bone remodelling cycle. *Annals of clinic. Biochem*. 55(3), 308–327.
156. Méndez-Ferrer S, Scadden DT, Sánchez-Aguilera A. (2015). Bone marrow stem cells: current and emerging concepts. *Annals of the New York Acad. of Sci*. 1335, 32–44.
157. Ono T, Hayashi M, Sasaki F, Nakashima T. (2020). RANKL biology: bone metabolism, the immune system, and beyond. *Inflammation and regeneration*, 40, 2.
158. Tanaka Y, Nakayamada S, Okada Y. (2005). Osteoblasts and osteoclasts in bone remodeling and inflammation. *Current drug targets. Inflammation and allergy*, 4(3), 325–328.
159. Marin E, Boschetto F, Pezzotti G. (2020). Biomaterials and biocompatibility: An historical overview. *J. of biomedic. Mat. res. Part A*, 108(8), 1617–1633.
160. Li Y, Xu Z, Wang J, Pei X, Chen J, Wan, Q. (2023). Alginate-based biomaterial-mediated

regulation of macrophages in bone tissue engineering. *Intern. J. of biology. Macromolec*. 230, 123246.

161. Liu Z, Zhu J, Li Z, Liu H, Fu C. (2023). Biomaterial scaffolds regulate macrophage activity to accelerate bone regeneration. *Front. in bioeng. and biotech*. 11, 1140393.
162. Davenport L, Pascual-Gil S, Wang Y, Mandla S, Yee B, Radisic M. (2020) Advanced Strategies for Modulation of the Material–Macrophage Interface. *Adv. Funct. Mater*. 30, 1909331. License Number 5515850282931. Mar 25, 2023. Publisher John Wiley and Sons.
163. Witherel, C. E., Abebayehu, D., Barker, T. H., Spiller, K. L., Adv. (2019) Macrophage and Fibroblast Interactions in Biomaterial-Mediated Fibrosis. *Healthcare Mater*. 8, 1801451.
164. Chandorkar Y, Ravikumar K, Basu B. (2019) The Foreign Body Response Demystified. *ACS biomat. Sci. & engineer*. 5(1), 19–44.
165. Gareb B, Van Bakelen NB, Vissink A, Bos RRM, Van Minnen B. (2022) Titanium or Biodegradable Osteosynthesis in Maxillofacial Surgery? In Vitro and In Vivo Performances. *Polymers*, 14(14), 2782.
166. Zhang D, Chen Q, Shi C, Chen M, Ma K, Wan J, Liu R. (2021) Dealing with the Foreign-Body Response to Implanted Biomaterials: Strategies and Applications of New Materials. *Adv. Funct. Mater*. 31, 2007226.
167. Branemark PI, Adell R, Breine U, Hansson B0, Lindstrom J, Ohlsson A. (1969) Intra-osseous anchorage of dental prostheses. I. Experimental studies. *Scand J Plast Reconstr Surg* 3(2), 81-100.
168. Branemark PI, Hansson B0, Adell R, Breine U, Lindstrom J, Hallen 0, Ohman A. (1977) Osseointegrated implants in the treatment of the edentulous jaw. Experience from a 10 year period. *Scand J Plast Reconstr Surg* (16), l-132.
169. Brånemark PI. (1992) Osseointegration-a method of anchoring prostheses. *The Swedish Society of Medicine* 7-15.
170. Branemark PI. Introduction to osseointegration. In: Tissue integrated Prostheses. Osseointegration in Clinical Dentistry (Eds. Branemark P I, Zarb G, Albrektsson T.) Quintessence, Berlin, Chicago, Tokyo 1985, 1-76.
171. Sullivan RM. (2001). Implant dentistry and the concept of osseointegration: a historical perspective. *J. of the Calif. Dental Assoc*. 29(11), 737–745.
172. Buser D, Sennerby L, De Bruyn H. (2017). Modern implant dentistry based on

osseointegration: 50 years of progress, current trends and open questions. *Periodontology* 2000, 73(1), 7–21.

173. Albrektsson T, Wennerberg A. (2005). The impact of oral implants - past and future, 1966-2042. *Journal (Canadian Dental Association)*, 71(5), 327.
174. Mavrogenis AF, Dimitriou R, Parvizi J, Babis GC. (2009) Biology of implant osseointegration. *J. of musculosk. & neur. Interact*. 9(2), 61–71.
175. Albrektsson T, Johansson C. (2001). Osteoinduction, osteoconduction and osseointegration. European spine journal: official publication of the European Spine Society, the European Spinal Deformity Society, and the European Section of the Cervical Spine Research Society, 10 Suppl 2(Suppl 2), S96–S101.
176. Xing G, Manon F, Guillaume H. (2019) Biomechanical behaviours of the bone–implant interface: a review. *J. R. Soc. Interface*.162019025920190259.
177. Folkman M, Becker A, Meinster I, Masri M, Ormianer Z. (2020) Comparison of bone-to-implant contact and bone volume around implants placed with or without site preparation: a histomorphometric study in rabbits. *Sci Rep* 10, 12446.
178. Shah FA, Thomsen P, Palmquist A. (2019) Osseointegration and current interpretations of the bone-implant interface. Acta Biomater. 84, 1–15.
179. Albrektsson T, Branemark PI, Hansson HA, Lindstrom J. (1981) Osseointegrated titanium implants requirements for ensuring a long-lasting, direct bone-to-implant anchorage in man. *Acta. Orthop Scand*. 52(2), 155–170.
180. Esposito M, Hirsch JM, Lekholm U, Thomsen P. (1998) Biological factors contributing to failures of osseointegrated oral implants. (I). Success criteria and epidemiology. *Eur. J. Oral Sci*. 106 (1), 527–551.
181. Brånemark RA. (1996) Biomechanical Study of Osseointegration. PhD Thesis, Göteborgs Universitet, Göteborg.
182. Schroeder A, Pohler O, Sutter F. (1976) Tissue reaction to an implant of a titanium hollow cylinder with a titanium surface spray layer. SSO Schweiz Monatsschr Zahnheilkd. 86(7), 713–27
183. Wang Y, Zhang Y, Miron RJ. (2016), Soft Tissues around Implants. *Clin. Imp. Dent. and Relat. Res*. 18, 618-634. License Number 5516350662694, Mar 26, 2023.
184. He Y, Gao Y, Ma Q, Zhang, X, Zhang Y, Song, W. (2022). Nanotopographical cues for regulation of macrophages and osteoclasts: emerging opportunities for osseointegration. *J. of nanobiotech*. 20(1), 510.

185. Guglielmotti MB, Olmedo DG, Cabrini RL. (2019). Research on implants and osseointegration. *Periodontology 2000*, 79(1), 178–189.
186. Kagan R, Adams J, Schulman C, Laursen R, Espana K, Yoo J, Doung YC, Hayden J. (2017) What Factors Are Associated With Failure of Compressive Osseointegration Fixation? *Clinic. orthopaed. and related res*. 475(3), 698–704.
187. Frost HM. (1994) Wolff's Law and bone's structural adaptations to mechanical usage: an overview for clinicians. *Angle Orthod*. 64, 175–188.
188. Guillaume B. (2016). Dental implants: A review. *Morphologie : bulletin de l'Association des anatomistes*, 100(331), 189–198.
189. Lekholm U, Zarb GA. (1985) Patient selection and preparation. In Brånemark P-I, Zarb GA, Albrektsson T, editors, Tissue integrated protheses, osseintegration in clinical denistry, Chicago, Quintessence.
190. Zarb GA. (1984) *Proceedings of the Toronto conference on osseointegration in clinical dentistry*. Mosby.
191. Misch CE. (2005) Short dental implants: a literature review and rationale for use. *Dentistry today*, 24(8), 64–68.
192. Misch CE. (1989) Bone classification, training keys to implant success. *Dentistry today*, 8(4), 39–44.
193. Scortecci GM, Misch CE, Odin G. (2019). Principles of Basal Implantology. In: Scortecci, G. (eds) Basal Implantology. Springer, Cham.
194. Misch CE. (1990) Density of bone: effect on treatment plans, surgical approach, healing and progressive bone loading. *Int J Oral Implant*. 6, 23–31.
195. Boyan BD, Sylvia VL, Liu Y, Sagun R, Cochran DL, Lohmann CH, Dean DD, Schwartz Z (1999) Surface roughness mediates its effects on osteoblasts via protein kinase A and phospholipase A2. Biomaterials 20(23-24):2305-10.
196. Donnelly E, Baker SP, Boskey AL, van der Meulen MC (2006) Effects of surface roughness and maximum load on the mechanical properties of cancellous bone measured by nanoindentation. *J Biomed Mater Res A* 77(2), 426-35.
197. Andreucci CA, Fonseca EMM, Jorge RN - A new simple machine that converts torque into steady-state pressure in solids. Poster presentations nº 46 – Session III, 7th Portuguese Meeting on Bioengineering ENBENG, Porto, Portugal, 22-23 june 2023.
198. Carlos Aurelio Andreucci, Elza M.M. Fonseca, Renato Natal Jorge. A new biomechanical simple machine, poster #87, DCE23 | 5th Doctoral Congress of

Engineering, Symposium on Biomedical Engineering, 15-16 junho 2023, Porto, Portugal.

199. Gobbi, S.J., Reinke, G., Gobbi, V.J., Rocha, Y., Sousa, T.P. & Coutinho, M.M. (2020) Biomaterial: Concepts and Basics Properties. *European International Journal of Science and Technology*, 9(2), 23-42.
200. Bertollo N, Walsh WR (2011) Drilling of bone: practicality, limitations and complications associated with surgical drill bits. In: Vaclav Klika (Ed.), Biomechanics in Applications. InTech.
201. Fernandes MG, Fonseca EM, Natal RM. Vaz M, Dias MI. (2017) Thermal analysis in drilling of ex vivo bovine bones. *Journal of Mechanics in Medicine and Biology*. 17(5), 1750082-98. DOI: https://doi.org/10.1142/S0219519417500828.
202. Sato M, Grese TA, Dodge JA, Bryant HU, Turner CH (1999) Emerging therapies for the prevention or treatment of postmenopausal osteoporosis. *J Med Chem* 42(1), 1- 24.
203. Jee WSS (2001) Integrated bone tissue physiology: anatomy and physiology. In: Cowin SC (Eds), Bone Mechanics Handbook. Second Edition, New York: CRC Press, pp. 1-34.
204. Cole JH, van der Meulen MC (2011) Whole bone mechanics and bone quality. Clin *Orthop Relat Res* 469(8), 2139-49.
205. Dahotre N, Joshi S (2016) Machining of bone and hard tissues. Springer International Publishing, Switzerland, pag.12. ISBN: 978-3-319-39158-8 (e-Book).
206. Rho JY, Kuhn-Spearing L, Zioupos P (1998) Mechanical properties and the hierarchical structure of bone. *Med Eng Phys* 20(2), 92-102.
207. Wu Z, Ovaert TC, Niebur GL (2012) Viscoelastic properties of human cortical bone tissue depend on gender and elastic modulus. *J Orthop Res* 30(5), 693-699.
208. An YH (2000) Mechanical properties of bone. In: An YH and Draughn RA (Eds), Mechanical Testing of Bone and the Bone-Implant Interface. Boca Raton, CRC press, pp.41-58.
209. Spatz HC, O'Leary EJ, Vincent JF (1996) Young's moduli and shear moduli in cortical bone. *Proc Biol Sci* 263(1368), 287-94.
210. Guo XE (2001) Mechanical Properties of Cortical Bone and Cancellous Bone Tissue. In: Cowin SC (Eds), Bone Mechanics Handbook. Second Edition, New York: CRC Press, pp. 10-1-10-18.
211. Reingewirtz Y, Szmukler-Moncler S, Senger B (1997) Influence of different parameters on bone heating and drilling time in implantology. *Clin Oral Implants Res* 8(3), 189-97. 155.

212. Eriksson AR, Albrektsson T, Albrektsson B (1984) Heat caused by drilling cortical bone. Temperature measured in vivo in patients and animals. *Acta Orthop Scand* 55(6), 629-31.
213. Li S, Wahab AA, Demirci E, Silberschmidt VV (2014) Penetration of cutting tool into cortical bone: Experimental and numerical investigation of anisotropic mechanical behaviour. *J Biomech* 47, 1117-1126.
214. Pandey RK, Panda SS (2013) Drilling of bone: A comprehensive review. *J Clin Orthop Trauma* 4, 15-30.
215. Karmani S, Lam F (2004) The design and function of surgical drills and K-wires. *Current Orthopaedics* 18(6), 484-490.
216. Comuzzi L, Tumedei M, Romasco T, et al. (2022) Insertion Torque, Removal Torque, and Resonance Frequency Analysis Values of Ultrashort, Short, and Standard Dental Implants: An In Vitro Study on Polyurethane Foam Sheets. *J Funct Biomater*. 14(1), 10. doi:10.3390/jfb14010010.
217. Kohli N, Stoddart JC, van Arkel RJ (2021) The limit of tolerable micromotion for implant osseointegration: a systematic review. *Sci Rep* 11, 10797 . https://doi.org/10.1038/s41598-021-90142-5.
218. Makary C, Rebaudi A, Mokbel N, Naaman N, (2011) Peak Insertion Torque Correlated to Histologically and Clinically Evaluated Bone Density. *Implant Dentistry* 20(3), 182-191. DOI: 10.1097/ID.0b013e31821662b9.
219. Stocchero M, Jinno Y, Toia M, et al. (2023) Effect of Drilling Preparation on Immediately Loaded Implants: An In Vivo Study in Sheep. *Int J Oral Maxillofac Implants*. 38(3), 607-618. doi:10.11607/jomi.9949.
220. Raz P, Meir H, Levartovsky S, Sebaoun A, Beitlitum I (2022). Primary Implant Stability Analysis of Different Dental Implant Connections and Designs-An In Vitro Comparative Study. *Materials*. 15(9), 3072. https://doi.org/10.3390/ma15093072.
221. Bulaqi HA, Mousavi Mashhadi M, Geramipanah F, Safari H, Paknejad M (2015) Effect of the coefficient of friction and tightening speed on the preload induced at the dental implant complex with the finite element method. *J Prosthet Dent*. 113(5), 405-411. doi:10.1016/j.prosdent.2014.09.021.
222. Hao CP, Cao NJ, Zhu YH, et al. (2021) The osseointegration and stability of dental implants with different surface treatments in animal models: a network meta-analysis. *Sci Rep*. 11, 13849. https://doi.org/10.1038/s41598-021-93307-4.

223. Kamel Saeed, Mohamed Nadim, Sherif Morcos, Hee-Moon Kyung, Abbadi El-Kady. (2017) In vitro assessment of maximum insertion and removal torque with three different miniscrews on artificial maxilla and mandible. *Journal of the World Federation of Orthodontists* 6, (3), 115-119. https://doi.org/10.1016/j.ejwf.2017.08.003.
224. Andreucci CA, Fonseca EMM, Jorge RN. A New Simplified Autogenous Sinus Lift Technique. (2023). *Bioengineering*. 10, 505. doi.org/10.3390/bioengineering10050505
225. Andreucci CA, Fonseca EMM, Jorge RN. (2023) Immediate Autogenous Bone Transplantation Using a Novel Kinetic Bioactive Screw 3D Design as a Dental Implant. *BioMedInformatics*. 3, 299-305. doi.org/10.3390/biomedinformatics3020020
226. Andreucci CA, Fonseca EMM, Natal Renato J. (2023) Bio-Lubricant Properties Analysis of Drilling an Innovative Design of Bioactive Kinetic Screw into Bone. *Designs*. 7, 21. doi.org/10.3390/designs7010021.
227. Zhao, R.; Yang, R.; Cooper, P.R.; Khurshid, Z.; Shavandi, A.; Ratnayake, J. (2021) Bone Grafts and Substitutes in Dentistry: A Review of Current Trends and Developments. *Molecules* 26, 3007.
228. Schmidt, A.H. (2021) Autologous bone graft: Is it still the gold standard? *Injury* 52, 18–22.
229. Azi, M.L.; Aprato, A.; Santi, I. (2016) Autologous bone graft in the treatment of post-traumatic bone defects: A systematic review and meta-analysis. *BMC Musculoskelet. Disord*. 17, 465.
230. Titsinides, S.; Agrogiannis, G.; Karatzas, T. (2019) Bone grafting materials in dentoalveolar reconstruction: A comprehensive review. *Jap. Dent. Sci Rev* 55, 26–32.
231. Cypher, T.J.; Grossman, J.P. (1996) Biological principles of bone graft healing. *J. Foot Ankle Surg*. 35, 413–417.
232. Shah, T.; Chacko, L.; Rakhewar, P.S.; Kale, R. (2017) Autogenous Bone Harvesting and Grafting: Intraoral Sites and Techniques’. *Int. J. Curr. Ad. Res*. 6, 4811–4819.
233. Doonquah, L.; Holmes, P.J.; Ranganathan, L.K.; Robertson, H. (2021) Bone grafting for implant surgery. *Oral Maxillofac. Surg. Clin*. 33, 211–229.
234. Athanasiou, V.T.; Papachristou, D.J.; Panagopoulos, A.; Saridis, A.; Scopa, C.D.; Megas, P. (2009) Histological comparison of autograft, allograft-DBM, xenograft, and synthetic grafts in a trabecular bone defect: An experimental study in rabbits. *Med. Sci. Monit*. 16, BR24–BR31
235. Jang, K.Y.; Lee, J.H.; Oh, S.H.; Ham, B.D.; Chung, S.M.; Lee, J.K.; Ku, J.K. (2020)

Bone graft materials for current implant dentistry. *J. Dent. Res*. 39, 1

236. Gehrke, S.A.; Mazón, P.; Del Fabbro, M.; Tumedei, M.; Aramburú Júnior, J.; Pérez-Díaz, L.; De Aza, P.N. (2019) Histological and histomorphometric analyses of two bovine bone blocks implanted in rabbit calvaria. *Symmetry* 11, 641.
237. Bae, E.B.; Kim, H.J.; Ahn, J.J.; Bae, H.Y.; Kim, H.J.; Huh, J.B. (2019) Comparison of bone regeneration between porcine-derived and bovine-derived xenografts in rat calvarial defects: A non-inferiority study. *Materials* 12, 3412.
238. Janjua, O.S.; Qureshi, S.M.; Shaikh, M.S.; Alnazzawi, A.; Rodriguez-Lozano, F.J.; Pecci-Lloret, M.P.; Zafar, M.S. (2022) Autogenous Tooth Bone Grafts for Repair and Regeneration of Maxillofacial Defects: A Narrative Review. *Int. J. Environ. Res. Public Health* 19, 3690. https://doi.org/10.3390/ijerph19063690
239. Pripatnanont, P.; Nuntanaranont, T.; Vongvatcharanon, S. (2019) Proportion of deproteinized bovine bone and autogenous bone affects bone formation in the treatment of calvarial defects in rabbits. *Int. J. Oral Maxillofac. Surg* 38, 356–362.
240. Chang, L.C. (2021) Comparison of Clinical Parameters in Dental Implant Therapy between Implant Site Development Using Porcine-and Bovine-Derived Xenografts. *Technologies* 9, 72.
241. Brink, O. (2021) The choice between allograft or demineralized bone matrix is not unambiguous in trauma surgery. *Injury* 52 (Suppl. 2), S2–S28.
242. Zamborsky, R.; Svec, A.; Bohac, M.; Kilian, M.; Kokavec, M. (2016) Infection in Bone Allograft Transplants. *Exp. Clin. Transplant* 14, 484–490.
243. Dziki, J.L.; Huleihel, L.; Scarritt, M.E.; Badylak, S.F. (2017) Extracellular Matrix Bioscaffolds as Immunomodulatory Biomaterials. *Tissue Eng. Part A* 23, 1152–1159
244. Anitua, E. (2018) Biological drilling: Implant site preparation in a conservative manner and obtaining autogenous bone grafts. *Balk. J. Dent. Med*. 22, 98–101
245. Xing, G.; Manon, F.; Guillaume, H. (2019) Biomechanical behaviours of the bone–implant interface: A review. *J. R. Soc. Interface* 16, 20190259
246. Giesenhagen, B.; Martin, N.; Jung, O.; Barbeck, M. (2019) Bone Augmentation and Simultaneous Implant Placement with Allogenic Bone Rings and Analysis of Its Purification Success. *Materials* 12, 1291.
247. Raghoebar, GM, Onclin, P, Boven, GC, et al. (2019) Long-term effectiveness of maxillary sinus floor augmentation: A systematic review and meta-analysis. *J Clin Periodontol*. 46(Suppl. 21): 307– 318.

248. Lie N, Merten HA, Yamauchi K, Wiltfang J, Kessler P. (2019) Pre-implantological bone formation in the floor of the maxillary sinus in a self-supporting space. *Journal of Cranio-Maxillofacial Surgery* 1, 47(3), 454-60.
249. Kuik K, Putters TF, Schortinghuis J, van Minnen B, Vissink A, Raghoebar GM. (2016) Donor site morbidity of anterior iliac crest and calvarium bone grafts: a comparative case-control study. *Journal of Cranio-Maxillofacial Surgery* 1, 44(4), 364-8.
250. Lie SAN, Claessen RMMA, Leung CAW, Merten HA, Kessler PAWH. (2022) Non-grafted versus grafted sinus lift procedures for implantation in the atrophic maxilla: a systematic review and meta-analysis of randomized controlled trials. *International Journal of Oral and Maxillofacial Surgery* 51, 1 122-132.
251. Andreucci CA (2022). Constructive arrangement applied in screw for bone implant (Brazil/International Patent No. WO2022036425A1). WIPO (PCT). URL WO2022036425A1-Constructive arrangement applied to screw for bone implant-Google Patents.
252. Andreucci CA, Fonseca EMM, Natal RJ. Bioactive Kinetic Screw Drill-And-Seal Technique: Innovative Design and Aseptic Bone Implant, Livro de Resumos, Ana Amaro, Luis Roseiro et al. (Eds), X Congresso da Sociedade Portuguesa de Biomecânica, pp.271-272, 5-6 maio 2023, Figueira da Foz, ISBN: 978-989-33-4641-9, Portugal.
253. Marco M, Rodríguez-Millán M, Santiuste C, Giner E, Henar Miguélez M (2015) A review on recent advances in numerical modelling of bone cutting. *J Mech Behav Biomed Mater* 44, 179-201.
254. Fernandes, M. (2017). Analysis of bone damage during drilling processes. Thesis of Doctorate. Faculdade de Engenharia da Universidade do Porto.
255. Chang CH, Lin LY, Roberts WE. (2021) Orthodontic bone screws: A quick update and its promising future. *Orthod Craniofac Res*. 24 Suppl 1, 75-82. doi:10.1111/ocr.12429.
256. Morarend C, Qian F, Marshall SD, et al. (2009) Effect of screw diameter on orthodontic skeletal anchorage. *Am J Orthod Dentofacial Orthop* 136(2), 224-229.
257. Huja SS, Litsky AS, Beck FM, Johnson KA, Larsen PE. (2005) Pull-out strength of monocortical screws placed in the maxillae and mandibles of dogs. *American Journal of Orthodontics and Dentofacial Orthopedics* 127, 3, 307-313.
258. Vieira CA, Pires F, Hattori WT, de Araújo CA, Garcia-Junior MA, Zanetta-Barbosa D. (2021) Structural resistance of orthodontic mini-screws inserted for extra-alveolar anchorage. Resistência estrutural de mini-aparafusos ortodônticos inseridos para

ancoragem extra-alveolar. *Acta Odontol Latinoam*. 34(1), 27-34.

259. Morarend C, Qian F, Marshall SD, Southard KA, Grosland NM, Morgan TA, McManus M, Southard TE. (2009) Effect of screw diameter on orthodontic skeletal anchorage. *American Journal of Orthodontics and Dentofacial Orthopedics* 136, 2, 224-229.
260. Morarend C, Qian F, Marshall SD, Southard KA, Grosland NM, Morgan TA, McManus M, Southard TE. (2009) Effect of screw diameter on orthodontic skeletal anchorage. *American Journal of Orthodontics and Dentofacial Orthopedics* 136, 2, 224-229.
261. Roberts WE, Chang CH, Chen J, Brezniak N, Yadav S. (2022) Integrating skeletal anchorage into fixed and aligner biomechanics. *J World Fed Orthod*. 11(4), 95-106.
262. Chang CH, Lin LY, Roberts WE. (2021) Orthodontic bone screws: A quick update and its promising future. *Orthod Craniofac Res*. 24 Suppl 1, 75-82.
263. Coletti DP, Salama A, Caccamese JF Jr. (2007) Application of intermaxillary fixation screws in maxillofacial trauma. *J Oral Maxillofac Surg*. 65(9), 1746-1750.
264. Rai AJ, Datarkar AN, Borle RM. (2009) Customised screw for intermaxillary fixation of maxillofacial injuries. *Br J Oral Maxillofac Surg*. 47(4), 325-326.

CHAPTER III

New biomechanism: A Bioactive Kinetic Screw*

Carlos Aurelio Andreucci[1], Elza Fonseca[2], Renato Natal Jorge[3]

[1]Faculty of Engineering of the University of Porto (FEUP), Portugal
[2]School of Engineering, Polytechnic of Porto (ISEP), Mechanical Engineering Department, Portugal
[3]Faculty of Engineering of the University of Porto (FEUP), Portugal

**Chapter in book: Advances and Current Trends in Biomechanics*. 2021 1st edition, Taylor & Francis, CRS press, ISBN 9781003217152

DOI: 10.1201/9781003217152-1

Abstract

A new biomechanism, Bioactive Kinetic Screw (BKS), for bone screws created by the first author will be presented through a bone implant screw, in which the bone particles, cells and molecules removed during bone drilling will be used as an autogenous homogeneous transplant in the same implant site, aiming to obtain primary and secondary bone stability simplifying the surgical procedure (one step) and improving healing process. With this new biomechanism we will have the possibility to be proven, of obtaining an intermediate phase of healing between primary and secondary bone stability, using the natural process of inflammation, healing, repair and in the final stage of osseointegration, we could have a bone remodelling through the implant screw.

1 Introduction

The Develop a biomechanism for bone fixation that involves desirable biological and mechanical characteristics in a biomechanical rehabilitation in a safe and practical way, are the founding principles of all the specialties involved in these studies; from research with molecules, proteins and genetic therapies to the functional biomechanical restoration of limbs and organs (Ad-ell et al. 1981). The successful close interaction of implant surfaces with their biological environment is one of the most crucial issues in biomechanics of implantology (Albrektsson and Johansson 2001). Bone is a strong and lightweight composite multi-scale anisotropic material which presents a hierarchy of microstructures. Besides its multi-scale nature, bone can adapt its structure through remodelling phenomena, after a primary mechanical stability, which induces changes in its structure and biomechanical properties to accommodate the presence of an implant (secondary stability). Despite the difficulties, the industrial design of implants has often been driven by an aggressive ‘copycat’ marketing approach rather than by fundamental advances in biomechanic (Abraham 2014). The difficulty also comes from the multi-factorial determinants of the problem, given by the implant properties, by the surgical protocol (which is not standardized) and by the patient's bone quality and its mechanical behaviour. The implant osseointegration is far from being understood, and measuring peri-prosthetic bone properties remains a challenge. Implant surface treatment and coatings (surface topography) are responsible for increase the surface area of the bone-implant contact (BIC), decrease the stresses, and enhance adhesion qualities to the BIC interface at initial healing. Today we have improvements in biomechanical characteristics that optimize primary and secondary stability, mainly related to the screw threads (primary stability) and the surface of the screws (secondary stability) (Abuhussein et al. 2010). Using Finite Element Analysis (FEA), some authors (Chang et al. 2012) evaluated the pattern of micro motion within implants and surrounding bone with different thread designs under immediate loading. The results revealed that all micro motion was located near the interface of cortical and cancellous bone and the square thread profile had the most favourable micro motion value. Multiple studies (Abuhussein et al. 2010) demonstrated that implants with smaller pitch showed the greater surface area and better stress distribution particularly in low-density bone. It has been a common clinical observation that bone is often lost to the first thread after loading, regardless of the manufacturer type or design the bone loss often stops at the first thread be-cause changes the shear load created by the crest module to a component of compressive loading (Abuhussein et al. 2010).The bone response, which means rate, quantity and quality, are related to implant surface properties, the composition and charges are critical for protein adsorption and cell attachment. Hydrophilic surfaces seem to favor the interactions with biological fluids and cells when compared to the hydrophobic ones and hydrophilicity is affected by the surface chemical composition (Adell et al. 1981). Anodized surfaces interfere positively in bone response with higher values for biomechanical and histomorphometric tests when compared to machined surfaces. Calcium phosphate (CaP) coatings, mainly composed by hydroxyapatite, have been used as a biocompatible, osteoconductive and resorbable blasting materials. The idea behind the clinical use of hydroxyapatite is to use a compound with a similar chemical composition as the mineral phase of the bone to avoid connective tissue encapsulation and promote peri-implant bone apposition. In some studies (Su et al. 2013) nano-hydroxyapatite/polyamide 66/glass fiber (n-HA/PA66/GF) was used as bioactive bone screws in comparison with metallic screws to investigate the in vivo biocompatibility, internal fixation properties and osteogenesis. The n-HA/PA66/GF screws exhibited good biocompatibility, high mechanical strength, and extensive osteogenesis in the host bone; the maximum push-out load of the bioactive screws was greater than that of the metallic screws. Bioactive materials, able to induce hydroxyapatite precipitation in contact with body fluids, are of great interest because of their bone bonding capacity. A comparison among bioactive materials with different surface features (chemistry, charge, morphology) was performed to verify case by case the mechanism of action and the relationship with kinetics and type of precipitated hydroxyapatite over time. The results suggest that the OH groups on the surface have several effects on the surface chemical behaviour: a detailed description of their abundance and chemical acidic/basic reactivity can be helpful for a better understanding of surface chemistry. Abundance of OH groups mainly affect hydrophilicity of surfaces, while the isoelectric point, surface charge and ions adsorption from the solution mainly depends on the OH acidic/basic strength. The main outcome of the present research is a detailed understanding of the bone implant screwing processes, contributing for the application of optimum implant screw insertion parameters that will minimize the bone damage due the invasive procedure, trying to obtain primary and secondary stability optimizing healing process. The results on this new model BKS contribute to a comprehensive understanding of thermomechanical aspects of bone drilling and screwing process and associated predictive models creating a new simplified protocol for implant screws surgery. The new developed model and protocol if succeeds in results, can be used in any bone surgery when implant screw integration is needed. The drilling and the new implant screwing process under different aspects provide an important tool that will enable for the health professionals to plan an accurate and safe surgery with better post-surgery patient recovery.

2 Materials and Methods

The use of screws for bone implants and fixations has been done in a safe and systematic way since 1985 (Albrektsson and Albrektsson 1987). Biomechanics has not improved real changes since then, with the focus given more over the last four decades to the surfaces and threads of the screws. The innovation of a new biomechanism (BKS) indicated in Figure 1, using biomechanical concepts already well known and structured in the same implant screw, will be described In the new biomechanism the particles removed during bone drilling and screwing at the same time due to the new characteristics, will use the chips (particulate bone, cells and molecules) to fill the through hole by the drill flutes in the new screw. The screw was created based on the concepts of using drill bits for bone drilling and screws for fixing bone implants. Bearing in mind that the traditional drill flutes eliminate the particulate material to be removed after cutting, the author created a limit for these flutes that are found in a through hole connecting and limiting these cutting grooves avoiding the removal of particles coming from the drilling. This drilling particulate material will be compacted in and through the screw, increasing the bone contact surface and creating a bone bridge of particulate material through the screw (Elsayed 2019).Developing a screw that will also be the drill bit for bone implants fixation, creates the opportunity to decrease the drilling stages in the surgical protocols, using and not discarding the bone from the site where the implant will be screwed, taking advantage of the natural characteristics of the particulate bone, blood, molecules and cells of the implanted site, stimulating the biological processes of bone healing. The advantages obtained with the simplification of surgical protocols for implants and the optimization of immediate and long-term results, justify the research of a new biomechanism and its practical results in genetic, molecular and cellular levels in bone healing for biomechanical efficiency (Degirmenci and Atala 2019).The new biomechanism can be applied to any biomaterial for implants screws, any kind of surfaces, coatings and threads, which provides more possibilities for practical applications and optimization of results. The characteristics that were considered today to optimize the success rate in situations of low quality and bone quantity were chosen, where the risks of implant failures are lower when related to implant design. Commercially pure titanium will be used as standard biomaterial for being the oldest, accepted and well-studied short and long term results for dental implants; remembering that the new biomechanism can be applied to any biomaterial for bone screws, for example nano-hydroxyapatite/polyamide 66/glass fiber (n-HA/PA66/GF),(Su et al. 2013) any kind of surfaces, coatings and threads (Abuhussein et al. 2010), which pro-vides more possibilities for practical applications and optimization of results.

3 Results and Discussion

The studies are in their manufacturing phase of the new biomechanism in the form of a dental implant to perform the laboratory tests that will be used to validate the computational models. The resources and financing for the research have already been approved and are in their final phase for the beginning of data collection. The possibility of obtaining bone healing through the screw can become a new reality for bone implants, where we will have for the first time direct bone to bone contact through the screw. In every bone drilling for insertion of an implant screw, there is a bone loss with almost all the measurements of the screw used. Clearly taking advantage of this particulate bone, which is normally discarded during drilling, is in itself already a great benefit for the patient and the surgeon. The simplification of the surgical technique is also a great natural benefit of the new bio-mechanism, since with a lower number of intermediate drills and the direct self-drilling of the implant in cases of low bone quality (trabecular bones) we can decrease the time and the risks related to the surgical technique (Steigenga 2003).In every bone drilling for insertion of an implant screw, there is a bone loss with almost all the measurements of the screw used. Clearly taking advantage of this particulate bone, which is normally discarded during drilling, is in itself already a great benefit for the patient and the surgeon. The natural presence of bone through the screw and direct bone contact through the hole pre-sent in the new biomechanism as seeing on Figure 1, will enable the new formation of blood vessels and better bone quality around the implant, to be tested (Elsayed 2019).

Figure 1. New Bioactive Kinetic Screw (BKS) made by the first author.

4 Conclusions

As The new BKS created by the first author allows the use of the bone, blood, cells, and molecules removed in the bone drilling to be introduced through the screw using an innovative insertion and compacting biomechanism, based on biomechanical concepts already proven and used since the initial use of screws for fixations and bone implants. The innovation is based on the system created by associating different biomechanical concepts in the same screw, optimizing efficiency in molecular, cellular, and macroscopic levels. Determining the design of a bone implant for all the practical clinical conditions that present itself to achieve osseointegration is not yet fully possible. In cases of low quality and bone quantity, we find the greatest number of implant failures. With this factor in mind, we opted to use anodized surface with calcium phosphate coating (CaP), square threads and small pitch in the new biomechanism to be tested. All these features can be modified according to individual surgery plan. More studies should confirm these properties and their consequences for bone healing of screws.

References

Abuhussein, H., Pagni, G., Rebaudi, A., Wang, H. L. 2010. The effect of thread pattern upon implant osseointegration. Clinical Oral Implants Research. 21: 129-136.

Abraham, C. M. 2014. A Brief Historical Perspective on Dental Implants, Their Surface Coatings and Treatments. The Open Dentistry Journal, 8(Suppl 1-M2): 50-55.

Adell, R., Lekholm, U., Rockler, B., Branemark, P. 1981. A 15 year study of osseointegrated implants in the treatment of the edentulous jaw. International J. Oral Surgery, 10(6): 387-416.

Albrektsson, T., Johansson, C. 2001. Osteoinduction, osteoconduction and osseointegration. Europe Spine J. 10(Suppl 2): S96–S101.

Albrektsson, T., Albrektsson, B. 1987. Osseointegration of bone implants: A review of an alternative mode of fixation. Acta Orthopaedica Scandinavica, 58(5): 567-577.

Chang, P. K., Chen, Y. C., Huang, C. C., Lu, W. H., Chen, Y. C., et al. 2012. Distribution of micromotion in implants and alveolar bone with different thread profiles in immediate loading: a finite element study. International J Oral Maxillofacial Implants, 27: 96-101.

Degirmenci, K., Atala, M. H. 2019. The impact of different dental implant surface properties to osseointegration success of dental implants: A systematic review. Clinical Oral Implants Research, 30(19): 280.

Elsayed, M.D. 2019. Biomechanical Factors That Influence the Bone-Implant-Interface. Research Rep Oral Maxillofacial Surgery. 3: 1-14.

Steigenga, J. T., al-Shammari, K. F., Nociti, F. H., Misch, C. E., Wang, H. L. 2003. Dental implant design and its relationship to long-term implant success. Implant Dentistry. 12: 306-317.

Su, B., Peng, X., Jiang, D., Wu, J., Qiao, B., Li, W., et al. 2013. In Vitro and In Vivo Evalua-tions of Nano-Hydroxyapatite/Polyamide 66/Glass Fiber (n-HA/PA66/GF) as a Novel Bioac-tive Bone Screw. PloS one, 8(7): 1-9.

CHAPTER IV

Static in Bone Implants: Standard Steady-State Torque and Primary Stability in a Bioactive Kinetic Screw*

Carlos Aurelio Andreucci[1], Elza Fonseca[2], Renato Natal Jorge[3]

[1]Faculty of Engineering of the University of Porto (FEUP), Portugal
[2]School of Engineering, Polytechnic of Porto (ISEP), Mechanical Engineering Department, Portugal
[3]Faculty of Engineering of the University of Porto (FEUP), Portugal

**Submitted to an International Journal (under review), July 2023*

Abstract

The Establishing a standard measurement for drilling and screwing bone implants in different amounts and qualities of bone tissue, in a simple and adequate way to control and predict results, is the gold standard for successful primary stability and better results on long-term osseointegration. So far, the maximum insertion torque (MIT) has been used as the main parameter to achieve success in primary stability and osseointegration, although it has shown conflicting results in the literature for over four decades when predicting standard or minimum values. Basically, the surgeon's experience guides the planning and execution of the surgical procedure, adapted in each case according to his tactile experience, guided by X-ray analysis and the bone and general conditions of the patient. In this work, using a new biomechanical simple machine as a dental implant, a new method will be described mathematically and experimentally, which standardizes the compression and torque in the implant-bone contact, in five different bone densities, during the achievement of mechanical primary stability. The results described the relationship between the MIT, maximum removal torque (MRT), and maximum force of static friction between implant-bone and bone-to-bone, achieving a controlled and predictable standard steady-state torque that maintains equilibrium in elastic stress for the primary stability of bone implants, hereby established for an innovative simple machine Bioactive Kinetic Screw (BKS).

Keywords: Statics; Bone Implants; Maximum Insertion Torque; Maximum Removal Torque; Standard Torque.

1 Introduction

Torque (T) is a special kind of force that applies rotational or angular acceleration in an object. If it is not moving it is going to start spinning faster or slower inherent to the force applied. Rotational equilibrium means that there is no torque, no rotational or angular acceleration in an object. Anytime a force goes straight through the center of rotation of an object, there is no torque from that force ($T_{net} = 0$) [1]. Torque equals the force applied times the distance between this force and the centre of rotation (T = Fr) and its unit Nm, a transcription of kg m/s^2.

In bone osteotomies, drilling, and screwing, torque is manually or by motor applied into the bone, controlled by the surgeon tactile experience. Especially for drilling and screwing bone implants, using an electric surgical motor enhance the predictable results for the surgeon by describing torque, speed, and rotational parameters for future improvements in the surgical techniques [2]. Three factors determine the type of work a motor can produce, speed, torque, and horsepower. Speed is defined as how fast the motor performs its work, the typical units of measurement for rotational motor speed are revolutions per minute (rpm). Work is defined as a force applied over a distance, the same definition of torque that produces rotation when a force acts on a radius (r). Horsepower (HP) is defined as the rate at which work is accomplished being another unit of measurement for power and can be translated into Watts (1 HP = 746 Watts), BTUs (1HP = 2545 BTU), Joules (1 HP = 1.055 J), or any unit of power [3].

Manipulating the connection among speed, torque, and horsepower, an understanding of how they are related to surgical motors, increases the precision during bone osteotomies, and offers parameters for controlled results. If torque remains constant, speed and horsepower are proportional. As the speed or rpm increases, HP increases to maintain constant torque. If speed decreases, HP decreases to maintain constant torque [4].

Friction occurs when two materials resists moving against one another like titanium screwed into the bone. The coefficient of static friction depends on the combined effects of material deformation characteristics and surface roughness, both of which originate from the chemical bonding between the atoms of the materials between their surfaces and any adsorbed material. The fractality of surfaces, a parameter that describes the integration of structural and molecular interactions across a range of scales of surface roughness, plays an important role in determining the magnitude of static friction [5]. The amount of friction generated depends primarily on the materials which are in sliding contact, the coefficient of friction (μ) is a dimensionless quantity that describes the ratio of the force of the friction between two bodies and the force of them pressing together. This coefficient can be used to help to determine the amount of force required to move a drill bit, a screw, or a saw in the bone. The amount of force required to slide a load and overcome the maximum static friction (μ_s), and start the kinetic friction, is calculated by multiplying the coefficient of friction (μ) by the weight of the load for horizontal forces, where F_f is the frictional force and N is the normal force (mg), as seen in equation [6].

$$F_f = \mu N \tag{1}$$

If an object is on a flat surface and subjected to an external force sliding, then the normal force between the object and the surface is N = mg + Fd only where mg is the object's weight and Fd is the component of the external force (MIT). The coefficient of friction has different values for static friction and kinetic friction. In static friction, the frictional force resists force that is applied to an object, and the object remains at rest, like dental implants totally screwed into the bone, resulting from molecular interactions between the implant and the bone surface. In kinetic friction, the frictional force resists the motion of an object like during the drilling bone. The frictional force itself is directed oppositely to the motion of the object.

How hard the materials are pressed together puts more of their surfaces in contact with each other, and that's where the BKS increased material density plays an advantage [8]. Static friction is required for dental implants primary stability or mechanical stability avoiding micromovements that lead to increased failure in osseointegration. Maximum insertion torque (MIT) is mistakenly used as a parameter for mechanical initial stability in dental implants clinical and experimental procedures, as observed by conflicting results in literature for decades [9]. Over-tightening the implant into the bone will strip the bone threads, while under-tightening may cause the screws to loosen.

Achieving higher torques in dental implants due to an increased coefficient of friction and not due to undersized drilling compression, increases the bone-implant contact (BIC) surface area without overloading the bone with high stress/strain, as is the case with MIT, mainly due to the difference between the undersized drilling in the bone (smaller diameter) and the geometry of the metal bone implant (screwed under pressure). The different hardness of bone and metal implants increase the stress/strain in the bone, increasing the risk of osseointegration failure

[10]. As bone density varies, it is impossible to accurately predict the optimised undersize of the holes for each specific implant geometry. It is used in the literature on different undersized drilling protocols, related to bone densities and implant properties without clear correlation of the results [11]. The higher torque obtained by compression of the implant screw into the bone can cause initial mechanical stability, but it also shows an osteoclastic increase in the early days of the healing process, increasing the risk of implant failure [12]. Once fully screwed into the bone, the dental implant reaches static friction (stability). This is the parameter that prevents micro-movements of the implant in the bone and its value determines the load that can be mechanically supported at this stage of the healing process without compromising short and long term osseointegration.

If, immediately after obtaining MIT, we apply an anti-torque (MRT) to the same implant, as soon as it begins to move, we obtain exactly the value of torque (force) required to overcome maximum force of static friction, or maximum static friction torque (MSFT) applied to screw removal, equivalent to the maximum removal torque (MRT) in implants, which has already been robustly described in the literature. This is only possible in experimental studies in the laboratory or on animals, otherwise, osseointegration is compromised by loosening the implant [13]. The implant site preparation protocol should be carefully chosen to reduce implant micromovement below the 50-150 μm threshold and to provide adequate stability and prosthetic support according to the planned loading protocol (delayed, early, or immediate) [14]. This implant-bone interface contact (BIC) does not consider the contact volume between these materials. With different drilling parameters and protocols, its unpredictable in humans that the maximum static friction torque (MSFT) or MRT, and different MIT standards are described in the literature as ideal, with differences between 10 to 150 Ncm, showing discrepancies and inconsistencies in the results [15, 16]. There are also no correlations between different primary stability analysis tests, such as resonance frequency analysis (RFA), implant stability quotient (ISQ), insertion energy (IE) measurements, i.e., the total energy required to place the implant in its site, and implant to bone MIT [17]. In a systematic review, the mean value of micromotion for implants that osseointegrated was 32% of the mean value for those that did not (112 ± 176 μm versus 349 ± 231 μm, $p < 0.001$) [14].

As it is also a drill bit, with BKS there is no lateral compression after total insertion into the bone bed due to the bone being cut by the flutes of the same size and geometry as the BKS implant. The retention and immobilization of the BKS being done primarily by the resulting force (torque) applied through the implant into the bone, correlated with the coefficient of kinetic friction of the implant into the bone (μ_{KIB}) and the coefficient of kinetic friction (μ_{KBB}) of the compacted bone (chips) inside and through the BKS to the bone bed site (μ_{KBB}, or bone to bone kinetic friction) until the torque is removed, becoming the BKS coefficient of static friction (BKSμ_{SF}) [18, 19]. The depth where the torque increases more abruptly has been considered as the point of flute clogging (bone chips) and used as a performance criterion for chip-evacuation capability [20, 21]. In BKS insertion (μ_{KIB}), the increase in torque indicates the start of compaction of the collected material, where the addition of more torque continuously reaches the limit (μ_{KBB}) allowed and established by the properties of the materials used, without breaking the integrity of the system and causing rupture (ultimate strength) [21].

Chips can be classified as granular solids, which are characterised as a group of particles of approximately the same size. Granular solids have characteristics of both fluids and solids. They occupy the internal geometry of the BKS, as shown in Figure 1, where they fill, exert pressure on the container boundaries, and flow through openings like fluids. However, like solids, they have cohesive strength, can have non-isotropic stress distributions, and have shear stresses proportional to normal stress [20].

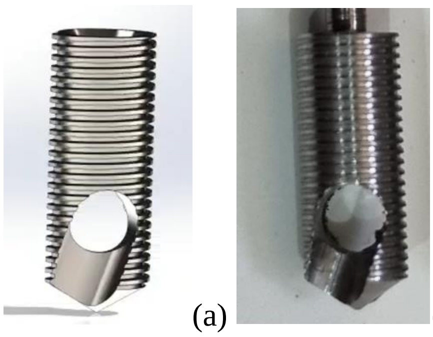

(a) (b)

Figure 1. (a) BKS, innovative biomechanism for bone screws and implants; (b) BKS machined for the experiment in steel 304.

Bone drilling chips (bone graft) collected during implant site preparation can be reused as homogenous autologous bone graft material to increase the coefficient of friction values due to cohesive molecular retention of bone particles in the bone bed site [20, 21]. It is well known in the literature that living cells have been found in bone chips even after drilling with twist drills [22]. The measured value obtained in vitro, and ex vivo experiments determined the torque values for five different synthetic bone densities (polyurethane foam) PCF 10, 15, 20, 30, and 40. The biomechanical results can be mathematically hypothesized for human application by the similar and proportional relationship observed in this and other experimental tests [23] even with different bone densities, using the same protocol [24].

2 Materials and Methods

The forces of torque (MIT and MRT), and coefficient of friction analysis, covered by this study, aim to find the required rotational moment to push (insertion) and pull (removal) BKS to impending motion. As impending motion is the threshold between the system holding still and moving, the knowledge of the moments required at impending motion allows you to interpret what happens to the BKS system in static-but-not-impending conditions as well. Since all friction is impending, we will use the maximum coefficient of static friction (μ_{SF}) after reaching the MIT (equal to F_d) and the related friction force (F_f or MRT) to describe the maximum insertion force associated directly to (μ_{SF}) by the equation (2), where the normal force (N) equals to weight (mg), applied as follows:

$$\mu_{SF} = \frac{F_f}{N+F_d} = \frac{MRT_{BKS}}{mg+MIT_{BKS}} \qquad (2)$$

The innovation presented by the BKS bone implant is that after the implant is fully screwed in (MIT), it achieves static friction without lateral pressure into the bone, due to its drill properties [25-28]. By applying the anti-torque (MRT) to the BKS, as soon as the BKS implant starts to move, we can precisely measure the value of the maximum static friction force limit that will avoid micro-movements of the implant inside the bone to achieve successful primary stability (mechanical stability).

In the experiment to determine the maximum static friction force (F_{SF}), a new standard torque (ST) obtained will be proposed, correlated with success or failure probabilities in osseointegration. Our *ST* proposal is described by the *MIT* relationship with *MRT*, obtaining the amount of force (F_{SF}) to start unscrewing the implant (BKS). This approach is only valid for individual measurements on implants that are inserted without any bone bed compression when the bone bed size is drilled the same size as the implant geometry. It is not possible to obtain controlled similar values and predictions using this method, in any protocol of undersized bone drilling, and perforations with unthreaded holes, applied in bone implants. The equation (3) to determine the standard torque (*ST*) for BKS is:

$$ST_{BKS} = MRT_{BKS} \tag{3}$$

The ST will be a non-absolute value but proportional to the bone densities applied. The higher the MIT the higher the MRT, but due to the properties of BKS the measured difference between MIT and MRT remains proportional and predictable. The Coefficient of Friction (μ) is the measure of the amount of interaction between two surfaces related to the friction between them, as they slide over one another, roll over one another, or two surfaces are in contact but not moving. They are acted upon by forces in opposite directions, and then, since they do not move and there is still an interaction, the amount of interaction depends on the coefficient of friction between them. In maximum static friction when a force (F_{SF}) is applied and eventually the object begins to move this is defined as the static coefficient of friction (μ_{SF}), distinct from the kinetic coefficient of friction. Mathematically it can be represented by an equation (4) between the MRT_{BKS} that is equal to static friction force (F_{SF}), the force required to start moving the implant anticlockwise, divided by the normal Force (N) sum with the external force (MIT) of the object as follows equations:

$$MRT_{BKS} = F_{SF} \tag{4}$$

$$\mu_{SF} = \frac{F_{SF}}{mg+F_d} \tag{5}$$

The force (MRT_{BKS} or F_{SF}) required to start moving the BKS implant divided by the normal force N = mg + Fd only where mg is the object's weight and Fd is the component of the external force (MIT), is equal to the maximum static coefficient of friction (μ_{SF}) of the BKS into the bone.

With the experimental results obtaining the MRT_{BKS} that is equal to F_{SF} we can precisely determine the static coefficient of friction (μ_{SF}) using equations (4), and (5), correlating it in different bone densities. Measuring the MRT_{BKS} and applying its correlation with a static coefficient of friction (μ_{SF}), we can predict the amount of force (F_{SF}) or standard torque (ST_{BKS}) that the mechanical primary stability will support to avoid micromotions and lead to secondary stability promoting osseointegration as seeing on equation (3).

Knowing μ_{SF} and N applying equation (5) we can determine F_{SF}. From equation (4) we know that F_{SF} is equal to MRT_{BKS}. Without applying MRT_{BKS} into the implant, the standard torque (ST_{BKS}) proposed can be mathematically determined with precision and safety, without compromising osseointegration, allowing to have improved data collection, precise adjustments on the surgical protocols planning, and controlling the osseointegration predictable results based on mechanical primary stability.

Twenty BKS implants [--] were machined in steel 304 with the size of 10 mm length and 4 mm diameter to be tested in synthetic bones (Nacional Ossos Ltda.) in five distinct densities, PCF 10, 15, 20, 30 and 40. Implants were inserted manually with a surgical electrical motor (Tech Drill) and the torques (MIT and MRT) was measured by TQ 8801 digital torquemeter. The MIT and MRT values were considered individually for each implant to achieve accuracy in comparing the results of the coefficient of friction and the amount of compacted bone inside. visual inspection of the quality of bone compaction was performed during the removal of bone from the BKS during weighing, as seen in figure 2.


(a)
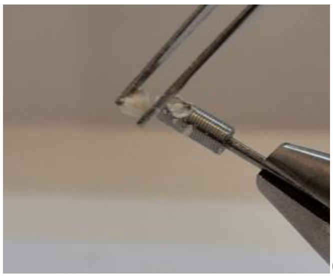
(b)

Figure 2. (a) Synthetic bones in five distinct densities (PCF 10, PCF 15, PCF 20, PCF 30, and PCF 40); (b) BKS filled with PCF 10 synthetic bone after insertion and removal and densification of the material.

All BKS implants were weighed before bone insertion and after total removal to accurately measure the amount of bone graft collected using the Brifit precision digital scale, and these values were used individually in the calculations as seen in Figure 3.

(a)


(b)

Figure 3. (a) BKS, innovative biomechanism for bone screws and implants dry weight before insertion into the bones; (b) and BKS filled with synthetic bone after insertion to achieve MIT and complete removal of the BKS after obtaining MRT.

3 Results and Discussion

A new measure of the volumetric coefficient of friction (μV) when there is full contact between the walls of a volume of material that is inserted into another material, with one of the surfaces being subjected to the insertion force was determined in this work. In all the measurements made, the MRT was always higher than the MIT, which is an innovative property of the BKS used as a dental implant in this work. A pattern was observed when obtaining the torque values. At the beginning of the simultaneous drilling and screwing, a constant torque is obtained, which gradually increases until it reaches the MIT as soon as the material begins to be compacted inside the BKS. It has been observed that the compaction and densification of the material inside the BKS (figure 2b) produces the superior locking of the BKS, requiring a higher torque (MRT) for its removal than that used for its insertion (MIT). This innovative feature represents a major advance in the field of implantology, considering the precise control of the values obtained and their standardisation to determine the torque and force that immediate connections and prostheses can withstand. In addition, the densification of the bone inside the BKS makes the low-density bones (PCF 10 and PCF 15) inside the BKS similar or superior to the amounts of higher density bones studied here (PCF 20, PCF 30) [8]. Considering the non-uniform biomechanical properties of the bones, obtaining a precise relationship proportional to the MIT obtained and its relationship with μ_{SF} and MRT, we have obtained a new fundamental tool through BKS properties for understanding the relationship of primary stability of bone implants, the contact surface and its relationship with bone quantity and quality.

Ten measurements were taken for each bone density and only the lowest values were used in this study to maintain a direct relationship between individual MIT and MRT values. It was decided not to use the average of the values obtained from all the measurements to accurately determine the values of the coefficient of friction for each bone density studied. The lower values of MIT and MRT determined and applied in this study make it possible to predict the torque and load that the BKS implant will support with a margin of safety to be tested.

The results presented in Table 1 show that in all different bone densities, the determined minimum friction factor was greater than 1. This standardisation of the μ_{SF} in the different bone densities is the desired solution for cases where the quantity and the quality of the bone is low.

Table 1. Obtain μ_{SF} values by applying MIT, and MRT values and determine the amount of bone collected by BKS at the different bone densities studied.

	Density g/cm3)*	MIT (N/cm)	MRT (N/cm)	collected weight (g)	total weight (g)	µsf
PCF 10	0.16	20	21	0.059	0.91	1.05
PCF 15	0.24	22	23	0.082	0.933	1.05
PCF 20	0.32	30	32	0.11	0.961	1.07
PCF 30	0.48	44	47	0.165	1.016	1.07
PCF 40	0.64	52	57	0.22	1.071	1.1

Knowing that the total volume of bone compacted inside the BKS is 96.91 mm^3 [8], the densification value of the different bone densities (Table 1) was accurately determined. The average compaction value found was 3.45 times higher than the original density of the bones, validating previous studies [8].

The stability parameters measured for dental implants in D1 bones (PCF 40) are all higher than those measured in the D4 bones (PCF 10). In general, a higher insertion speed results in a lower MIT while the insertion stability coefficient (ISQ) differed significantly among the insertion speeds [29]. The increase in MIT reduces the value of micromotions between the implant and bone interface. Some authors indicate immediate loading as a valid therapeutic choice in low-density D4 trabecular bones with at least 45 N/cm MIT obtained with the use of compression drilling techniques. [30]. Clinical determination of bone density during drilling can be obtained in cortical and trabecular bone but not in intermediate densities. Increasing peak MIT values correlated with increasing bone volume and higher MIT, does not seem to alter the osseointegration process [15, 31].

Histological imaging with those obtained by X-ray absorption images from synchrotron radiation micro-computed tomography, is considered the gold standard for analysing bone formation around metallic implants. Comparing statistically the results of bone-implant contact (BIC) showed a non-significant difference of 1.9 % ($p = 0.703$), and bone-implant volume (BIV) showed a non-significant difference by only 1.4 % ($p = 0.736$) [32].

The major factors affecting the MIT are bone density and hardness, use or not of under-dimensioned drills, and tapered implant design. The MIT achieved is directly proportional to the bone density, higher in D1 density and lowest in D4 density, without the use of compression techniques. Using under sized drilling techniques it is possible to achieve better stability by compression improving MIT in poor quality bone. Over-compression (high stress) could compromise the angiogenesis and new blood vessel formation [33]. leading to hypoxia in bone-implant tissues inhibiting bone formation and affecting Secondary biological stability.

The interstitial fluid supplying the bone cells transmits external stresses to bone cells through mechanical energy from external stresses are converted into bioelectric and biochemical signals modulating bone cell metabolism, called mechano-transduction. When these external stresses are too high, osteocytes die, and emerging osteoclasts and bone tissue breakdown affecting osseointegration [34]. MIT is reduced in implant macro-designs that incorporated cutting edges, and lower insertion torque (IT) is associated with decreased micromovement as this thread-cutting geometry creates a high level of bone to implant contact [35]. Findings in the literature suggest that a rough surface finish to cut bone, in a well-reduced fracture, should promote healing by stabilizing the fracture interface [36].

The tribological properties from the friction of the bone, and titanium and its alloys should be considered, both exhibiting friction wear. In the bone, wear is more severe than titanium and its alloys. The wear debris (chips) from the bones, should be considered influencing the micromotion by stiffness or looseness of the implants. [37]. The wear form of bone is a plastic deformation with critical digs, debris, and microcracks, whereas while that of the Titanium Alloy (Ti-6Al-4V) is a micro-cutting with scratches, denoting adhesive, and abrasive wear. [38].

Authors [39] validated testing methods to provide bone-implant friction data concluding that the rotation method, like when screwing, presented accurate friction estimates, and was less affected by normal force (N) and speed, than the sled method. The testing of bone against implant surfaces produced a variety of different force displacement curves and a wide range of friction coefficients in bovines, ranging from 0.19 to 0.78. A weak positive correlation was observed between bone porosity and friction coefficient.

A dental implant's macro geometry is critical to its primary stability. Primary stability is improved by increasing the contact surface of the implant with the surrounding bone through a larger diameter, conical shape, and roughened surface. This is considered the basis for successful implant osseointegration, which can be influenced by various factors such as implant design [40, 41].

The results obtained in the experiments with BKS in the form of a dental implant showed that the presented new biomechanism preserves the bone perforated in the same place inside the BKS, increases the MIT in proportion to the compacted bone inside it, makes the MRT superior in values to the MIT for bone adhesion and cohesion within the BKS in contact with the bone bed. The BKS also made it possible to control and predict the results in the different bone densities used in this study. If the recipient site does not have a flat base for direct insertion of the BKS, a previous guide hole of 1.6 mm in is indicated to ensure correct positioning of the implant, reducing the compacted bone density inside the BKS, but still increasing the density compared to the original bone [8]. If a temporary bone screw is chosen, the limitations of BKS must be considered, given the tendency to increase primary locking and thus optimise osseointegration in the medium and long term.

4 Conclusions

The new simple machine BKS in the form of a dental implant showed a higher MRT than MIT in all the experiments carried out. In soft bone (PCF 10 and PCF 15) the minimum values obtained were 21 N/cm and 23 N/cm respectively. In medium hard bone (PCF 20 and PCF 30) the minimum values obtained were 32 N/cm and 47 N/cm respectively. In hard bone (PCF 40) a minimum value of 57 N/cm was obtained. The coefficient of friction between bone and BKS remained above 1 in all measurements performed. The lowest MRT values obtained at all bone hardness set a standard for the maximum load that can be safely applied to BKS, where the maximum torque value (MIT) obtained as a standard in dental implant surgery, which is always lower than the MRT in all measurements, it indicates, without the need to apply the MRT, how much is the maximum force that can be applied for tighten and loosen abutment screws and temporary teeth. The value of MIT will vary with the hardness of the bone but will always present a higher MRT for its removal, making the value of MIT obtain a safe range of load that the bone implant can support. Using average values to determine MIT and MRT should be avoided in experimental studies. This work showed the importance of directly comparing MIT and MRT values in the same bone implant to obtain the true values of the coefficient of friction. This is only possible with the new technique used at BKS, where the insertion of the dental implant is standardised by its experimentally determined properties and characteristics. Future work with in vivo studies will determine whether this ratio of MRT greater than MIT is maintained in the organic environment.

Funding and/or Conflicts of interests/Competing interests:

The authors have no relevant financial or non-financial interests to disclose.

References

1. Hansen EA, Smith G (2009) Factors affecting cadence choice during submaximal cycling

and cadence influence on performance. Int J Sports Physiol Perform. 4(1):3-17. doi:10.1123/ijspp.4.1.

2. Kandavalli SR, Wang Q, Ebrahimi M, Gode C, Djavanroodi F, Attarilar S and Liu S (2021) A Brief Review on the Evolution of Metallic Dental Implants: History, Design, and Application. Front. Mater. 8:646383. doi: 10.3389/fmats.2021.646383.
3. Lee, D.-H., Cho, S.-A., Lee, C.-H. and Lee, K.-B. (2015), The Overuse of the Implant Motor. Clinical Implant Dentistry and Related Research, 17: 435-441. https://doi.org/10.1111/cid.12195.
4. Neugebauer J, Scheer M, Mischkowski RA, et al. (2009) Comparison of torque measurements and clinical handling of various surgical motors. Int J Oral Maxillofac Implants. 24: 469– 476.
5. Hanaor, DAH, Gan, Y, Einav, I (2016) Static friction at fractal interfaces. Tribology International, 93:229–238. doi:10.1016/j.triboint.2015.09.016.
6. Castagnetti D, Dragoni E (2012) Predicting the macroscopic shear strength of adhesively-bonded friction interfaces by microscale finite element simulations. Computational Materials Science. 64:146-50.
7. Gnecco E, Bennewitz R, Pfeiffer O, Socoliuc A, Meyer E (2011) Friction and wear on the atomic scale. Nanotribology and Nanomechanics II, Springer, pp 243-92.
8. Andreucci CA, Fonseca EMM, Jorge RN (2022) Increased Material Density within a New Biomechanism. Math. Comput. Appl. 27:90. https://doi.org/10.3390/mca27060090.
9. Wilkie J, Rauter G, Möller K (2022) Determining relationship between bone screw insertion torque and insertion speed: Bestimmung des Zusammenhangs zwischen dem Drehmoment beim Eindrehen von Knochenschrauben und der Eindrehgeschwindigkeit. at - Automatisierungstechnik. 70(11):976-991. https://doi.org/10.1515/auto-2022-0009.
10. Kochar SP, Reche A, Paul P (2022) The Etiology and Management of Dental Implant Failure: A Review. Cureus, 14(10), e30455. https://doi.org/10.7759/cureus.30455.
11. Jimbo R, Tovar N, Anchieta RB, et al. (2014) The combined effects of undersized drilling and implant macrogeometry on bone healing around dental implants: an experimental study. Int J Oral Maxillofac Surg. 43(10):1269-1275. doi:10.1016/j.ijom.2014.03.017.
12. Berardini M, Trisi P, Sinjari B, Rutjes AWS, Caputi S (2016) The Effects of High Insertion Torque Versus Low Insertion Torque on Marginal Bone Resorption and Implant Failure Rates: A Systematic Review With Meta-Analyses. Implant Dentistry. 25(4):532-540. DOI: 10.1097/ID.0000000000000422.

13. Comuzzi L, Tumedei M, Romasco T, et al. (2022) Insertion Torque, Removal Torque, and Resonance Frequency Analysis Values of Ultrashort, Short, and Standard Dental Implants: An In Vitro Study on Polyurethane Foam Sheets. J Funct Biomater. 14(1):10. doi:10.3390/jfb14010010.
14. Kohli N, Stoddart JC, van Arkel RJ (2021) The limit of tolerable micromotion for implant osseointegration: a systematic review. Sci Rep 11:10797 . https://doi.org/10.1038/s41598-021-90142-5.
15. Makary C, Rebaudi A, Mokbel N, Naaman N, (2011) Peak Insertion Torque Correlated to Histologically and Clinically Evaluated Bone Density. Implant Dentistry 20(3):182-191. DOI: 10.1097/ID.0b013e31821662b9.
16. Stocchero M, Jinno Y, Toia M, et al. (2023) Effect of Drilling Preparation on Immediately Loaded Implants: An In Vivo Study in Sheep. Int J Oral Maxillofac Implants. 38(3):607-618. doi:10.11607/jomi.9949.
17. Raz P, Meir H, Levartovsky S, Sebaoun A, Beitlitum I (2022). Primary Implant Stability Analysis of Different Dental Implant Connections and Designs-An In Vitro Comparative Study. Materials. 15(9):3072. https://doi.org/10.3390/ma15093072.
18. Bulaqi HA, Mousavi Mashhadi M, Geramipanah F, Safari H, Paknejad M (2015) Effect of the coefficient of friction and tightening speed on the preload induced at the dental implant complex with the finite element method. J Prosthet Dent. 113(5):405-411. doi:10.1016/j.prosdent.2014.09.021.
19. Hao CP, Cao NJ, Zhu YH, et al. (2021) The osseointegration and stability of dental implants with different surface treatments in animal models: a network meta-analysis. Sci Rep. 11:13849. https://doi.org/10.1038/s41598-021-93307-4.
20. Mellinger JC, Burak Ozdoganlar O, DeVor RE, Kapoor SG (2002) Modeling Chip-Evacuation Forces and Prediction of Chip-Clogging in Drilling. ASME. J. Manuf. Sci. Eng. 124(3):605–614. https://doi.org/10.1115/1.1473146.
21. Andreucci CA, Fonseca EMM, Jorge RN (2023) A New Simplified Autogenous Sinus Lift Technique. Bioengineering. 10:505. https://doi.org/10.3390/bioengineering10050505.
22. Babczyk P, Winter M, Kleinfeld C, Pansky A, Oligschleger C, Tobiasch E (2022) Examination of the Quality of Particulate and Filtered Mandibular Bone Chips for Oral Implants: An In Vitro Study. Appl. Sci. 12:2031. https://doi.org/10.3390/app12042031.
23. Andersen OZ, Bellón B, Lamkaouchi M, et al. (2023) Determining primary stability for

adhesively stabilized dental implants. Clin Oral Invest. https://doi.org/10.1007/s00784-023-04990-8.

24. Kamel S, Mohamed N, Sherif M, Hee-Moon K, Abbadi El-K (2017) In vitro assessment of maximum insertion and removal torque with three different miniscrews on artificial maxilla and mandible. Jour of the World Fed of Orthodon. 6:(3):115-119. https://doi.org/10.1016/j.ejwf.2017.08.003.
25. Andreucci CA, Alshaya A, Fonseca EMM, Jorge RN (2022) Proposal for a New Bioactive Kinetic Screw in an Implant, Using a Numerical Model. Appl. Sci. 12:779. https://doi.org/10.3390/app12020779.
26. Andreucci CA, Fonseca EMM, Jorge RN (2022) 3D Printing as an Efficient Way to Prototype and Develop Dental Implants. BioMedInformatics. 2(4):671-679. https://doi.org/10.3390/biomedinformatics2040044
27. Andreucci CA, Fonseca EMM, Natal RMJ (2022) Structural analysis of the new Bioactive Kinetic Screw in titanium alloy vs. commercially pure titanium. J. Comp. Art. Int. Mec. Biomec. 2:35–43. https://zenodo.org/badge/DOI/10.5281/zenodo.7406075.svg
28. Andreucci CA, Fonseca EMM, Jorge RN (2023) Bio-lubricant Properties Analysis of Drilling an Innovative Design of Bioactive Kinetic Screw into Bone. Designs. 7(1):21. https://doi.org/10.3390/designs7010021.
29. Hsu YY, Tsai MT, Huang HL, et al. (2022) Insertion Speed Affects the Initial Stability of Dental Implants. J. Med. Biol. Eng. 42:516–525. https://doi.org/10.1007/s40846-022-00742-3.
30. Trisi P, Berardi D, Paolantonio M, Spoto G, D'Addona A, Perfetti G (2013) Primary stability, insertion torque, and bone density of conical implants with internal hexagon: is there a relationship? J Craniofac Surg. 24(3):841-844. doi:10.1097/SCS.0b013e31827c9e01.
31. Andreucci CA, Fonseca EMM, Jorge RN (2023) Immediate Autogenous Bone Transplantation Using a Novel Kinetic Bioactive Screw 3D Design as a Dental Implant. BioMedInformatics. 3(2):299-305. https://doi.org/10.3390/biomedinformatics3020020.
32. Bernhardt R, Kuhlisch E, Schulz MC, Eckelt U, Stadlinger B (2012) Comparison of bone-implant contact and bone-implant volume between 2D-histological sections and 3D-SRµCT slices. Eur Cell Mater. 23:237-248. doi:10.22203/ecm.v023a18.
33. Checa S, Prendergast PJ (2010) Effect of cell seeding and mechanical loading on vascularization and tissue formation inside a scaffold a mechano-biological model using

a lattice approach to simulate cell activity. J Biomech. 43(5):961e968.

34. Burger EH, Klein-Nulend J (1999) Mechanotransduction in bonedrole of the lacuno-canalicular network. FASEB J. (13):S101eS112.
35. Freitas Jr AC, Bonfante EA, Giro G, Janal MN, Coelho PG (2012) The effect of implant design on insertion torque and immediate micromotion. Clin Oral Impl Res. 23:113e118. http:// dx.doi.org/10.1111/j.1600-0501.2010.02142.x.
36. Shockey JS, von Fraunhofer JA, Seligson D (1985) A measurement of the coefficient of static friction of human long bones. Surface Technology. 25:2:167-173. https://doi.org/10.1016/0376-4583(85)90030-5.
37. Bihai Z, Xiaofeng H, Tianliang Z (2015) Friction and wear characteristics of natural bovine bone lubricated with water, Wear. 322–323. https://doi.org/10.1016/j.wear.2014.10.013.
38. Chenchen W, Gangqiang Z, Zhipeng L, Xiangqiong Ze, Yong X, Shichang Z, Hongxing H, Yadong Z, Tianhui R (2019) Tribological behavior of Ti-6Al-4V against cortical bone in different biolubricants. Journal of the Mechanical Behavior of Biomedical Materials. 90:460-471. https://doi.org/10.1016/j.jmbbm.2018.10.031.
39. Dannaway J, Dabirrahmani D, et al. (2015) An investigation into the frictional properties between bone and various orthopedic implant surfaces - implant stability J. Musculoskelet. 18. 10.1142/S0218957715500153.
40. Heimes D, Becker P, Pabst A, et al. (2023) How does dental implant macrogeometry affect primary implant stability? A narrative review. Int J Implant Dent 9:20. https://doi.org/10.1186/s40729-023-00485-z.
41. Lemos CAA, Verri FR, de Oliveira Neto OB, et al. (2021) Clinical effect of the high insertion torque on dental implants: A systematic review and meta-analysis. J Prosthet Dent. 126(4):490-496. doi:10.1016/j.prosdent.2020.06.012.

Chapter V

Increased Material Density within a New Biomechanism*

Carlos Aurelio Andreucci[1], Elza Fonseca[2], Renato Natal Jorge[3]

[1]Faculty of Engineering of the University of Porto (FEUP), Portugal
[2]School of Engineering, Polytechnic of Porto (ISEP), Mechanical Engineering Department, Portugal
[3]Faculty of Engineering of the University of Porto (FEUP), Portugal

**Mathematical and Computational Applications.* 2022 November 27(6), 90

DOI: 10.3390/mca27060090

Abstract

A new mechanism, applied in this study as a biomechanical device, known as a Bioactive Kinetic Screw (BKS) for bone implants is described. The BKS was designed as a bone implant, in which the bone particles, blood, cells, and protein molecules removed during bone drilling are used as a homogeneous autogenous transplant at the same implant site, aiming to optimize the healing process and simplify the surgical procedure. In this work, the amount of bone that will be compacted inside and around the new biomechanism was studied, based on the density of the bone applied. This study allows us to analyze the average bone density in humans (1.85 mg/mm3 or 1850 μg/mm^3) with four different synthetic bone densities (Sawbones PCF 10, 20, 30 and 40). The results show that across all four different synthetic bones densities, the bone within the new model is 3.45 times denser. After a pilot drill (with 10 mm length and 1.8 mm diameter), in cases where a guide hole is required, the increase in ratio is equal to 2.7 times inside and around the new biomechanism. The in vitro test validated the mathematical results, describing that in two different materials, the same compact factor of 3.45 was determined with the new biomechanical device. It was possible to describe that BKS can become a powerful tool in the diagnosis and treatment of natural bone conditions and any type of disease.

Keywords: Bioactive Kinetic Screw; bone mass density; osteopenia; osteoporosis; DEXA

1 Introduction

The Bone tissue is frequently remodeled through bone resorption by osteoclasts and bone formation by osteoblasts, having osteocytes as mechano-sensors and organizers of the bone remodeling process. This mechanism is regulated by growth factors, cytokines, and systemic factors that achieve bone homeostasis [1]. Any dysregulation in this process can cause osteoporosis.

Osteoporosis is a metabolic pathology defined by bone mass reduction related with reduced bone strength and heightened skeletal fragility with bone tissue microarchitectural degradation. Osteoporosis is a frequent cause of bone fractures in the elderly [2]. Dual-energy-x-ray absorptiometry (DEXA) can grant an accurate diagnosis of osteoporosis and assessment of fracture risk. The World Health Organization has settled DEXA as the standard technique for measuring bone mineral density (BMD) [3].

Bone Screws in orthopedic surgery convert torsional forces into compression. The primary functional objective in the design of a screw is to dissipate and distribute the mechanical load. Thread design should maximize initial contact, enhance surface area, dissipate, and distribute stresses at the screw–bone interface and increase the pullout strength. Screws can be used for attachment of implants to bone, bone-to-bone fixation, or for soft tissue fixation or anchorage [4]. Bone volume and bone quality properties are fundamental prerequisites to ensure optimal mechanical stability of the implants and further osseointegration [5].

In the new biomechanism (BKS), Figure 1, the hard tissue is removed during bone drilling and screwed at the same time, due to the new characteristics, which uses the chips (bone particles, blood, cells, and protein molecules) to fill the hole passing through the drill grooves in the new screw. The screw was created based on the concepts of using drills for bone drilling and screws for fixation and implants [4]. Traditional drill flutes remove bone particulate after perforation. In the BKS model, a mechanical limit was created for these flutes through a hole joining the cut grooves, avoiding the removal of all particulate bones from the perforation. This bone material is compacted in and through the screw, increasing the bone contact surface and creating a graft bone bridge of particulate material through the screw, according to the authors project [6].

Figure 1. BKS of 4 mm width and 10 mm length, according to the authors project [6].

Developing a biomechanism for bone fixation that involves biological and mechanical characteristics that are desirable in biomechanical rehabilitation in a safe and practical way, are the founding principles of all the specialties involved in these studies, from research with molecules and proteins, to genetic therapies for the biomechanical functional restoration of limbs and organs [5,6].

In this ongoing research, as in the previous work from the authors [6], the main objective is to simulate and test in vitro and in vivo the new biomechanical function described by the new BKS model, applying the concepts of a modified drilling, and screwing in the same device. The new biomechanism will be mathematically described, and its fundamental study is to help and guide practical decisions and have a protocol to be validated. The new screw refers to a line of research initiated through a new biomechanical model for “Improvement in screw of fixations and bone implant” [6] developed to provide the fixation of osseointegrated screws, to facilitate and simplify the surgical protocol of insertion and fixation, obtaining primary stability and consequent secondary stability, through greater contact of the recipient bone with the surface of the new fixation screw and through it.

The filling through the screw hole, Figure 1, with the bone of the bed site to be drilled, used in the screw of the drills of the cross flutes system, limited by a through hole, allows the use of the bone present in the flutes in the moment of screwing-drilling; the chips (particulate bones) flow as a homogenous autogenous transplant that will be inserted and compacted in the through hole.

With this, physiological bone healing stimulus are obtained (particulate bone, cells, and molecules through the screw or implant) [7,8,9], optimizing natural bone healing by using the organic bone tissue repair to aid in integration, stability, and longevity of fixations, with direct bone contact through the implants, making it possible to be a unique and functional object. This could become a biological osseointegration.

2 Materials and Methods

In this work, the mean bone density in humans was analyzed (1.85 mg/mm3 or 1850 µg/mm^3) [10] with four different synthetic bone densities, such as closed cell polyurethane (PCF) from Sawbones with the references PCF 10, 20, 30, and 40, respectively, simulating natural bone density in four macroscopic classes (D1, D2, D3, and D4) [11].

PCF foam is used as an alternative test medium for human cancellous bone. It does not replicate the structure of human bone; however, it provides properties consistent in the range of human cancellous bone. PCF is mostly used to test screw pullout, insertion, and stripping torque at different densities.

To measure the volume of the internal space of the new biomechanical model in SolidWorks software, the volume of the complete screw design was used, as shown in Figure 2, and the volume with the new biomechanism was subtracted, Figure 3. According to the procedure, the entire new internal volume of the biomechanical device is equivalent to 28.10 mm^3. The difference between bone mass (m) and bone density (D) is that the first refers to the amount of bone tissue in the skeleton, and bone density refers to the mineral mass per unit volume of bones [12,13,14]. Density (D) can be calculated using Equation (1) related to volume (V). Density is commonly expressed in units of grams per cubic centimeter.

$$D = \frac{m}{V} \tag{1}$$

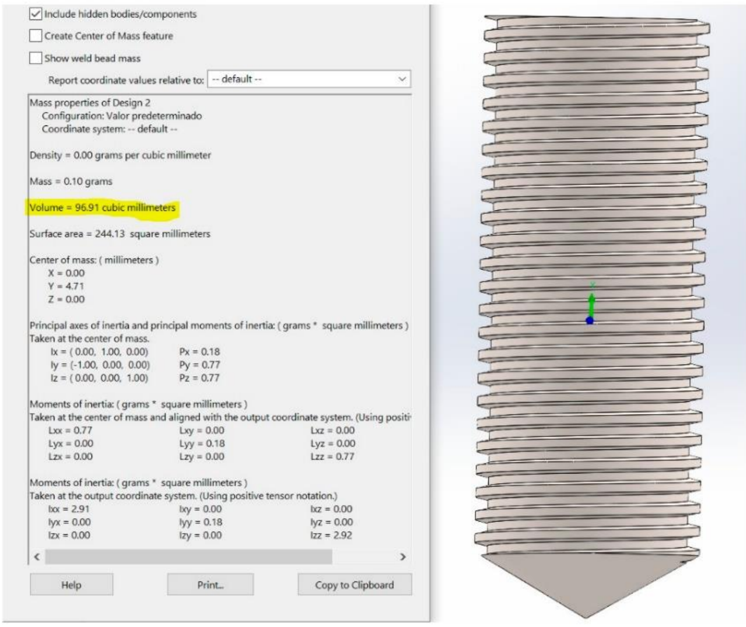

Figure 2. Complete model with a volume equal to 96.91 mm³.

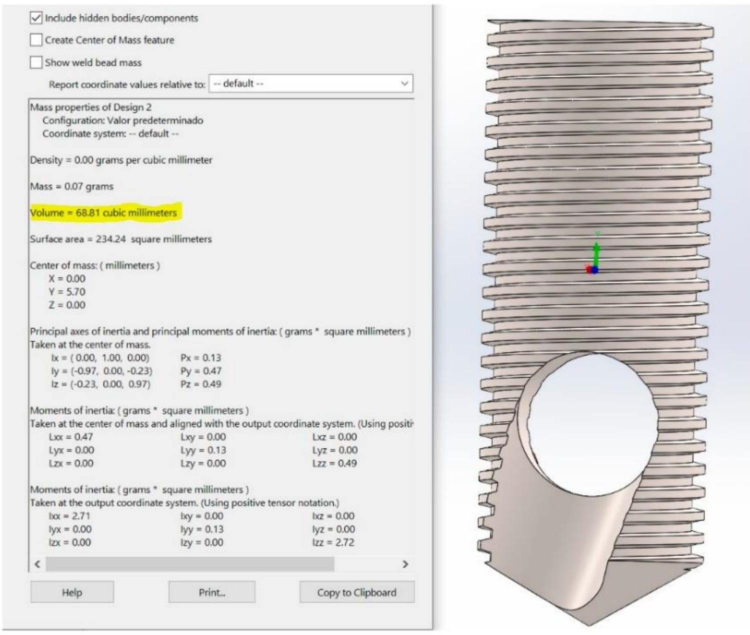

Figure 3. Final model with new biomechanism with a volume equal to 68.81 mm³.

To validate the mathematically proved concept, the new BKS model was 3D printed in Polylactic Acid (PLA), as shown in Figure 4, to be experimentally tested in Aluminum Phyllosilicates (clay) and Kinetic Sand. The BKS device was weighted before being manually screwed and unscrewed in the materials with a regular hexagonal spanner wrench. After collecting and compacting the material inside the BKS, another weight measurement was taken with all the material compacted. The difference between the weights before and after was determined by a Taylor Precision Compact Digital scale, using the calibration button before all weight measurements.

Figure 4. BKS device 3D printed and Taylor Precision Compact Digital scale before and after compacting Aluminum Phyllosilicates (clay).

Six measurements were performed in each material, obtaining an average of values, which was compared with the normal density of the materials itself and with the compaction factor described in the mathematical proof, validating it.

3 Results

3.1. Average Density in Human Bone

The volume inside the new biomechanism, measuring 4 mm in diameter and 10 mm in length, is 28.10 mm3. Thus, with bone density equal to 1850 µg/mm³, the calculated mass is 51,985 µg, approximately 0.05 g.

With bone density equal to 1850 µg/mm³, a total of 51,985 µg is determined inside and around the new biomechanism (28.1 mm3) for natural bone density, without measuring the effect of chip (particulate bone) compacting effect of the new biomechanism after cutting and insertion (total screw volume).

The total volume of the model is 96.91 mm3. The total amount of bone collected to be compacted will be the total volume of the screw multiplied by the density of the bone equal to 1850 µg/mm³. The mass obtained is equal to 179,283.50 µg. This value represents 0.18 g to be compacted into 28.10 mm³. Thus, with the effect of compacting inside the screw, a mass of 179,283.50 µg in the volume 28.10 mm3 was calculated, which allows a density calculation equal to 6380.19 µg/mm3 or 6.38 mg/mm3.

The density inside the screw after compacting bone will be 6.38 mg/mm3; in the same volume with natural bone density, it was equal to 1.85 mg/mm3. This means a density grow by 3.45 times inside and around the new biomechanical model optimizing the osseointegration is to be tested in vivo [15].

3.2. Average Density Using PCF

To test the amount of bone compacted in the BKS system in PCF foam material, in four different densities, the same introduced concept was used. Table 1 represents the chosen PCF densities, according to ASTM D1622 [16], the calculated results for the mass of the total screw drilled (volume of the model is 96.91 mm3) and the density of the total drilled screw compacted inside the BKS screw (in the volume 28.10 mm3).

3.1 Average Density in Human Bone

The volume inside the new biomechanism, measuring 4 mm in diameter and 10 mm in length, is 28.10 mm3. Thus, with bone density equal to 1850 µg/mm^3, the calculated mass is 51,985 µg, approximately 0.05 g.

With bone density equal to 1850 µg/mm^3, a total of 51,985 µg is determined inside and around the new biomechanism (28.1 mm3) for natural bone density, without measuring the effect of chip (particulate bone) compacting effect of the new biomechanism after cutting and insertion (total screw volume).

The total volume of the model is 96.91 mm3. The total amount of bone collected to be compacted will be the total volume of the screw multiplied by the density of the bone equal to 1850 µg/mm^3. The mass obtained is equal to 179,283.50 µg. This value represents 0.18 g to be compacted into 28.10 mm^3. Thus, with the effect of compacting inside the screw, a mass of 179,283.50 µg in the volume 28.10 mm3 was calculated, which allows a density calculation equal to 6380.19 µg/mm3 or 6.38 mg/mm3.

The density inside the screw after compacting bone will be 6.38 mg/mm3; in the same volume with natural bone density, it was equal to 1.85 mg/mm3. This means a density grow by 3.45 times inside and around the new biomechanical model optimizing the osseointegration is to be tested in vivo [15].

3.2 Average Density Using PCF

Temperature To test the amount of bone compacted in the BKS system in PCF foam material, in four different densities, the same introduced concept was used. Table 1 represents the chosen PCF densities, according to ASTM D1622 [16], the calculated results for the mass of the total screw drilled (volume of the model is 96.91 mm^3) and the density of the total drilled screw compacted inside the BKS screw (in the volume 28.10 mm^3).

Table 1. Calculated values for chosen PCF densities.

PCF	Density, g/cm^3 [10]	Mass, mg	Density, mg/mm^3
10	0.16	15.50	0.55
20	0.32	31.01	1.10
30	0.48	46.51	1.65
40	0.64	62.02	2.20

With the new BKS, a compacting effect was identified, making the synthetic bone inside the screw be 3.45 times denser in all types of densities (10, 20, 30 and 40 PCF) in a volume that represents almost 1/3 (28.10 mm^3) of the whole screw (96.91 mm^3).

BKS has a compacting factor increasing the density on the average human bone and synthetic bones equal to 3.45 times inside and around the new biomechanical model. It means that no matter the value of the bone density, the new biomechanical device increases 3.45 times the bone density in 29% of the total volume of the BKS in the deepest part of the perforation, usually attached in trabecular bone in surgeries.

3.3 In vitro Experiment

The in vitro test validated the mathematical results, describing that in two different materials, the same compact factor of 3.45 was determined inside the new biomechanical device. For this, a BKS model manufactured through 3D printing was experimentally tested in Aluminum Phyllosilicates (clay) and Kinetic Sand, with a mean density of fine silts and clays between 1.1 and 1.6 g/cm3 and Kinetic Sand 0.83 g/cm3 [17,18]. The results, as seen in Table 2, described the same results determined through the mathematical concept on the calculated mean (X), each score deviates from the mean by 0.06 points for aluminum phyllosilicates and 0.04 for Kinetic sand. It was possible to also observe the standard deviation (SD) of each one. A small standard deviation was obtained, which indicate the data observed is clustered tightly around the mean.

Table 2. Compacting factor analysis in two different materials to test and validate the mathematical proof of concept of the BKS device.

Material/Average Density(g/cm^3)	Volume Inside BKS (g/cm^3)	Volume Inside BKS/3.45 (g/cm^3)	Mean $(\overline{X})$ and Standard Deviation (SD) Density Inside BKS (g/cm^3)
aluminum phyllosilicates/1.10 to 1.60 g/cm^3	4.23	1.22	$\overline{X}$ = 1.23 SD = 0.02
	4.15	1.20	
	4.26	1.23	
	4.19	1.21	
	4.27	1.24	
	4.31	1.25	
Kinetic sand/0.83 g/cm^3	2.89	0.83	$\overline{X}$ = 0.84 SD = 0.01
	2.90	0.84	
	2.82	0.82	
	2.88	0.83	
	2.96	0.86	
	2.90	0.84	

3.4 Using a Pilot Drill in Cases a Guide Hole Is Needed

In the case of using a standard pilot drill with a length of 10 mm and a diameter of 1.8 mm to make a perforation to guide the insertion of the BKS screw, a volume of 20.10 mm^3 was removed from the bone bed site. If the volume of the drill (20.10 mm^3) is subtracted from the total volume of the screw (96.91 mm^3), it will result in 76.81 mm^3 as the total volume of bone to be compacted.

Table 3 shows the results of the mass of the total screw drilled at different bone densities after a pilot drilling (volume of 20.10 mm^3) and the density of the bone compacted inside the BKS screw at different synthetic bone densities, after a pilot drill (volume of 20.10 mm^3).

Table 3. Calculated values for chosen PCF densities after a pilot drilling.

PCF	Density, g/cm^3 [10]	Mass, mg	Density, mg/mm^3
10	0.16	12.28	0.43
20	0.32	24.58	0.87
30	0.48	36.86	1.31
40	0.64	49.15	1.74

BKS has a compacting factor that increases the density, on the average, human bone, and synthetic bones after a pilot drilling (10 mm in length and 1.8 mm in diameter) equal to 2.7 times inside and around the new biomechanical design.

4 Discussion

Dual-energy x-ray absorptiometry (DEXA) is the standard test for measuring bone mineral density since its approval by the Food and Drug Administration (FDA) for clinical use in 1988. The Bone Mass Measurements in 1998 solidified its validity considering other diagnostic modalities such as chemical analysis, direct dissection, quantitative ultrasonography, and later, CT/MRI images [19].

DEXA uses the attenuations of low and high-energy photon emissions that are detected above the patient and are combined to create a planar image to assess bone mass per unit volume (g/cm), for example, bone mineral density (BMD) [19,20].

World Health Organization (WHO) in 1994 provided a definition of bone mass loss using a standardized score, called T-scores as: greater than or equal to −1.0 is normal; less than −1.0 to greater than −2.5 considered as osteopenia; less than or equal to −2.5 as osteoporosis and less than or equal to −2.5 plus fragility fracture considered severe osteoporosis.

Correct interpretation of BMD requires attention to detail in anthropometric information, patient positioning, correct scan analysis, BMD pattern of individual vertebrae, and identification of artefacts [21].

With the new biomechanical screw, it is possible to directly access the BMD in cases where more reliable data are needed and when the clinical findings do not match with imaging tests (DEXA). The BKS screw can be used as a bone collector if removed immediately after full bone insertion. The amount of bone inside the new biomechanical screw will be measured and the BMD can be determined, according to the proposed Equation (2) for the ideal condition or Equation (3) when the guided hole is needed. As the bone inside the BKS is exactly 3.45 times denser than the bone of the same bed site, the proposed equation as the follow:

$$BMD = \frac{Bone\ inside\ BKS}{3.45} \tag{3}$$

$$BMD = \frac{Bone\ inside\ BKS - Bone\ Volume\ Pilot\ Drill}{3.45} \tag{3}$$

The average bone density in humans is 1.85 mg/mm3 [10]. The density inside the screw after compacting bone will be 6.38 mg/mm^3; in the same volume with natural bone density, the value is 1.85 mg/mm3.

For BMD calculation using the BKS screw, the vertebra L1 will be used as an example, as seen in a regular DEXA exam in Figure 5 [20]. The area is 8.92 cm^2, the bone mineral content (BMC) is 6.50 g, so the volume is equal to 892 mm^3 and the BMC will be 650 mg. Using Equation (1), BMD is equal to 0.244 mg/mm^3.

Region	Area (cm^2)	BMC (g)	BMD (g/cm^2)	T-score
L1	8.92	6.50	0.729	−2.4

Figure 5. Bone mineral density measured and reported on one vertebra L1 [18].

As the bone inside the BKS is exactly 3.45 times denser than the bone in the same bed site, the measure inside the BKS allows a value equal to 0.842 mg/mm3.

In conclusion, Bone Mass Density within the BKS (BKS-BMD) can always accurately define the BMD by dividing its value by 3.45, as per our proposal according to Equation (4).

$$BMD = \frac{BKS-BMD}{3.45} \tag{4}$$

Associating direct bone mass density measure through the new biomechanical screw (BKS) comparing and validating the images results (DEXA) will become a powerful tool in diagnosis and treatment of natural bone conditions and any kind of bone diseases to be tested.

Recent biomechanical studies [22,23,24,25] in implant osseointegration showed that the maintenance of bone viability at an osteotomy site is a critical variable for success. Analyzing the consequences of site preparation and the bone loss due the standard protocols, made some authors, including us, to rethink the design of bone-cutting drills for implant site preparation. In our new BKS, the screw is also a drill with a modified compacting factor. Some authors [22] developed a new protocol for drilling applying a new model of drill bit, with the unique design of the cutting flutes, making channels into the osteotomy maintaining on the site autologous bone chips and osseous coagulum that have inherent osteogenic potential. Collectively, these features resulted in robust, new bone formation at rates significantly faster than those observed with conventional drilling protocols.

5 Conclusions

A new biomechanism BKS for screws and bone implants developed by the first author was presented using a bone dental implant screw, in which the bone particles, blood, cells, and protein molecules removed during bone drilling are used as a homogeneous autogenous transplant in the same implant site, aiming to obtain primary and secondary bone stability, simplifying the surgical procedure, and improving the healing process. It was observed that at all four different synthetic bones densities the bone inside the new model is 3.45 times denser. After a pilot drill (10 mm in length and 1.8 mm in diameter), in cases where a guide hole is needed, the increased ratio is equal to 2.7 times inside and around the new biomechanical design. The in vitro test validated the mathematical results, describing that in two different materials, the same compact factor of 3.45 was determined with the new biomechanical device. With the new biomechanical screw, it is possible to directly access the BMD in cases where more reliable data are needed, during surgery treatments in patients with osteopenia to help confirm the diagnosis and treatment, and when the clinical findings do not match the imaging tests (DEXA), thus becoming a powerful tool in diagnosis and treatment of natural bone conditions and any type of bone disease.

Declaration of conflicting interests

The author(s) declared no potential conflicts of interest concerning the research, authorship, and/or publication of this article.

References

1. Florencio-Silva, R.; Sasso, G.R.; Sasso-Cerri, E.; Simões, M.J.; Cerri, P.S. Biology of Bone Tissue: Structure, Function, and Factors That Influence Bone Cells. Biomed Res.

Int. 2015, 2015, 421746.
2. Leslie, W.D.; Morin, S.N. Osteoporosis epidemiology 2013: Implications for diagnosis, risk assessment, and treatment. Curr. Opin. Rheumatol. 2014, 26, 440–446.
3. Kanis, J.A. Assessment of fracture risk and its application to screening for postmenopausal osteoporosis: Synopsis of a WHO report. Osteoporos. Int. 1994, 4, 368–381.
4. Albrektsson, T.; Johansson, C. Osteoinduction, osteoconduction and osseointegration. Eur. Spine J. 2001, 10 (Suppl. S2), S96–S101.
5. Ivanova, V.; Chenchev, I.; Zlatev, S.; Atanasov, D. Association between Bone Density Values, Primary Stability and Histomorphometric Analysis of Dental Implant Osteotomy Sites on the Upper Jaw. Folia Med. 2020, 62, 563–571.
6. Andreucci, C.A.; Alshaya, A.; Fonseca, E.M.M.; Jorge, R.N. Proposal for a New Bioactive Kinetic Screw in an Implant, Using a Numerical Model. Appl. Sci. 2022, 12, 779.
7. Zhu, G.; Zhang, T.; Chen, M. Bone physiological microenvironment and healing mechanism: Basis for future bone-tissue engineering scaffolds. Bioact Mater. 2021, 6, 4110–4140.
8. ElHawary, H.; Baradaran, A.; Abi-Rafeh, J.; Vorstenbosch, J.; Xu, L.; Efanov, J.I. Bone Healing and Inflammation: Principles of Fracture and Repair. Semin. Plast. Surg. 2021, 35, 198–203.
9. Marsell, R.; Einhorn, T.A. The biology of fracture healing. Injury 2011, 42, 551–555.
10. Chirchir, H.; Kivell, T.L.; Ruff, C.B. Recent origin of low trabecular bone density in modern humans. Proc. Natl. Acad. Sci. USA 2015, 112, 366–371.
11. Sawbones-Worldwide Leaders in Orthopaedic and Medical Models. Available online: www.sawbones.com (accessed on 15 June 2022).
12. Morgan, E.F.; Unnikrisnan, G.U.; Hussein, A.I. Bone Mechanical Properties in Healthy and Diseased States. Annu. Rev. Biomed. Eng. 2018, 20, 119–143.
13. Osterhoff, G.; Morgan, E.F.; Shefelbine, S.J.; Karim, L.; McNamara, L.M.; Augat, P. Bone mechanical properties and changes with osteoporosis. Injury 2016, 47 (Suppl. S2), S11–S20.
14. Aro, H.T.; Kelly, P.J.; Lewallen, D.G.; Chao, E.Y. The effects of physiologic dynamic compression on bone healing under external fixation. Clin. Orthop. Relat. Res. 1990, 256, 260–273.

15. Adell, R.; Lekholm, U.; Rockler, B.; Branemark, P. A 15 year study of osseointegrated im-plants in the treatment of the edentulous jaw. Int. J. Oral Surg. 1981, 10, 387–416.
16. ASTM D1622. Standard Test Method for Apparent Density of Rigid Cellular Plastics, 2020 ed; ASTM International: West Conshohocken, PA, USA, 2020.
17. Kumari, N.; Mohan, C. (Eds.) Basics of Clay Minerals and Their Characteristic Properties; IntechOpen Limited: London, UK, 2021.
18. Gago, F.; Vlcek, J.; Valaskova, V.; Florkova, Z. Laboratory Testing of Kinetic Sand as a Reference Material for Physical Modelling of Cone Penetration Test with the Possibility of Artificial Neural Network Application. Materials 2022, 15, 3285.
19. Alawi, M.; Begum, A.; Harraz, M. Dual-Energy X-Ray Absorptiometry (DEXA) Scan Versus Computed Tomography for Bone Density Assessment. Cureus 2021, 13, e13261.
20. El Maghraoui, A.; Mounach, A.; Rezqi, A.; Achemlal, L.; Bezza, A.; Ghozlani, I. Vertebral fracture assessment in asymptomatic men and its impact on management. Bone 2012, 50, 853–857.
21. Haseltine, K.N.; Chukir, T.; Smith, P.J.; Jacob, J.T.; Bilezikian, J.P.; Farooki, A. Bone Mineral Density: Clinical Relevance and Quantitative Assessment. J Nucl. Med. 2021, 62, 446–454.
22. Chen, C.-H.; Coyac, B.R.; Arioka, M.; Leahy, B.; Tulu, U.S.; Aghvami, M.; Holst, S.; Hoffmann, W.; Quarry, A.; Bahat, O.; et al. A Novel Osteotomy Preparation Technique to Preserve Implant Site Viability and Enhance Osteogenesis. J. Clin. Med. 2019, 8, 170.
23. Yao, Y.; Wang, L.; Li, J.; Tian, S.; Zhang, M.; Fan, Y. A novel auxetic structure based bone screw design: Tensile mechanical characterization and pullout fixation strength evaluation. Mat Des. 2020, 188, 108424.
24. Stahel, P.F.; Alfonso, N.A.; Henderson, C. Introducing the “Bone-Screw-Fastener” for improved screw fixation in orthopedic surgery: A revolutionary paradigm shift? Patient Saf. Surg. 2017, 11, 6.
25. Zhang, X.; Tiainen, H.; Haugen, H.J. Comparison of titanium dioxide scaffold with commercial bone graft materials through micro-finite element modelling in flow perfusion. Med. Bio.l Eng. Comput. 2019, 57, 311–324.

CHAPTER VI

3D Printing as an Efficient Way to Prototype and Develop Dental Implants*

Carlos Aurelio Andreucci[1], Elza Fonseca[2], Renato Natal Jorge[3]

[1]Faculty of Engineering of the University of Porto (FEUP), Portugal
[2]School of Engineering, Polytechnic of Porto (ISEP), Mechanical Engineering Department, Portugal
[3]Faculty of Engineering of the University of Porto (FEUP), Portugal

**BioMedInformatics.* 2022 December 2(4), 671-679

DOI: 10.3390/biomedinformatics2040044

Abstract

Individualized, serial production of innovative implants is a major area of application for additive manufacturing in the field of medicine. Individualized healthcare requires faster delivery of the implant to the clinic or hospital facility. The total manufacturing process, including data generation using 3D drawings, imaging techniques, 3D printing and post-processing, usually takes up to a week, especially implants from risk class III, which requires qualified equipment and a validated process. In this study, we describe how to develop a new biomechanical model for dental implants from its conception for the patent to the final product which is ready to be manufactured using additive manufacturing. The benefits and limitations of titanium metal printing for dental implant prototypes are presented by the authors.

Keywords: 3D printing; additive manufacturing; dental implant; biomedical devices; titanium metal printing

1 Introduction

Developing a new biomedical device, especially osseointegrated bone screws and/or implants for dentistry, orthopedics, neurosurgery, and all kinds of protheses fixed by bone implants, is a challenge that involves different professionals with different areas of expertise. The development of new concepts for biomedical devices can usually be performed by surgeons specialized in the field of innovation. The next steps involve a designer, engineer, and different technicians who will help to apply computational simulations, laboratory experiments, animal testing, and clinical trials where they are mandatory.

The aim of this study is to describe the whole process of developing a new biomechanism for bone screws for the application of dental implants, from concept creation by the author, initial patent design, and further needs, which will make individualized production possible using commercially pure titanium, or titanium alloy (Ti6Al4V), and where each component is fabricated by additive manufacturing (3D printing). This process can be applied to the research of innovative technologies, for companies and individuals, becoming a promising way to prototype new biomedical devices with all the advantages that 3D printing technology aggregates, including its quality and validated process.

The present and future of biomedical devices is in three-dimensional (3D) printing [1]. These technologies are having a remarkable impact on all aspects in the field of medicine, enhancing the possibilities to make precise, complex geometrical forms, from the initial concept and digital data, and in a variety of materials. It has been praised as a disruptive technology which will change manufacturing [2].

Three-dimensional printing by Selective Laser Sintering (SLS) has been available since 1986 [3]. Surgical applications using this method emerged later with improved technologies, making it possible for straightforward individualized or batch production of bone implants for surgeries in orthopedics, dentistry, neurosurgeries, and cranioplasties in both oral and maxillofacial surgery [3,4,5].

Direct metal laser sintering (DMLS) is the most widely used metal 3D printing technology. DMLS and SLM (selective laser melting) are used by technicians interchangeably, but they are also slightly different. Although the process is the same, DMLS is preferable when alloys are being created for metal parts, whereas SLM is used to create single element metals (Titanium CP) [6,7].

The additive manufacturing technology can also effectively integrate diverse types of living cells within a three-dimensional scaffold made up of conventional micro or nanoscale biomaterials to create an artificial bone graft capable of regenerating the damaged tissues [8,9,10,11,12,13].

In this work, we describe how to rapidly prototype a new biomechanical model for bone screws as a dental implant in 3D, improving the designs, optimizing the 3D printing process, and correlating desired functional aspects, and within the limitations of the additive manufacturing process. The purpose of this work is to describe how to prototype an innovative biomedical device by 3D printing.

2 Material and Methods

The bioactive kinetic screw (BKS), as seen in Figure 1, was created by the first author, and intended to reutilize the bone removed and discarded during the drilling for a dental implant's insertion into the bone. The original design was made by the first author on a sheet of paper. The goal at that point was to describe the new biomechanical concept and the possibility of applying for a patent request. A specialized company in Brazil, Modal Marcas e Patentes, for patent deposit, developed the first 3D design in Solidworks®. After six modifications by the author, finally the concept was ready to fill the patent request which was subsequently successfully completed.

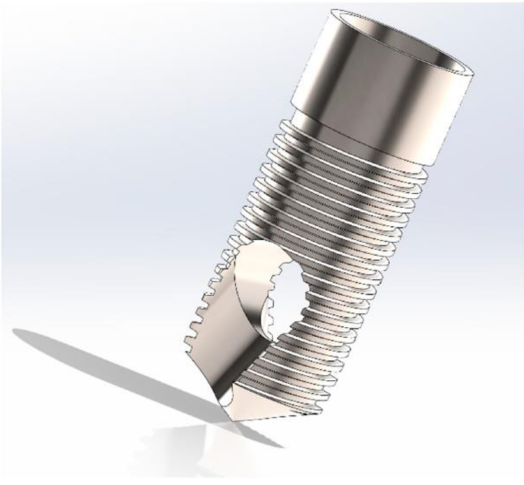

Figure 1. Prototype of BKS ready to be 3D printed.

An extensive literature review [14,15,16,17] was conducted after that to determine all the engineering and biological concepts to be applied in BKS, and given the possible sizes of the screw, flutes, through hole, threads, pitch, prothesis connections, angle of cut, angle of threads, every detail should be designed with the purpose of obtaining primary stability (mechanical) in the bone and secondary stability (biological) for as long a period as possible. Based on the literature review, these choices are made in relation to the purpose of the biomedical device and the characteristics desired by the author. The screw can be produced in any size according to the required bone specifications. In this study, we applied the size of 10 mm length and 4 mm diameter.

The next step was to evaluate by finite element analysis (FEA) the thermo-mechanical behavior of the BKS into the bone. At that point, modifications can be made by the authors, to achieve desired goals about the strain–stress levels which are required in order for the new prototype to be developed [14,15,16,17].

Once the computer simulations are finished, printing prototypes are mandatory to check if the desired outcomes observed in the project are fulfilled by the 3D printing process, and that they have an accuracy of 0.1 mm [2,5]. Prototypes can also be 3D printed in composites before the 3D metal printing; a filament extrusion system can be used because of the feasibility and similarity in the results of the printed device. The final concept design will be ready to metal 3D print by specialized additive manufacturing factories that have a validated process as seen in Figure 2.

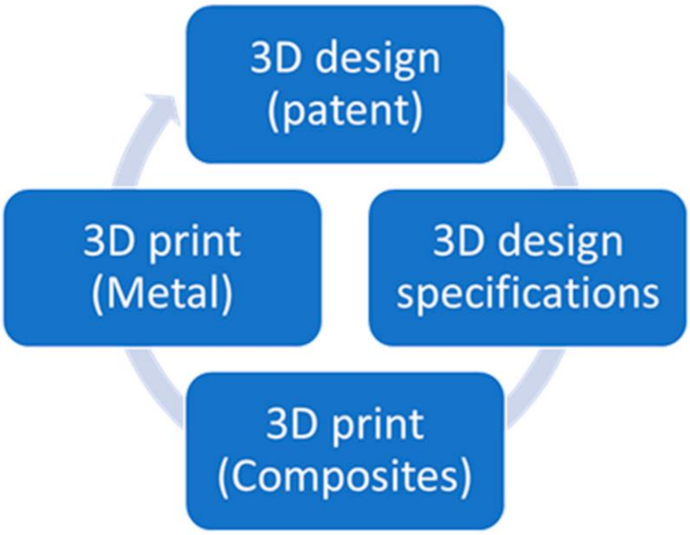

Figure 2. Methodology applied to develop a 3D-printed prototype of a dental implant.

Approved factories for biomedical devices manufacturing can deliver the final product ready to use, depending on the regulations applied for specific biomedical device [18,19]. Class III devices (biomedical devices) are subjected to higher regulatory scrutiny. However, the guidance lacks information on point-of-care manufacturing, which may be a significant gap as hospitals have rapidly invested in 3D printers over the past few years. Under the medical devices category, the FDA has also cleared software programs specifically intended to generate 3D models of a patient's anatomy. The FDA leaves it up to the medical facility to use the software correctly and within the scope of its intended use [18].

Within the European Union (EU), medical devices are regulated by European Council Directives 93/42/EEC (for medical devices, known as the MDD). The majority of 3D printed medical devices to date have been under MDD regulation and these are considered "custom-made", which is defined as being specifically made in accordance with a written prescription of any person authorized by national law by virtue of that person's professional qualifications. This allows for, under their responsibility, specific design characteristics and is intended for the sole use of a particular patient to exclusively meet.

3 Results

Since its first conceptualization for the patent, the BKS design was modified in Solidworks®, as seen in Figure 3, and printed in composites and metal for a visual analysis and for the efficacy of 3D printing in relation to the final desired outcome.

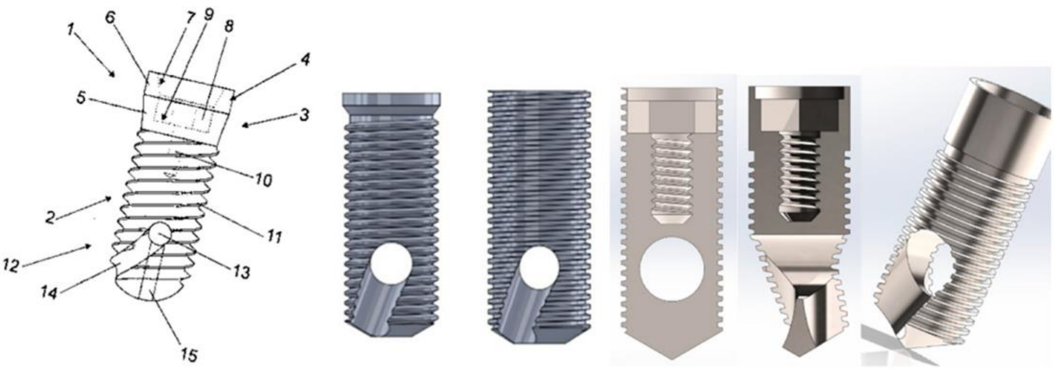

Figure 3. Evolution of the 3D design in Solidworks®. Characterized by a main body (1) that describes a cylindrical trunk (2), whose upper section (3) projects a head (4) with lower tapered section (5) from which extends a cylindrical trunk (6) that internally describes an oblique wall (7) that ends in an internal hexagon (8) whose bottom (9) projects centrally and longitudinally blind hole (10), cylindrical trunk (2) provided with a superb thread (11), whose lower section (12) has a through hole (13) that projects conductive grooves transversely (14), cylindrical trunk (2) is liable to receive a longitudinal hole (15) which communicates with the through-hole (13).

3.1 BKS 3D Printing

Three-dimensional printing in composites during the development process was a fundamental task before the metal printing. It is a feasible and faster way to evaluate the quality and features through a visual analysis and assess the connections for the prothesis and, at same time, the executability for the final titanium metal printing, as seen in Figure 4.

Figure 4. Testing connections in the BKS 3D printed in composite (Nylon).

During the metallic printing tests, as seen in Figure 5, we found unfavorable results with the initial 3D designs. This pointed out improvements to be completed in the final model. These changes helped not only for making possible the fabrication of the biomedical device BKS by additive manufacturing, but also improved the function for the primary stability insertion torque in the bone.

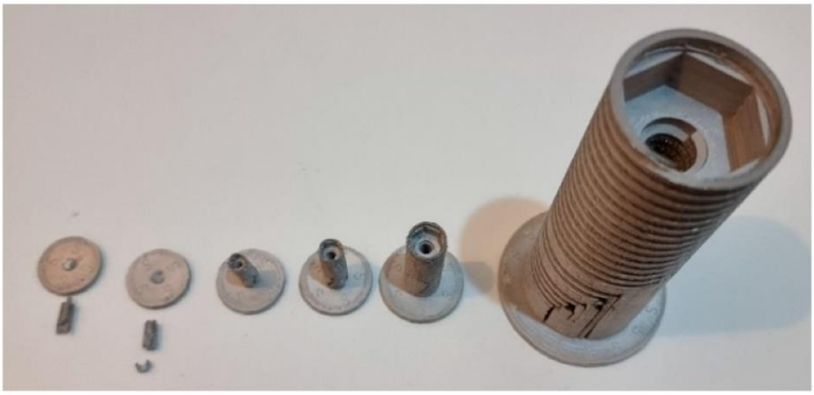

Figure 5. BKS printed in metal with varied sizes before the final printing process.

After all adjustments and tests, the final prototype is ready to be 3D printed by a specialized additive manufacturing factory that has a validated process for biomedical devices with all certifications required for class III devices.

All these procedures optimize the result and make it feasible for developing new prototypes for healthcare, especially because the inventor will be able to make and analyze the 3D concept in a printed device before sending for a more expensive way of production in titanium.

3.2 BKS FEM Model

In this work, a 3D numerical and structural linear model was developed by the authors, using ANSYS 2020 R2®–Workbench 2020 R2, with the new BKS biomechanism in Ti6Al4V (Grade 5) compared with a regular screw with the same size and threads of BKS. The mechanical properties of the material are shown in Table 1 [21].

Table 1. Mechanical properties [21].

	Ti6Al4V (Grade 5)
Young's Modulus, GPa	114
Poisson's Ratio	0.36
Ultimate Tensile Strength, MPa	896
Tensile Yield Strength, MPa	827

The application of the finite element modelling (FEM) aims to simulate the BKS biomechanism and evaluate the distribution of mechanical stresses and strains in the screw with or without the new biomechanism. The 3D model was built by the authors, using Solidworks® and ANSYS 2020 R2®–Workbench 2020 R2 software, as shown in Figure 6. Accordingly, the mesh adopted to use in our simulations consists of a total of 23,215 tetrahedron elements in BKS screw and 47,722 elements in the regular screw without biomechanism. The same element size was adopted equal to 0.3 mm.

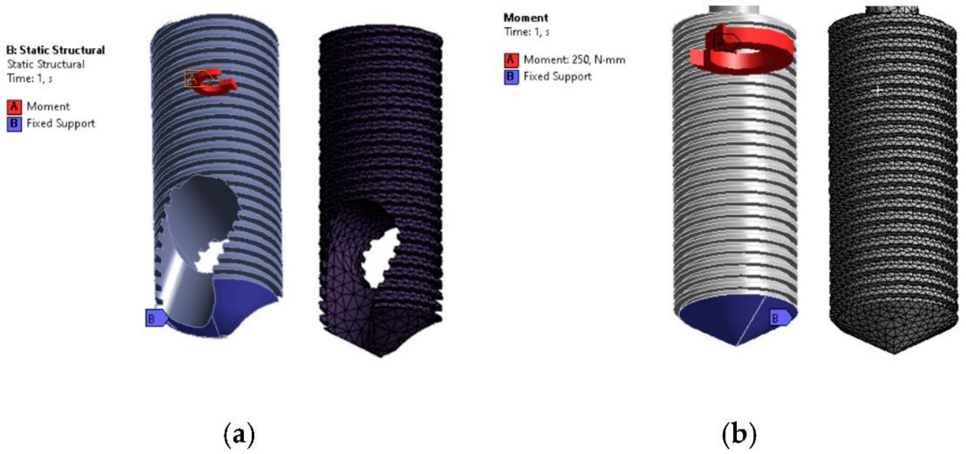

Figure 6. Static structural analysis. Boundary conditions and mesh. (a) BKS screw. (b) Regular screw without biomechanism.

Based on the geometrical model, volumetric finite element meshes were generated using SOLID187 element. SOLID187 element is a higher order, defined by 10 nodes having three degrees of freedom at each node (translations in the nodal x, y, and z directions). This tetrahedron element has a quadratic displacement behaviour with four-point integration and is suitable for modelling irregular meshes, such as those produced from CAD/CAM systems.

In the present study, an electric motor EM-12L with a maximum power of 59 W was selected, and angular speeds between 100 and 40,000 rpm [22]. The new BKS tool, intended for use in ongoing research, will work with different angular speeds depending on the material with which it is made, and with a constant feed rate of 0.5 mm/s vertically downwards. In this study, only the mechanical load due to the cutting torque Mt was considered in the model and the thermal effect produced by the BKS was not considered in this simulation. The relation between the torque (Mt in Nm), the maximum electrical power during drilling (P in W) and the speed of rotation (n in rpm) is determined according by Equation (1).

$$M_t = 9.55\ \frac{P}{n} \tag{1}$$

Boundary conditions, which represent typical drilling phenomena, are established on the lower surface of the BKS as fixed, and on the upper surface with the application of torque equal to 250 Nm, according to the rotational speed of 2250 rpm, using Equation (1).

The obtained results from equivalent stress and equivalent elastic strain are shown in Figure 7 and Figure 8.

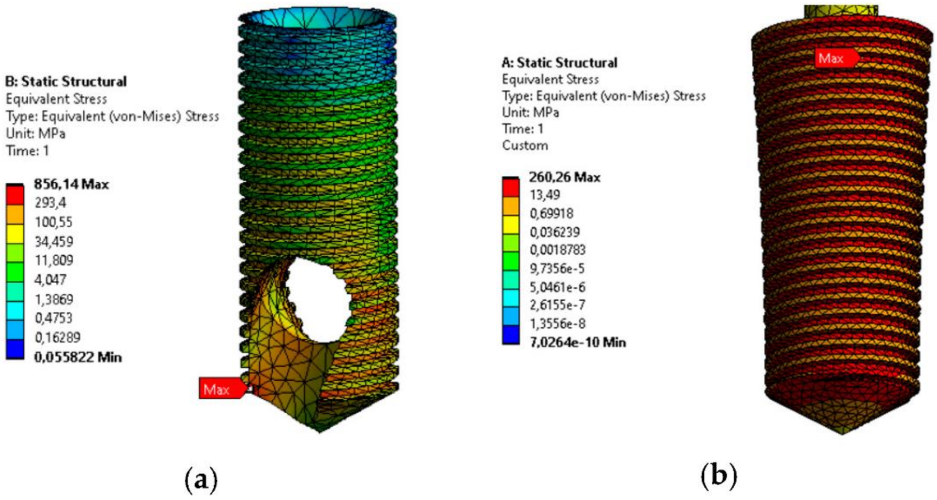

Figure 7. Equivalent stress in BKS screw (a) and regular screw without biomechanism (b).

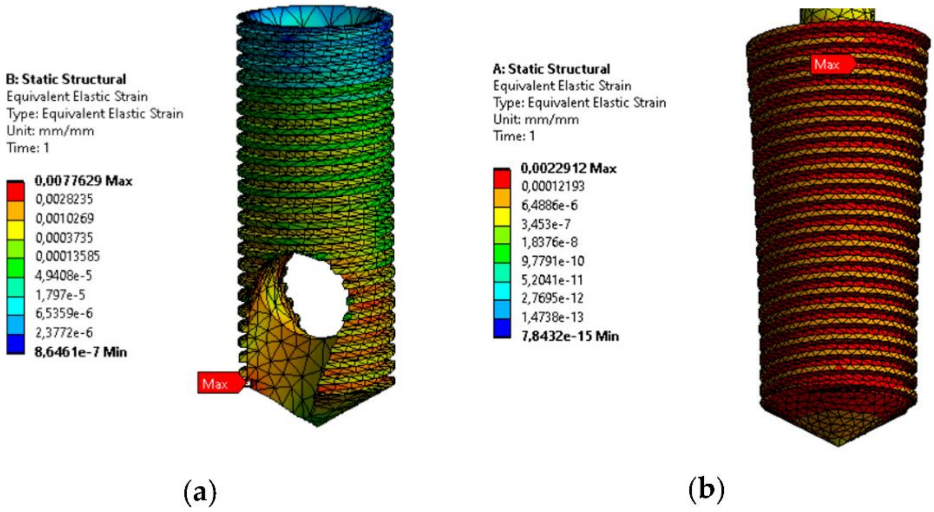

Figure 8. Equivalent elastic strain in BKS screw (a) and Regular screw without biomechanism (b).

Numerical results show that stress and strain levels increase 3.3 and 3.4 times more (respectively) in the BKS screw when compared with regular screw without the new biomechanism.

At the tip of the screw, the BKS presents higher stress and strain. The equivalent elastic stress determines the level of stress in the BKS that can be transmitted in the drilling process to the bone material.

The calculated stresses and strains vary along the entire length of the BKS, and this can be justified by the inertia of its cross section, with free space existing in the BKS mechanism. The inertia cross section at the bottom decreases, hence the strain increases. The strain level follows the same behavior.

The use of the geometry with the new biomechanics induces greater stresses and strains, but always within the ultimate admissible limit.

4 Discussion

Additive manufacturing or 3D printing is a disruptive technology, and it impacts multiples disciplines, including tissue engineering and biomedical engineering. Biomaterials are natural, synthetic, or combined materials used to improve the healing process of damaged body parts while cooperating with living systems [20]. Since the improvements obtained with osseointegration after Branemark's work, metallic, ceramic, and polymeric biomaterials have stablished unique innovations to biomedical devices, improving the quality of human life.

Biocompatibility is recognized by the literature as the primary goal for the biological assessment of a biomaterial. The elastic modulus is observed in an equal manner for mechanical performance. Metals are mostly bioinert, whereas ceramics, glasses and polymers can be bioinert or bioactive [23,24].

Metals and their alloys are applied in all biomedical devices, such as commercially pure titanium and its alloy (Ti6Al4V), for orthopedic, maxillofacial surgeries and load-bearing hip and knee implants, respectively. Stainless steel 316L is used for fracture treatment, and CoCr alloys for mobility surfaces [8,20,24].

It is crucial to invent new biomaterials with individual properties and mandatory to settle proved manufacturing standards to build distinct biomedical devices. Three-dimensional printing has updated biomedical device manufacturing, especially for porous scaffolds and patient-matched implants, increasing the design possibilities of biomedical devices [25,26].

Three-dimensionally printed metallic implants in the initial stages of development were intended to create porous structures to reduce the natural stiffness of the material and the methods for biological integration [27].

The new BKS presented all of the following desired factors combined in one biomedical device: the possibility to be 3D printed in commercially pure titanium and its alloy (Ti6Al4V); the presence of grooves and a hole making it porous decreasing the stiffness of the device; and can be a patient-matched implant.

One of the greatest benefits added on this new BKS prototype is the innovation for patient-matched dental implants and can be performed in a straightforward manner through a validated and certified company, after biomechanical tests, and following international regulatory rules [13,14].

Three-dimensionally printed patient-matched implants are being increasingly and continually developed and applied in the last years. Over 100,000 mass-produced metallic implants for human use are being additive manufactured every year only in the United States and used regularly in hospitals worldwide. Regulatory approval for 3D-printed devices can be slow if the operations are significantly different from traditional approaches [18,19,20].

Metal powders are the raw materials for additive manufacturing technologies. It is still questionable how long these powders can be reused, and what proper techniques should be applied to guarantee the robustness of the process [3,4].

With improved design flexibility and materials options in additive manufacturing, diversified innovative biomedical devices will be available to benefit long-established challenges in human care.

Creativity and imagination are needed to solve problems, and healthcare innovations in biomedical devices are a reality and will become the primary founders of disruptive technologies, both aggregating and increasing economic value. Three-dimensional printing is described to be the fourth industrial revolution and it is changing the traditional manufacturing process, being sustainable for the environment, economy, and society [28,29].

The final design of BKS was reinforced in the crest module diameter (top of the dental implants, as seen in Figure 1) after failures in metal 3D printing, while improving the prosthesis connection surface, decreasing stress within the bone where higher stresses occur. The gain in crest module diameter enhances the prosthesis adaptation with lesser stresses during loading [30]. We realized that techniques to minimize the part volume and using additive manufacturing technologies that do not require support structures can help keep costs as low as possible. Metal filament for 3D printers is not suited for industrial metal 3D printing, both from a throughput and from a quality perspective.

The best solution for biomedical devices is DMLS (direct metal laser sintering). SLM (selective laser melting) uses a combination of heat and pressure to make particles stick together. Melting (DMLS) uses high enough temperatures to cause the particles to fully melt and join. Sintered parts have high porosity and require heat treatments to be strengthened, though they will never be as strong as forged metal parts; melted parts are fully solid and do not require heat treatments.

Macro design in implants focuses on the relationship between osseointegration and mechanical features of implant design engineering and helps to understand which implant to select depending on different clinical conditions. Micro design features include the study of the biological aspect of implant design and focuses on the host response patterns and implant survival. It influences cell behavior on the surface such as adhesion, proliferation, and differentiation of cells as well as the mineralization of the extracellular matrix at the implant's surfaces [14,17,24].

BKS, the new biomechanism presented in this work, aims to bring biomechanical benefits to all types of screws and their designs in which bone integration is necessary in the short and long term. The disadvantage is when a temporary fixation of the screw is needed. In this case, the BKS is contra-indicated.

5 Conclusions

The creation, development, and prototyping of innovative biomedical devices has seen a huge improvement with the recent technologies and software, especially related to 3D printing and 3D drawings, respectively. DMLS (direct metal laser sintering) additive manufacturing offers a better quality and faster process of developing a complete prototype to be used for experiments or human application, following international regulatory rules.

The numerical results obtained by FEM showed that the BKS has structural strength for its proposed biomechanics and pointed out that the region on the top of the screw (crest module), where bone-implant contact occurs and the prosthesis is fixed in a dental implant, was designed to be most reinforced area of the screw.

Future studies will describe the results of the BKS prototype in vivo. These results can be used to add novel changes in the 3D model, applying the same method described in this work.

6 Patents

Carlos Aurelio Andreucci, C.A.A. (2022). Disposição construtiva aplicada em parafuso para implante ósseo (Brasil/Internacional Patent No. WO2022036425A1). WIPO (PCT). URL WO2022036425A1–Disposição construtiva aplicada em parafuso para implante ósseo–Google Patents.

Conflict of interest statement

The authors declare that no conflicts of interest associated with the presented work.

References

1. Coriaty, N.; Pettibone, K.; Todd, N.; Rush, S.; Carter, R.; Zdenek, C. Titanium Scaffolding: An Innovative Modality for Salvage of Failed First Ray Procedures. J. Foot Ankle Surg. 2018, 57, 593–599.
2. Dawood, A.; Marti, B.M.; Sauret-Jackson, V.; Darwood, A. 3D printing in dentistry. Br. Dent. J. 2015, 219, 521–529.
3. Deckard, C. Method and Apparatus for Producing Parts by Selective Sintering. U.S. Patent US4863538A, 5 September 1989.
4. Melchels, F.P.W.; Feijen, J.; Grijpma, D.W. A review on stereolithography and its applications in biomedical engineering. Biomaterials 2010, 31, 6121–6130.
5. Zhou, X.; Yang, Y.; Bharech, S.; Lin, B.; Schröder, J.; Xu, B. 3D-multilayer simulation of microstructure and mechanical properties of porous materials by selective sintering. GAMM-Mitteilungen 2021, 44, e202100017.
6. Cerea, M.; Dolcini, G.A. Custom-Made Direct Metal Laser Sintering Titanium Subperiosteal Implants: A Retrospective Clinical Study on 70 Patients. BioMed Res. Int. 2018, 2018, 5420391.
7. Jaivignesh, M.; Babu, A.S.; Arumaikkannu, G. In-vitro Analysis of Titanium Cellular Structures Fabricated by Direct Metal Laser Sintering. Mater. Today Proc. 2020, 22, 2372–2377.
8. Cheng, L.; Shoma, K.; Suresh, S.; He, H.; Rajput, R.S.; Feng, Q.; Ramesh, S.; Wang, Y.; Krishnan, S.; Ostrovidov, S.; et al. 3D Printing of Micro- and Nanoscale Bone Substitutes: A Review on Technical and Translational Perspectives. Int. J. Nanomed. 2021, 16, 4289–4319.
9. Cox, S.C.; Thornby, J.A.; Gibbons, G.J.; Williams, M.A.; Mallick, K.K. 3D printing of porous hydroxyapatite scaffolds intended for use in bone tissue engineering applications. Mater. Sci. Eng. C 2015, 47, 237–247.
10. Kim, J.I.; Kim, D.Y.; Kwon, D.Y.; Kang, H.J.; Min, B.H.; Kim, M.S. An injectable biodegradable temperature-responsive gel with an adjustable persistence window. Biomaterials 2012, 33, 2823–2834.
11. Kantaros, A.; Piromalis, D. Fabricating Lattice Structures via 3D Printing: The Case of Porous Bio-Engineered Scaffolds. Appl. Mech. 2021, 2, 18.
12. Inzana, J.A.; Olvera, D.; Fuller, S.M.; Kelly, J.P.; Graeve, O.A.; Schwarz, E.M.; Kates,

S.L.; Awad, H.A. 3D printing of composite calcium phosphate and collagen scaffolds for bone regeneration. Biomaterials 2014, 35, 4026–4034.
13. Kantaros, A.; Chatzidai, N.; Karalekas, D. 3D printing-assisted design of scaffold structures. Int. J. Adv. Manuf. Technol. 2015, 82, 559–571.
14. Andreucci, C.A.; Fonseca, E.M.M.; Jorge, R.N. Advances and Current Trends in Biomechanics, 1st ed.; Taylor & Francis: London, UK, 2021; pp. 1–4.
15. Fernandes, M.G.; Fonseca, E.M.; Natal, R.M. Three-dimensional dynamic finite element and experimental models for drilling processes. Proc. Inst. Mech. Eng. Part L J. Mater. Des. Appl. 2015, 232, 35–43.
16. Fernandes, M.G.; Fonseca, E.M.; Jorge, R.N. Thermo-mechanical stresses distribution on bone drilling: Numerical and experimental procedures. Proc. Inst. Mech. Eng. Part L J. Mater. Des. Appl. 2019, 233, 637–646.
17. Andreucci, C.A.; Alshaya, A.; Fonseca, E.M.M.; Jorge, R.N. Proposal for a New Bioactive Kinetic Screw in an Implant, Using a Numerical Model. Appl. Sci. 2022, 12, 779.
18. Available online: https://www.fda.gov/medical-devices/3d-printing-medical-devices/3d-printing-medical-devices-point-care-discussion-paper (accessed on 28 October 2022).
19. Available online: https://www.ema.europa.eu/en/human-regulatory/overview/medical-devices (accessed on 28 October 2022).
20. Bandyopadhyay, A.; Ghosh, S.; Boccaccini, A.R.; Bose, S. 3D printing of biomedical materials and devices. J. Mater. Res. 2021, 36, 3713–3724.
21. Shah, F.A.; Trobos, M.; Thomsen, P.; Palmquist, A. Commercially pure titanium (cp-Ti) versus titanium alloy (Ti6Al4V) materials as bone anchored implants—Is one truly better than the other? Mater. Sci. Eng. C 2016, 62, 960–966.
22. Available online: https://www.wh.com/en_global/dental-products/restoration-prosthetics/electric-motor/em-12l/ (accessed on 22 November 2022).
23. Ashtiani, R.E.; Alam, M.; Tavakolizadeh, S.; Abbasi, K. The Role of Biomaterials and Biocompatible Materials in Implant-Supported Dental Prosthesis. Evidence-Based Complement. Altern. Med. 2021, 2021, 3349433.
24. Albrektsson, T.; Johansson, C. Osteoinduction, osteoconduction and osseointegration. Eur. Spine J. 2001, 10 (Suppl. S2), S96–S101. [Google Scholar]
25. Bose, S.; Ke, D.; Sahasrabudhe, H.; Bandyopadhyay, A. Additive manufacturing of biomaterials. Prog. Mater. Sci. 2018, 93, 45–111.

26. Bandyopadhyay, A.; Mitra, I.; Bose, S. 3D Printing for Bone Regeneration. Curr. Osteoporos. Rep. 2020, 18, 505–514.
27. Dumas, M.; Terriault, P.; Brailovski, V. Modelling and characterization of a porosity graded lattice structure for additively manufactured biomaterials. Mater. Des. 2017, 121, 383–392.
28. Liu, Z.; Jiang, Q.; Zhang, Y.; Li, T.; Zhang, H. Sustainability of 3D Printing: A Critical Review and Recommendations. In Proceedings of the ASME 2016 11th International Manufacturing Science and Engineering Conference, Blacksburg, VA, USA, 27 June–1 July 2016; Volume 2, p. 4.
29. Jiang, Q.; Liu, Z.; Li, T.; Cong, W.; Zhang, H.-C. Emergy-based life-cycle assessment (Em-LCA) for sustainability assessment: A case study of laser additive manufacturing versus CNC machining. Int. J. Adv. Manuf. Technol. 2019, 102, 4109–4120.
30. Shetty, P.; Yadav, P.; Tahir, M.; Saini, V.; Prajapati, D.; Mahesh, L. Implant Design and Stress Distribution. Int. J. Oral Implant. Clin. Res. 2016, 7, 34–39.

CHAPTER VII

*A New Simplified Autogenous Sinus Lift Technique**

Carlos Aurelio Andreucci[1], Elza Fonseca[2], Renato Natal Jorge[3]

[1]Faculty of Engineering of the University of Porto (FEUP), Portugal
[2]School of Engineering, Polytechnic of Porto (ISEP), Mechanical Engineering Department, Portugal
[3]Faculty of Engineering of the University of Porto (FEUP), Portugal

**Bioengineering 2023.* 2023 April 10(5), 505

DOI: 10.3390/bioengineering10050505

Abstract

Oral maxillofacial rehabilitation of the atrophic maxilla with or without pneumatization of the maxillary sinuses routinely presents limited bone availability. This indicates the need for vertical and horizontal bone augmentation. The standard and most used technique is maxillary sinus augmentation using distinct techniques. These techniques may or may not rupture the sinus membrane. Rupture of the sinus membrane increases the risk of acute or chronic contamination of the graft, implant, and maxillary sinus. The surgical procedure for maxillary sinus autograft involves two stages: removal of the autograft and preparation of the bone site for the graft. A third stage is often added to place the osseointegrated implants. This is because it was not possible to do this at the same time as the graft surgery. A new bioactive kinetic screw (BKS) bone implant model is presented that simplifies and effectively performs autogenous grafting, sinus augmentation, and implant fixation in a single step. In the absence of a minimum vertical bone height of 4 mm in the region to be implanted, an additional surgical procedure is performed to harvest bone from the retro-molar trigone region of the mandible to provide additional bone. The feasibility and simplicity of the proposed technique were demonstrated in experimental studies in synthetic maxillary bone and sinus. A digital torque meter was used to measure MIT and MRT during implant insertion and removal. The amount of bone graft was determined by weighing the bone material collected by the new BKS implant. The technique proposed here demonstrated the benefits and limitations of the new BKS implant for maxillary sinus augmentation and installation of dental implants simultaneously.

Keywords: scaffold; sinus lift; dental implant

1 Introduction

The maxillary sinuses are air-filled spaces located in both maxilla, lateral to the nasal cavity, superior to the maxillary teeth, inferior to the orbital floor, and anterior to the infratemporal fossa. Furthermore, the maxillary sinus is second to the ethmoid as a source of orbital infection [1]. With an average volume of 12.5 mL, these sinuses are the largest of the paranasal sinuses. The maxillary sinuses are surrounded by a thin bilaminar mucoperiosteal membrane (Schneider's membrane). This membrane consists of a ciliated pseudostratified columnar epithelium on the luminal side and a single-cell osteogenic periosteal layer on the bony side [2]. In occlusal rehabilitation, the simultaneous placement of osteotome-mediated sinus floor elevation implants with autogenous bone grafting can be considered a successful and predictable treatment approach for deficient posterior maxillary ridges. Different classes of biomaterials, from platelet concentrates to harvested bone and dentin derivatives, are indeed used in sinus lift interventions [3]. This contributes to bone remodeling, resulting in increased endosinus bone gain and a significant reduction in marginal bone loss [4]. Studies systematically reviewed the current evidence on the effect of non-graft versus graft-supported sinus floor elevation on implant survival/failure, endosinus bone gain, crestal bone loss, and bone density around dental implants. Implant survival/failure was the primary outcome. Endosinus bone gain, crestal bone loss, and bone density around dental implants were secondary outcomes. Non-graft maxillary sinus floor elevation appears to be characterised by the new bone formation and high implant survival comparable to bone-graft-supported maxillary sinus floor elevation [5]. There is still no robust evidence on the best techniques for oral rehabilitation with implants in the atrophic maxilla, with or without sinus augmentation. The existence of a wide variety of techniques, implant models, and graft materials in use is evidence of these observations, which are supported by the extensive literature [6,7,8,9,10,11]. All these techniques have their own advantages and disadvantages, ranging from the amount of time involved, to the level of security, cost, and learning curve, such as minimally invasive endoscopic-assisted sinus augmentation [12].

A retrospective study of maxillary sinus lift showed it to be a viable surgical technique allowing implant placement with predictable long-term success regardless of bone graft material type. The success rate of grafts and implants was not affected by the presence of sinus membrane perforation [13]. Another study prospectively evaluated implant status, marginal bone loss, and maxillary sinus floor augmentation outcomes in patients undergoing sinus lift and simultaneous implant placement using bone grafts harvested adjacent to the actual surgical site. Bone grafts can be harvested locally at the site of maxillary sinus augmentation with successful implant placement and healing [14]. One of the most common complications of sinus floor elevation in highly atrophic alveolar ridge augmentation is the perforation of the maxillary sinus membrane. In terms of long-term success, there is no increased risk of implant failure or other persistent complications, such as sinusitis after intraoperative perforation [15,16]. A direct sinus lift, the conventional method of elevating the maxillary sinus, requires surgical access through the lateral wall of the maxilla and elevation of the sinus membrane with the insertion of a bone graft under direct vision. A modified, less invasive method uses a crestal approach without direct membrane visualization, called indirect sinus lift [17].

Tatum in 1970 augmented the posterior maxilla with an autogenous rib and in 1974 developed a Caldwell–Luc surgical technique by fracturing the crest of the alveolus, modifying his own procedure to lift the membrane via a lateral approach [18]. In 1994, Summers developed an internal approach to lift the membrane via an osteotomy, a less invasive procedure for sinus membrane elevation in conjunction with dental implant placement, referred to as osteotome/crestal sinus membrane elevation (OCSME) [7,16,17]. It is indicated for patients with a minimum of 5.0 to 6.0 mm of adequate remaining alveolar bone below the sinus floor. Chen (1996) developed the technique of hydraulic sinus condensation with an osteotomy on the lateral wall of the maxillary ridge [17,19]. The development of hydraulic sinus condensation relies on pressure on the graft material and trapped fluids to hydraulically compress the sinus membrane, creating a blunt force over an expanded area larger than the osteotome tip. In the early days of sinus lift (1974–1979), most grafts were autogenous bone, followed by deproteinized bovine bone mineral (DBBM), and then synthetic grafts, such as beta-tricalcium phosphate (ß-TCP) and calcium phosphosilicate (CPS) [20].

With the introduction and studies of the new bioactive kinetic screw (BKS) dental implant, it is possible to perform a homogeneous autogenous autograft (from the same individual at the same site), transporting the harvested bone to the apical region of the implant [21,22,23,24,25,26]. In the case of implants placed in the atrophic maxilla close to the maxillary sinus, the apical region coincides with the limit defined by the amount of bone and the extension of this sinus. As a natural process of the characteristics and properties of BKS, in which it perforates, screws, collects, and compacts the perforated bone, retaining it in its internal volume, it is possible to lift the sinus membrane using the material's compression technique in the same simplified surgical procedure. As the transplanted homogeneous autogenous bone is compressed in the internal volume of the BKS, it is transported into the maxillary sinus after the sinus membrane is lifted by pressure and stabilized by the properties of the BKS.

Using a synthetic maxilla and sinus, it is possible to develop and describe an innovative technique for simplified sinus lift using only the concept of simultaneous drilling and screwing, unique inherent characteristics of the BKS, whereby a novel dental implant technique now also simultaneously lifts the maxillary sinus with the pressure provided by the implant apex assembly, densified particulate bone in the internal volume of the BKS, and the controlled insertion torque obtained in the experiment and technique described here. The BKS sinus lift is proven to be a simple and safe technique for immediate indirect sinus lift with homogeneous autogenous bone in cases where a minimum bone height of 4 mm is available. The use of a low rotational speed (60 to 600 rpm) during implantation ensures that implant insertion into the maxillary sinus is safely avoided, and the increased maximum insertion torque achieved by the BKS optimizes implant fixation in bone of low density and volume. This technique was developed experimentally for use in further in vivo studies.

2 Materials and Methods

In this study, five bioactive kinetic screws (BKS) were machined by Usiform Ltd.a (304 stainless steel) to a length of 10 mm and a diameter of 4 mm with a 15 mm shaft to be connected to the Techdrill Surgical Motor-1 implant motor with a power of 150 watts and a pre-set torque of 45 N/cm for simultaneous drilling and screw insertion. A Lutron TQ 8801 digital torquemeter was used to measure MIT and MRT during implant insertion and removal, and the amount of bone graft was determined by weighing the bone material collected by the new BKS implant using a Brifit precision professional digital mini scale (0.001 to 20.00 g). The technique proposed here, using the innovative BKS dental implant, was performed using a synthetic replica of the constituent bones of the maxillary sinus walls and floor and the sinus membrane, with biomechanical properties such as these structures (Nacional Ossos) used in studies of maxillary sinus augmentation, as seen in Figure 1.

(a) (b)

Figure 1. (a) Synthetic maxillary sinus bone; (b) and maxillary sinus membrane attached to the bone.

In view of the biomechanical characteristics of the BKS already determined [26], the technique proposed here for maxillary sinus augmentation to place dental implants in the atrophic maxilla consists of the simple simultaneous drilling and screwing of the innovative BKS. After the selection of the dental region to be rehabilitated with a dental implant, the BKS is inserted with a surgical motor using the standard initial drilling procedure for placing dental implants. The difference in the technique lies in the properties and characteristics of the BKS itself, which simultaneously drills, screws, collects, and condenses the bone in its internal volume and, in the case of an atrophic maxilla, transplants the bone into the maxillary sinus without exposing it to the oral environment, as seen in Figure 2.

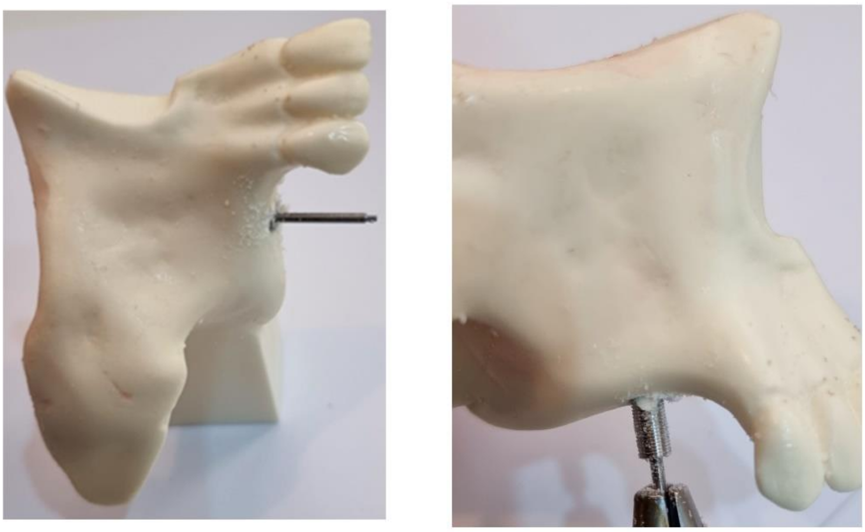

(a) (b)

Figure 2. (a) BKS totally implanted in atrophic maxilla ready to measure the MRT with the digital torquemeter; (b) BKS removed with the compacted collected bone inside to weight measurement.

The MIT torque was measured at the end of implant insertion, as well as its removal and weighing the volume and amount of bone transplanted. After complete insertion of the BKS and augmentation of the maxillary sinus, the sinus membrane was removed to allow direct visualization of the bone graft, as seen in Figure 3.

(a) (b)

Figure 3. (a) Properties of the sinus membrane lifted without rupture by BKS drilling and screwing simultaneously; (b) sinus membrane removed showing the bone transplanted between the maxillary sinus floor and the lifted membrane without rupture.

3 Results

The results obtained corroborate with previous studies, adding the values of MIT and MRT measured during the insertion and removal of the BKS, respectively. Considering that one of the properties of BKS is to compact the material in its internal volume, increasing the density of the material applied by 3.45 times [24] densification and solidification of the material was observed, as seen in Figure 4. After perforation of the floor of the maxillary sinus by continuous insertion of BKS, it was noted that the maxillary sinus membrane was lifted without rupture and that the transplanted bone was retained in the BKS implant. Removal of the sinus membrane for direct visualization of the experiment also revealed the presence of bone particles between the sinus floor and this membrane, as seen Figure 3b.

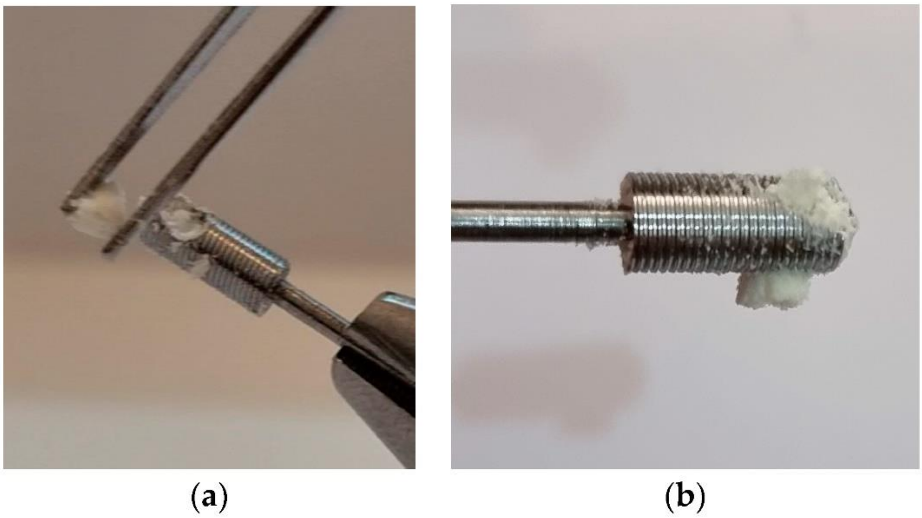

Figure 4. (a) and (b) Condensation and solidification of the bone particles (chips) inside BKS inherent in its properties of compacting material.

3.1 *MIT and MRT*

During the insertion of the BKS into the atrophic maxilla, a constant insertion torque was observed, which increased as the entire internal volume was filled with bone. A progressive increase in the rotation was performed automatically by the surgical motor, which was limited to 600 rpm. Even after disruption of the bone floor of the maxillary sinus, the BKS did not reduce the torque and the MIT was measured at 16 N/cm. During the removal of the BKS, the MRT showed a value of 17 N/cm during most of this unscrewing process. The MRT greater than MIT observed in this study was not reported as an occurrence in the literature for bone implants, with it being stated that the removal torque is always less than the insertion torque in both synthetic and natural bone [17,27,28,29].

3.2 *Weight Measurement*

The weight of the compacted and densified bone in the internal volume of the BKS was measured directly on a high-precision Brifit scale, thus determining the amount of bone transplanted during the indirect maxillary sinus augmentation procedure proposed here. With the value obtained, it was also possible to determine the bone mass density (BMD) of the synthetic bone used in this experiment using Equation (1) determined in a previous study [24]:

$$BMD = \frac{Bone\ inside\ BKS}{3.45} \tag{1}$$

Density (D) can be calculated using the Equation (2) related to volume (V):

$$D = \frac{m}{V} \tag{2}$$

The value of bone weight measured inside the BKS was 43 milligrams (mg), as seen in Figure 5. Therefore, the bone mass density found for the synthetic bone used in this study using Equation (1) is 0.44 mg/mm^3. The bone transplanted into the maxillary sinus was 3.45 times denser (1.53 mg/mm^3) than the bone from the atrophic maxilla used in this experiment with a BKS inner volume of 28.10 mm^3. The total volume of bone transplanted without densification is 63.86 mm^3.

(a) (b)

Figure 5. (a) BKS original weight; (b) BKS and bone weight measurement after total bone removal. The total bone weight is obtained by subtracting the weight of the BKS with bone from the original weight (43 mg).

In previous studies, the measurement of the total BKS volume determined was 96.91 mm^3 [24]. Since the total volume of bone transplanted was 63.86 mm^3 (bone volume available in the atrophic maxilla), it is possible to determine with a tenth of a millimeter accuracy the minimum bone volume of 33.05 mm^3 required for complete bone filling in the maxillary sinus to optimise the contact between the bone and the BKS implant to promote the desired sinus augmentation. The bone augmentation achieved was almost twice the minimum required (63.86 mm^3).

4 Discussion

The innovative bioactive kinetic screw (BKS) described here, a simple machine, has the characteristics of a drill, a screw, and a compression machine, combined simultaneously by the application of an insertion torque to fix this device in any material it is capable of drilling, such as bone. It has the characteristics of a self-tapping screw combined with a drill bit with modified flow grooves to hold and compress the material inside. It can be used to drill in the way of a drill bit, to fix in the way of a screw, to collect material for analysis in the way of a biopsy needle, and to graft in the way of a bone graft collector; it can be adapted to any system that uses a screw as a fixation system or a drill bit as an anchor. These combined features allow this new simple machine (BKS) to be used in many ways [21,22,23,25]. As a drill bit, it can be used for more accurate drilling due to the presence of threads that stabilize the drill and help with penetration speed. As there is an established limit to the chip flow of the drilled material, it is also possible to accurately determine the geometry and depth of the hole. The compacted material inside the BKS can be safely removed for analysis, transport, and reuse with minimal handling [26]. It has a higher removal torque than insertion torque and increases the maximum insertion torque. It can be tested for use on bone screws, dental and other limb implants, and prostheses. It can be used as an instrument for measuring the density of materials, including bone [24].

Maxillary sinus augmentation to increase volume and bone quality in the atrophic maxilla became an important tool in oral rehabilitation with dental implants. Autogenous grafts are still considered the gold standard for bone grafting, but they have some disadvantages in their execution. It usually involves another surgical procedure to remove the bone graft from the patient's donor site and most often a third surgical procedure after an average of 6 months of healing of the grafted bone [4,5]. The proposed new technique, BKS sinus lift, was shown to be similar to conventional dental implant surgery in a single surgical procedure for autogenous bone grafting, sinus lift, and dental implant fixation simultaneously. It also simplified the technique for placing dental implants by using fewer drills to perforate the recipient bone bed site. Care should be taken not to insert the implant into the maxillary sinus, respecting the torque values obtained by simultaneous drilling and screwing of the BKS. This is facilitated by the stability achieved in the simultaneous insertion and drilling of the BKS and its square threads [22].

The increase in MRT in relation to MIT observed in this experiment demonstrates the ability to increase the coefficient of friction between the BKS implant surface and the bone because the densified bone inside it increases the friction between the surfaces by adhesion and cohesiveness between the similar materials bone–implant and bone–bone, respectively [30,31]. In the case of the sinus lift technique proposed here, the hypothesis is that the transferred bone above the floor of the maxillary sinus can also become a mechanical barrier to the removal of the dental implant. The square threads present in the BKS helped to maintain the stability of the implant during and after insertion, including its removal [32]. Regardless of the torque achieved, continuous stability was observed throughout the drilling and removal of the BKS. Although there was no rupture of the sinus membrane in this study, this is a limitation of this experiment because we cannot say that this will happen in clinical practice. Even if the rupture of this membrane were to occur, it is already known in the literature that the rupture of the membrane does not significantly interfere with clinical outcomes [15,16]. We also have the advantage that the technique proposed here is indirect, i.e., without exposing the maxillary sinus to the oral environment and its contaminants.

The densification of the particulate bone (chips) coming from the drill cut was an important observation (Figure 4a,b). It enables the stability of the bone graft used in the maxillary sinus lift. It is expected that the clot that is formed in the natural inflammatory response to the surgical trauma caused by the technique will help to perfuse the graft. This hypothesis should be confirmed in further studies. Since the first theoretical and clinical studies on bone implantation to partially fill with bone the maxillary sinuses, much developed to improve the surgical technique of sinus exposure and augmentation, first with autogenous bone and later with biomaterials [2,3,4,5]. Although the evolution of these techniques contributed to better control the results over the years, the very concept of exposing the maxillary sinus membrane during the surgical procedure increases the risk of infection and other complications [4]. Therefore, authors proposed indirect techniques of maxillary sinus augmentation to avoid sinus exposure, thereby reducing the risk of complications with bone grafting and the success of osseointegration of dental implants [2,19].

The technique of increasing the volume of the maxillary sinus using hydraulic pressure exerted by the bone filling material became an option in cases where there is a vertical height of up to 5 mm in the atrophic maxilla where a dental implant is to be placed [19]. With this concept of indirect augmentation of the maxillary sinus, modified using a new model of dental implant BKS, it is possible to simplify the procedure using autogenous homogeneous bone, i.e., from the patient himself, with bone from the site to be implanted being moved into the maxillary sinus by the biomechanical properties of BKS. In cases where the vertical bone height of the maxillary sinus is less than 4 mm, it is possible to harvest bone from the retromolar region of the patient’s own mandible using the BKS itself as a bone collector [26], as seen in Figure 6, and to transplant the harvested bone in its internal volume to the atrophic maxilla where sinus augmentation for rehabilitation with dental implants is desired. In these cases, an additional surgical procedure is required during the BKS sinus lift surgery, without the need for a new surgery to fix the dental implant.

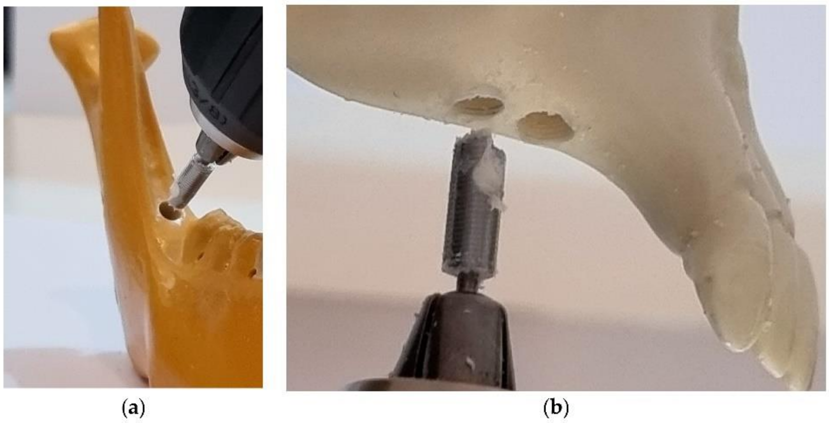

Figure 6. (a) Collecting bone from the retromolar region of the synthetic mandible using the BKS itself as a bone collector; (b) transplanting the harvested bone in BKS internal volume to the atrophic maxilla.

As the bone quality of the atrophic maxilla is of low density and volume, the proposed study allows simultaneous drilling and screw insertion with the BKS in a single step. In cases where the bone density is higher, an initial guide hole of 1.8 mm diameter can be drilled [24]. This pre-drilling should also be performed (Figure 6b) in cases where transplanted bone from the mandibular retromolar region is used, considering the smaller drilling capacity of the BKS that transports the bone inside. This is desired to increase the bone volume of the atrophic maxilla. The BKS demonstrated the ability to form threaded walls in the perforated bone regardless of the change in rpm (Figure 6b).

Filling the maxillary sinus with synthetic biomaterials, such as hydroxyapatite, was shown to be effective in surgical clinical practice [2,29].

The study proposed here that using synthetic bone became an effective means of demonstrating the feasibility and simplification of the technique of augmenting the maxillary sinus with homogeneous autogenous bone in a single step. Since one of the factors related to the success of osseointegrated implants and maxillary sinus augmentation surgery is related to the specific training of the surgeon, simplifying the technique tends to reduce the risks of performing it [2,33]. It was observed in the literature [2,5,19] that all experiments performed on MIT and MRT measurements and comparisons used mean values for analysis and conclusions. With the technique and experiment described here, the importance of directly comparing MIT and MRT values of the same bone perforation, without comparing other perforations among themselves, became apparent. In this way, it was possible to determine the increase in MRT that could be masked by calculating the average of the values found. Ongoing studies will apply the proposed technique and analyse the benefits of healing and simplification of the sinus floor augmentation technique, comparing the results with other direct and indirect sinus lift procedures.

The main advantage of the BKS is to make the use of fixation screws more efficient by controlling the insertion and stability parameters inherent in its combined characteristics of a modified screw and drill, in which the material from the drill is used to compress in its internal volume, increasing the torque through the internal compression of the applied material, distributing the applied forces in a controlled manner, and increasing the stability of the BKS. The unexpected effect when it was created was the ability to compress material in its internal volume with a precisely estimated amount, to measure the density of the material, to increase the value of the removal torque, and above all, to be able to collect the material when desired, for analysis, transport, and re-insertion or reimplantation in the case of organic materials, such as bone.

5 Conclusions

The BKS sinus lift technique proposed and described here was found to be simple and feasible for simplified autogenous transplantation for maxillary sinus augmentation, being similar to the conventional drilling and screwing of dental bone implants. Simultaneous drilling and screwing with square threads provided greater stability for the BKS implant, even with 1/3 of its volume inserted into the maxillary sinus cavity. The experimental tests did not show the “falling into a void” sensation with loss of stability that is usually observed when the implant loses its bone anchorage during implantation. With the limitations described here, the proposed technique proved to be effective in raising the maxillary sinus indirectly, without exposure to the external environment of the sinus membrane. Further studies will evaluate the biological response to this technique.

Conflict of interest statement

The authors declare that no conflicts of interest associated with the presented work.

References

1. Raponi, I.; Giovannetti, F.; Buracchi, M.; Priore, P.; Battisti, A.; Scagnet, M.; Genitori, L.; Valentini, V. Management of orbital and brain complications of sinusitis: A practical algorithm. J. Craniomaxillofac. Surg. 2021, 49, 1124–1129.
2. Stern, A.; Green, J. Sinus Lift Procedures: An Overview of Current Techniques. Dent. Clin. N. Am. 2012, 56, 219–233.
3. Bernardi, S.; Macchiarelli, G.; Bianchi, S. Autologous Materials in Regenerative Dentistry: Harvested Bone, Platelet Concentrates and Dentin Derivates. Molecules 2020, 25, 5330.
4. Rahate, P.S.; Kolte, R.A.; Kolte, A.P.; Bodhare, G.H.; Lathiya, V.N. Efficacy of simultaneous placement of dental implants in osteotome-mediated sinus floor elevation with and without bone augmentation: A systematic review and meta-analysis. J. Indian Soc. Periodontol. 2023, 27, 31–39.
5. Nasr, S.; Slot, D.E.; Bahaa, S.; Dörfer, C.E.; Fawzy El-Sayed, K.M. Dental implants combined with sinus augmentation: What is the merit of bone grafting? A systematic review. J. Craniomaxillofac. Surg. 2016, 44, 1607–1617.
6. Boyne, P.J.; James, R.A. Grafting of the maxillary sinus floor with autogenous marrow and bone. J. Oral Surg. 1980, 38, 613–616.
7. Summers, R.B. A new concept in maxillary implant surgery: The osteotome technique. Compendium 1994, 15, 152, 154–156, 158.
8. Ferrigno, N.; Laureti, M.; Fanali, S. Dental implants placement in conjunction with osteotome sinus floor elevation: A 12-year life-table analysis from a prospective study on 588 ITI implants. Clin. Oral Implant. Res. 2006, 17, 194–205.
9. Del Fabbro, M.; Corbella, S.; Weinstein, T.; Ceresoli, V.; Taschieri, S. Implant survival rates after osteotome-mediated maxillary sinus augmentation: A systematic review. Clin. Implant Dent. Relat. Res. 2012, 14 (Suppl. 1), e159–e168.
10. Gu, Y.X.; Shi, J.Y.; Zhuang, L.F.; Qian, S.J.; Mo, J.J.; Lai, H.C. Transalveolar sinus floor elevation using osteotomes without grafting in severely atrophic maxilla: A 5-year prospective study. Clin. Oral Implants Res. 2016, 27, 120–125.
11. Krennmair, S.; Hunger, S.; Forstner, T.; Malek, M.; Krennmair, G.; Stimmelmayr, M. Implant health and factors affecting peri-implant marginal bone alteration for implants placed in staged maxillary sinus augmentation: A 5-year prospective study. Clin. Implant

Dent. Relat. Res. 2019, 21, 32–41.
12. Giovannetti, F.; Raponi, I.; Priore, P.; Macciocchi, A.; Barbera, G.; Valentini, V. Minimally-Invasive Endoscopic-Assisted Sinus Augmentation. J. Craniofac. Surg. 2019, 30, e359–e362.
13. Jamcoski, V.H.; Faot, F.; Marcello-Machado, R.M.; Melo, A.C.M.; Fontão, F.N.G.K. 15-Year Retrospective Study on the Success Rate of Maxillary Sinus Augmentation and Implants: Influence of Bone Substitute Type, Presurgical Bone Height, and Membrane Perforation during Sinus Lift. Biomed. Res. Int. 2023, 2023, 9144661.
14. Johansson, L.A.; Isaksson, S.; Lindh, C.; Becktor, J.P.; Sennerby, L. Maxillary sinus floor augmentation and simultaneous implant placement using locally harvested autogenous bone chips and bone debris: A prospective clinical study. J. Oral Maxillofac. Surg. 2010, 68, 837–844.
15. Beck-Broichsitter, B.E.; Gerle, M.; Wiltfang, J.; Becker, S.T. Perforation of the Schneiderian membrane during sinus floor elevation: A risk factor for long-term success of dental implants? Oral Maxillofac. Surg. 2020, 24, 151–156.
16. Khehra, A.; Levin, L. Maxillary sinus augmentation procedures: A narrative clinical review. Quintessence Int. 2020, 51, 578–584.
17. Gandhi, Y. Sinus Grafts: Science and Techniques—Then and Now. J. Maxillofac. Oral Surg. 2017, 16, 135–144.
18. Tatum, H. Maxillary and sinus implant reconstruction. Dent. Clin. N. Am. 1986, 30, 207–229.
19. Chen, L.; Cha, J. An 8-year retrospective study: 1100 patients receiving 1557 implants using the minimally invasive hydraulic sinus condensing technique. J. Periodontol. 2005, 76, 482–491.
20. Browaeys, H.; Bouvry, P.; De Bruyn, H. A literature review on biomaterials in sinus augmentation procedures. Clin. Implant Dent. Relat. Res. 2007, 9, 166–177.
21. Andreucci, C.A.; Fonseca, E.M.M.; Natal, R.M.J. Structural analysis of the new Bioactive Kinetic Screw in titanium alloy vs. commercially pure titanium. J. Comp. Art. Int. Mec. Biomec. 2022, 2, 35–43.
22. Andreucci, C.A.; Alshaya, A.; Fonseca, E.M.M.; Jorge, R.N. Proposal for a New Bioactive Kinetic Screw in an Implant, Using a Numerical Model. Appl. Sci. 2022, 12, 779.
23. Andreucci, C.A.; Fonseca, E.M.M.; Jorge, R.N. 3D Printing as an Efficient Way to

Prototype and Develop Dental Implants. BioMedInformatics 2022, 2, 44.

24. Andreucci, C.A.; Fonseca, E.M.M.; Jorge, R.N. Increased Material Density within a New Biomechanism. Math. Comput. Appl. 2022, 27, 90.
25. Andreucci, C.A.; Fonseca, E.M.M.; Jorge, R.N. Bio-lubricant Properties Analysis of Drilling an Innovative Design of Bioactive Kinetic Screw into Bone. Designs 2023, 7, 21.
26. Andreucci, C.A.; Fonseca, E.M.M.; Jorge, R.N. Immediate Autogenous Bone Transplantation Using a Novel Kinetic Bioactive Screw 3D Design as a Dental Implant. BioMedInformatics 2023, 3, 299–305.
27. Comuzzi, L.; Tumedei, M.; Romasco, T.; Petrini, M.; Afrashtehfar, K.I.; Inchingolo, F.; Piattelli, A.; Di Pietro, N. Insertion Torque, Removal Torque, and Resonance Frequency Analysis Values of Ultrashort, Short, and Standard Dental Implants: An In Vitro Study on Polyurethane Foam Sheets. J. Funct. Biomater. 2023, 14, 10.
28. Ravidà, A.; Wang, I.C.; Sammartino, G.; Barootchi, S.; Tattan, M.; Troiano, G.; Laino, L.; Marenzi, G.; Covani, U.; Wang, H.L. Prosthetic Rehabilitation of the Posterior Atrophic Maxilla, Short (≤6 mm) or Long (≥10 mm) Dental Implants? A Systematic Review, Meta-analysis, and Trial Sequential Analysis: Naples Consensus Report Working Group A. Implant Dent. 2019, 28, 590–602.
29. Pierfelice, T.V.; D’Amico, E.; Iezzi, G.; Piattelli, A.; Di Pietro, N.; D’Arcangelo, C.; Comuzzi, L.; Petrini, M. Nanoporous Titanium Enriched with Calcium and Phosphorus Promotes Human Oral Osteoblast Bioactivity. Int. J. Environ. Res. Public Health 2022, 19, 6212.
30. Shockey, J.S.; von Fraunhofer, J.A.; Seligson, D. A measurement of the coefficient of static friction of human long bones. Surf. Technol. 1985, 25, 167–173.
31. Rosenholm, J.B.; Peiponen, K.P.; Gornov, E. Materials cohesion and interaction forces. Adv. Colloid Interf. Sci. 2008, 141, 48–65. [Google Scholar] [CrossRef]
32. Steigenga, J.T.; Al-Shammari, K.F.; Nociti, F.H.; Misch, C.E.; Wang, H. Dental Implant Design and Its Relationship to Long-Term Implant Success. Implant Dent. 2003, 12, 306–317.
33. Lu, B.; Zhang, X.; Liu, B. A systematic review and meta-analysis on influencing factors of failure of oral implant restoration treatment. Ann. Palliat. Med. 2021, 10, 12664–12677.Brett PN, Baker DA, Taylor R, Griffiths MV (2004) Controlling the penetration of flexible bone tissue using the stapedotomy microdrill. *Proc IMechE Part I: J Systems*

and Control Engineering 218(5):343-351.

CHAPTER VIII

*A new simple machine that converts torque into steady-state pressure in solids**

Carlos Aurelio Andreucci[1], Elza Fonseca[2], Renato Natal Jorge[3]

[1]Faculty of Engineering of the University of Porto (FEUP), Portugal
[2]School of Engineering, Polytechnic of Porto (ISEP), Mechanical Engineering Department, Portugal
[3]Faculty of Engineering of the University of Porto (FEUP), Portugal

**IEEE 7th Portuguese Meeting on Bioengineering (ENBENG)*. 2023 July pp. 148-150
DOI: 10.1109/ENBENG58165.2023.10175336

Abstract

The proposed new mechanism, BKS, converts the movement of rotation into linear movement, torque into compression by increasing the density of the mass on which it acts decreasing its original volume under measured conditions. The chosen material for BKS must be more resistant than the material on which it will be applied, making it possible to drill it. To do this, it makes the collected mass smaller than the original by cutting and breaking its original structure, forming granular solids, moving them like fluids into the internal volume of the BKS due to the insertion torque applied, increasing the coefficient of friction between these materials. This is an innovative simple machine that can compact particles within its internal volume, making the material collected denser under mechanical pressure. Previous experimental studies from the authors have shown that the BKS modifies its original surface, incorporating inside its volume the same material on which's applied, standardizing inner volume measurement under given precise conditions. With the introduction of this new simple machine, the possibility to create and develop new mechanical and biomechanical devices is expanded by applying the mechanical advantage determined in this work.

Keywords: Simple Machine; Self-Locking; Friction

1 Introduction

Bone A Simple Machine (SM) is a mechanical device that changes the direction or magnitude of a force, defined as the simplest mechanism that transfers energy allowing work to be done with Mechanical Advantage (MA) [1]. The energy transferred during the operation of the SM can be described by the work input into the SM equal to the work that is output. In operation, deflection, friction, and wear will reduce the Ideal Mechanical Advantage (IMA) to the Actual Mechanical Advantage (AMA) defined by Efficiency, a value that is determined by tests. The Work done by a Force is calculated as the product of Force (F) and Distance (d) moved by the object, so the SM equation with their equivalent expressions in terms of F and d is (1):

$$F_{in}d_{in} = F_{out}d_{out} \tag{1}$$

Torque is very useful for leverage to multiply a Force by adjusting the lever arm of a Simple Machine obtaining AMA, which is the ratio between the Output Force (Fout) and the Input Force (Fin), as seen (2):

$$AMA = \frac{F_{out}}{F_{in}} \tag{2}$$

The IMA of the Screw [2] starts with the transferred rotational movement of the torque being translated into linear downward movement. The expected mechanical advantage produced is calculated by IMA = dE/dR, where dE is the effort (input) distance and dR is the resistance (output) distance. Once the screw is inserted with one complete rotation, a thread penetrates a linear distance to the applied material, and it is possible to measure the IMA by the ratio of the circumference of the screw (dE) to the Pitch (dR) as represented in (3):

$$IMA = \frac{2\pi r}{Pitch} \tag{3}$$

In the experimental application, deflection, friction, and wear will reduce the MA. The amount of this reduction from the AMA is defined by a factor called Efficiency (%E), a quantity which is determined by testing, as seen (4):

$$\%E = \left(\frac{AMA}{IMA}\right)100 \tag{4}$$

The innovation of the new BKS simple machine, as shown in Figure 1, is to use the same characteristics of the screw [3-7] by adding angles and cutting grooves at its apex, reducing the area of contact with the perforated material, and thus increasing the cutting pressure of a conventional screw. In addition to this advantage, the innovation introduced was the ability to store and compact the chips from the drilling and insertion of the BKS through its double flutes, by flowing the chips which meet at a common point in the internal volume of the BKS and are pressed together. After the material to which the new BKS has been applied has filled the entire internal volume with its chips, compaction increases the density of the material [4], transmitting the torque exerted in the pressure area to the entire internal volume of the BKS in all directions, acting as a fluid when there is torque and increasing the coefficient of static friction, and self-locking in the absence of torque. Conventional screws have a very low efficiency due to the amount of friction between the materials. In BKS this has become an advantage.

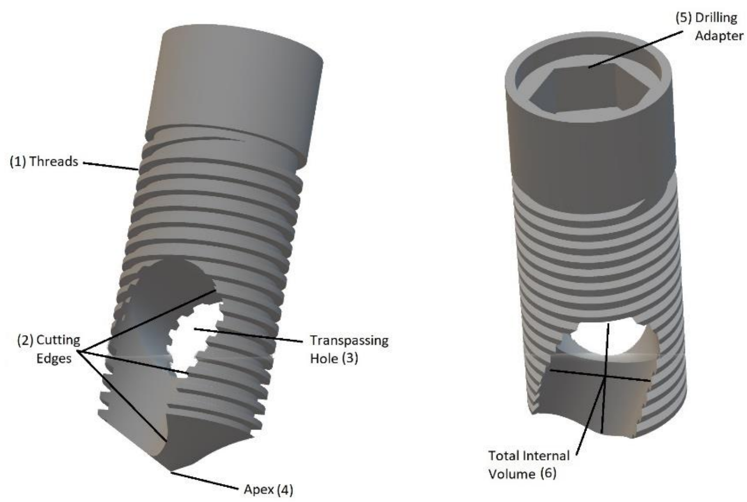

Figure 1. BKS innovative Simple Machine: (1) Screw thread; (2) adding angles and cutting grooves; (3) Trespassing hole connecting flutes; (4) Apex; (5) Drilling or spanner adapter for insertion torque; (6) Inner volume.

2 Materials and Method

2.1 Simple machine BKS

A BKS model manufactured through 3D print in Polylactic Acid (PLA), was experimentally tested in Aluminum Phyllosilicates (clay), with a mean density of fine silts and clays between 1.1 and 1.6 g/cm^3 [4]. The pressure exerted by the BKS Torque on its inner volume makes the collected granular matter denser in proportion to the size of the grains formed, and the amount of Force applied to the Torque. This process occurs until a limit is established between the materials (Self-Locking), experimentally given by the amount of force applied and the innovative Mechanical Advantage Pressure created, without rupturing the system.

The depth where the torque increases more abruptly is considered as the point of flute clogging [8-10] or full-filling the BKS inner volume marked as beginning the compaction of the material, the same criterion for chip-evacuation capability. This provides the means to make comparisons of the BKS performance of different tooling parameters drill geometry, substrate material, coating and cutting conditions.

2.2 Experimental Methodology

Experimental studies in material with a similar density of Synthetic Bone (aluminium phyllosilicates) were conducted to demonstrate the torque increase at the start of compaction (Ti) of the material and the MIT at the full insertion of the BKS. The values were measured using a Lutron digital torque wrench (TQ8801). With the values obtained, the formulas were applied to determine the efficiency of the innovative simple machine BKS by subtracting the MIT of Ti, which determines the mechanical advantage of the BKS in compacting the material in its internal volume.

Figure 2. The Lutron Digital Torque Wrench (TQ8801) displays 35 N/cm (MIT).

3 Results and Discussion

The innovative BKS Mechanical Advantages (MABKS) combines the mechanical advantages of the screw, which are the inclined spiral plane (MA1) and the wheel and axle (MA2), adding the compaction of material in its inner volume under mechanical pressure (MA3) through the resistance movement of the material being drained by double cutting grooves like a drill, densifying the material in which it is applied. The ability to in the same movement of simultaneous insertion and screwing create pressure in its inner volume determines a new MA and therefore becomes an innovative Simple Machine, according to (5):

$$MA_{BKS} = MA_1 MA_2 MA_3 \quad (5)$$

3.1 Results

The BKS model determines two depths of interest when drilling: the depth that can be drilled before being subjected to an increasing torque at which compaction (chip jamming) begins to occur, and the limit based on the material's breaking torque, and thus the maximum desired depth. These two critical depths can be used jointly to change the BKS design accordingly with process planning and materials applied. For a given specified depth, the BKS model can be used to determine if the hole can be drilled in one pass without exceeding the chosen torque limit. If the hole cannot be drilled without violating the limit, a pilot or more previous drilling should be made.

- When the BKS started to compact the material inside, the maximum initial torque (Ti) obtained was 21 N/cm.
- The MIT obtained after full insertion of the BKS was 31 N/cm, the moment at which the increasing force reaches the breaking limit of the material.
- The MRT obtained after removal of the BKS was 25 N/cm, the moment at which the BKS start to move.

The efficiency of the BKS in compacting and densifying the material collected in its internal volume (figure 3) is indicated by the increase in output torque. By applying the formula for efficiency, an increasing value of 84% was obtained for the materials and the method described here.

Figure 3. BKS with the material inside after total collection and removal. The MRT result was 25 N/cm.

3.2 Discussion

Since a system under pressure has the potential to perform work on its surroundings [1], pressure is a measure of potential energy stored per unit volume, equation (6). It is therefore related to energy density and may be expressed in units such as joules per cubic meter (J/m^3, which is equal to Pascal).

$$P = \frac{Work}{Volume} \tag{6}$$

By increasing the pressure that compresses the material in the internal volume of the BKS when it is inserted, the work done is increased by this simple machine [2]. If the aim of the work is to increase the energy of the system, the BKS is more efficient than other devices such as screws, bone screws and dental implants, among others.
Further studies will be necessary to determine the ideal measures for each case in which BKS is applied. It should be noted that there is a limited maximum torque at which the insertion cannot be carried out if the ultimate strength of the materials is compromised. These limits have been experimentally determined for the used materials in the proposed work.

4 Conclusions

This The new, simple BKS machine has been shown to be 84% more efficient than a standard screw that is used in a variety of mechanical and biomechanical applications. It was observed that the removal torque of the BKS was 4 N/cm higher than the initial torque of maximum insertion (Ti), indicating an increase in mechanical locking in screws modified by the proposed new simple machine.

It was possible to standardize the maximum insertion torque in the dimensions and design of the BKS used in the proposed experiment and establish a ratio relationship between the initial moment of compaction of the material (Ti) and the MIT obtained after full insertion of the BKS, due to the characteristics of the collection and compaction of the material inside. Future studies are planned to evaluate other dimensions and different materials to correlate the results described in this work.

Conflict of interest statement

The authors declare that no conflicts of interest associated with the presented work.

References

1. T.G. Chondros, "Archimedes life works and machines," Mech. and Machi. The. , vol. 45(11), pp.1766-1775, november 2010.
2. C. Wang, B. Wang, M. Liu, and Z. Xing, "A Review of Recent Research and Application Progress in Screw Machines," Machines, vol. 10(1), pp. 62, january 2022.
3. C. A. Andreucci, A. Alshaya, E. M. M. Fonseca, and R. N. Jorge, " Proposal for a New Bioactive Kinetic Screw in an Implant, Using a Numerical Model," Appl. Sci., vol. 12, pp. 779, january 2022.
4. C. A. Andreucci, A. Alshaya, E. M. M. Fonseca, and R. N. Jorge, " Increased Material Density within a New Biomechanism," Math. Comput. Appl., vol. 27, pp. 90, november 2022.
5. C. A. Andreucci, A. Alshaya, E. M. M. Fonseca, and R. N. Jorge, "3D Printing as an Efficient Way to Prototype and Develop Dental Implants," BioMedInformatics, vol. 2, pp. 44, december 2022.
6. C. A. Andreucci, A. Alshaya, E. M. M. Fonseca, and R. N. Jorge, "Structural analysis of the new Bioactive Kinetic Screw in titanium alloy vs. commercially pure titanium," J. Comp. Art. Int. Mec. Biomec., vol. 2, pp. 35–43, december 2022.
7. C. A. Andreucci, A. Alshaya, E. M. M. Fonseca, and R. N. Jorge, "Bio-lubricant Properties Analysis of Drilling an Innovative Design of Bioactive Kinetic Screw into Bone," Designs, vol. 7(1), pp. 21, february 2023.
8. J. B. Rosenholm, K. E. Peiponen, E. Gornov E. "Materials cohesion and interaction forces," Adv. in Coll. and Interf. Sci., vol. 141, pp. 1–2, 48-65, september 2008.

9. D. K. Ameur. “Tribological Study of the Friction between the Same Two Materials (RAD Steel),” Tribol. in Mat. and Manuf. - Wear, Friction and Lubrication. doi: 10.5772/intechopen.93478, february 2021.
10. D. A. H. Hanaor, Y. Gan, I. Einav. “Static friction at fractal interfaces,” Tribol. Inter., vol. 93, pp. 229–238, june 2016.
11. J. C. Mellinger, O. B, Ozdoganlar, R. E. DeVor, and S. G. Kapoor, “Modeling Chip-Evacuation Forces and Prediction of Chip-Clogging in Drilling,” ASME. J. Manuf.

CHAPTER IX

Concluding Remarks and Future Directions

8.1 Introduction

The study presented in this thesis aimed to improve the understanding of the main properties and biomechanical characteristics of the new SM BKS, to determine its advantages and disadvantages, obtaining more data on the simultaneous drilling and screwing properties in different materials. The development of new concepts capable of predicting the biomechanical behaviour of BKS was based on all the experimental data obtained and on theoretical and numerical analyses of the response of materials under different drilling and screwing conditions. The main findings, conclusions and some issues for further analysis and development are presented in this final chapter.

8.2 Conclusions and remarks

Osteotomies for bone perforations, with or without the insertion of fixation screws or implants, are practiced in several medical specialties. From bone biopsies to organ and limb rehabilitation, a thorough understanding of this procedure is essential to the advancing sciences. There is a consensus in the reviewed literature that the practical experience of the surgeon who performs bone drilling is one of the most important factors in the success of the procedure, along with the technique used, the materials used and the parameters to control and predict results, which are the most important indicators for optimising osseointegration and its outcomes. The primary or mechanical stability of the bone screws and implants is the main factor mentioned in the reviewed literature to predict the likelihood of successful osseointegration. It was observed that there are different conclusions without a common sense based on evidence. Different MIT measurements are indicated, and the MIT value is considered equally at all bone densities. No relationship based on experimental or clinical evidence was found in the reviewed literature between the importance of obtaining the MIT and its relationship with the μ, MRT individually, and the importance of determining the compression exerted by the bone screw on the walls of the recipient bone. It is stated that excessive compression can lead to bone resorption, but there are no clear parameters for avoidance in different clinical situations and bone densities.

Undersized bone drilling techniques for bone screw implantation are used as standard to obtain a larger MIT. Given the characteristics and properties of bone, simple standardised undersized drilling depends entirely on radiographic analysis according to the surgeon's experience. The development of a new biomechanism, in which the bone screw itself is responsible for passively adapting to the recipient bone in different bone densities and qualities, still achieving an MIT for optimal mechanical stability, becomes a great advance through the standardisation and simplification of the technique. Achieving controlled and accurate parameters is essential for monitoring results in a controlled manner and optimising evidence-based procedures. The use of an innovative MA during drilling, in which the material to be drilled itself is used to fill the internal *V* of the BKS, obtaining a material densification, increased friction and a MRT superior to the MIT, has allowed the development of a new SM studied in the form of a dental implant with the properties described here and others yet to be determined. In this thesis, a comprehensive experimental test and literature review was presented, with particular emphasis on the results obtained and their relation to evidence-based research. Based on the findings and literature, the following conclusions, limitations, and challenges were identified:

- There are no standard parameters to study the direct relationships between MIT, MRT, μ_S and the BIC surface under controlled conditions that can be replicated. Most of the techniques and methodologies studied present the effects of different drilling parameters on the temperature rise and drilling forces obtained during bone drilling, without proper observation and analysis of the mechanical damage and strain levels produced during drilling and screwing;
- There is no complete agreement on the exact and optimal parameters for drilling and screw insertion. Different types of surgery (e.g., orthopaedic, maxillofacial, implantology, etc.) require different drilling parameters and several studies recommend the use of high drill speeds, feed rates and higher drilling forces, taking into account the bone and tissues involved;
- Regarding the geometry of bone screws, most studies recommend the use of cylindrical or conical screws of different sizes, with differences only related to the pitch size and the type of thread. These different geometries used do not correlate with improvement or biomechanical innovations, with results not showing significant differences. Simultaneous drilling and screwing of a dental implant were not found in the literature review;
- The BKS geometry, due to its innovative properties, presented another limitation for computational simulations that require the understanding of the chip flow within its internal volume. Most FE models from a numerical point of view only include

thermal issues, assuming the application of a heat source without simulating chip removal, using simple constitutive models (isotropic, elastic-plastic) and simplifying bone geometry. The development of FE models based on real bone geometry and all real drilling characteristics is one of the challenges in this field.

Considering the above literature review and their limitations, the most relevant contributions of this thesis were:

- development of a new SM, the BKS, in which it was possible to determine its properties of increasing the μ between its surface and the applied material, collecting the material and compacting it in the internal V of the BKS, possibility of transporting the collected material, precise volumetric measurement of the amount of material obtained and evaluation of its volumetric D;

- identified a process for the computational design and manufacture of titanium and titanium alloy (Ti6Al4V) biomaterials, specifically a dental implant, using additive manufacturing and machining for prototyping and the final BKS product ready for commercialization. A new patent was proposed in collaboration with the University of Porto, following the identification of the innovative characteristics of the BKS through the results of the experiments carried out;

- the use of the BKS as a densitometer will allow the accurate validation of images and laboratory measurements of BMD when absolute values are required for accurate dosing of medications on an individual patient basis and planning of bone screw fixation;

- the use of BKS as a dental implant will increase bone D in the trabecular bone regions and make MIT favourable for osseointegration, especially in cases of low bone D, a common cause of failure to achieve primary stability for the future achievement of secondary or biological stability;

- Standardize and simplify the technique of simultaneous drilling and screwing of bone screws with precise parameters for drilling, removing, and determining the μ.

8.3 Future directions

The author sees this thesis as a lever for new developments and improvements with several research fronts. There are main future perspectives that can follow this thesis:

- development of robotic and navigation systems for the operating room. These systems would minimise human error by allowing the use of precise drilling and screwing parameters simultaneously;

- use of the new SM BKS to develop new specific projects for bone screws, such as prostheses for limbs and organs (femur, shoulder, knee, temporomandibular joint, etc.) and to obtain new patents;

- analysis of the effects and results on healing, repair and remodelling in studies that determine the advantages and disadvantages in the secondary stability of BKS;

- to develop and validate a study method to assess the bone *D* obtained by BKS in bones used for radiographic analysis for the diagnosis of BMD;

- use the data obtained from the experiments to develop new means of simulating the study of drilling and screwing into the bone, while at the same time compacting the material cut and collected inside the BKS.

APPENDIXES

Autorização de Compilação

Elza Maria Morais Fonseca e Renato Manuel Natal Jorge na qualidade de coautores do artigo "New Biomechanism: A Bioactive Kinetic Screw" publicado no capítulo do livro *Advances and Current Trends in Biomechanics 2021*, declaram que autorizam a inclusão do mesmo na dissertação de doutoramento do candidato Carlos Aurelio Andreucci, intitulada "Biomechanical applications of a novel simple machine"

Porto, 1 de novembro de 2023

(Elza Maria Morais Fonseca)

(Renato Manuel Natal Jorge)

Autorização de Compilação

Elza Maria Morais Fonseca e Renato Manuel Natal Jorge na qualidade de coautores do artigo "Static in Bone Implants: Standard Steady-State Torque and Primary Stability in a Bioactive Kinetic Screw" submetido a revista *Journal of the Brazilian Society of Mechanical Sciences and Engineering*, declaram que autorizam a inclusão do mesmo na dissertação de doutoramento do candidato Carlos Aurelio Andreucci, intitulada "Biomechanical applications of a novel simple machine"

Porto, 1 de novembro de 2023

(Elza Maria Morais Fonseca)

(Renato Manuel Natal Jorge)

Autorização de Compilação

Elza Maria Morais Fonseca e Renato Manuel Natal Jorge na qualidade de coautores do artigo "Increased Material Density within a New Biomechanism" publicado na revista *Mathematical and Computational Applications,* declaram que autorizam a inclusão do mesmo na dissertação de doutoramento do candidato Carlos Aurelio Andreucci, intitulada "Biomechanical applications of a novel simple machine"

Porto, 1 de novembro de 2023

(Elza Maria Morais Fonseca)

(Renato Manuel Natal Jorge)

Autorização de Compilação

Elza Maria Morais Fonseca e Renato Manuel Natal Jorge na qualidade de coautores do artigo "3D Printing as na Efficient Way to Prototype and Develop Dental Implants" publicado na revista *Biomedinformatics*, declaram que autorizam a inclusão do mesmo na dissertação de doutoramento do candidato Carlos Aurelio Andreucci, intitulada "Biomechanical applications of a novel simple machine"

Porto, 1 de novembro de 2023

(Elza Maria Morais Fonseca)

(Renato Manuel Natal Jorge)

Autorização de Compilação

Elza Maria Morais Fonseca e Renato Manuel Natal Jorge na qualidade de coautores do artigo "A New Simplified Autogenous Sinus Lift Technique" publicado na revista *Bioengineering*, declaram que autorizam a inclusão do mesmo na dissertação de doutoramento do candidato Carlos Aurelio Andreucci, intitulada "Biomechanical applications of a novel simple machine"

Porto, 1 de novembro de 2023

(Elza Maria Morais Fonseca)

(Renato Manuel Natal Jorge)

Autorização de Compilação

Elza Maria Morais Fonseca e Renato Manuel Natal Jorge na qualidade de coautores do artigo "A New Simple Machine that converts torque into steady-state pressure in solids" publicado na revista *IEEE 7th Portuguese Meeting on Bioengineering*, declaram que autorizam a inclusão do mesmo na dissertação de doutoramento do candidato Carlos Aurelio Andreucci, intitulada "Biomechanical applications of a novel simple machine"

Porto, 1 de novembro de 2023

(Elza Maria Morais Fonseca)

Glossary

Abbreviation	Definition
Additive manufacturing	Additive manufacturing is the process of creating an object by building it one layer at a time.
Alveolar bone	Is the thickened ridge of bone that contains the tooth sockets on the jaw bones (in humans, the maxilla, and the mandible).
Anabolism	The synthesis of complex molecules in living organisms from simpler ones together with the storage of energy; constructive metabolism.
Angiogenesis	Angiogenesis is the physiological process through which new blood vessels form from pre-existing vessels, formed in the earlier stage of vasculogenesis.
Anisotropic	Substance having a physical property which has a different value when measured in different directions.
Anterior Cruciate Ligament	Is one of the key ligaments that help stabilize the knee joint. The ACL connects the thighbone (femur) to the shinbone (tibia).
Apoptosis	The death of cells which occurs as a normal and controlled part of an organism's growth or development.
Appositional bone growth	Growth by forming new layers on the surface of pre-existing layers; process of increasing in thickness rather than length.
Atrophic alveolar ridge	Decrease in size of the alveolar bone.
Autologous	Derived from the same individual.
Bicortical screw	Bicortical screws are bone screws that penetrate the bone cortex twice, adjacent the bone plate and opposite the bone plate.

Bioactivation	Is a term used in biochemistry to describe the process of making a molecule reactive, active, or effective in carrying out its function.
Biocompatibility	Especially of material used in surgical implants, not harmful or toxic to living tissue.
Blood clot	Are gel-like clumps of blood.
Bone matrix	Is the intercellular substance of bone tissue consisting of collagen fibers, ground substance, and inorganic bone salts.
Bone morphogenetic proteins	(BMPs) are a group of growth factors that induce the formation of bone and cartilage.
Calcitonin	A hormone secreted by the thyroid that has the effect of lowering blood calcium.
Callus	The bony healing tissue which forms around the ends of broken bone.
Catabolism	The breakdown of complex molecules in living organisms to form simpler ones, together with the release of energy, destructive metabolism.
Cephalocaudal growth gradient	Gradient of growth is a pattern of changing spatial proportions during human growth.
Cephalometric x-ray	Is a type of dental x-ray that shows a side view of the head, including the teeth, jaw, and soft tissues.
Circumferential lamellae	Are layers of bone matrix that go all the way around the bone.
Connective tissue	Tissue that connects, supports, binds, or separates other tissues or organs, typically having relatively few cells embedded in an amorphous matrix, often with collagen or other fibers, and including cartilaginous, fatty, and elastic tissues.
Chips	A small piece of something removed in the course of chopping, cutting, or breaking a hard material such as wood or bone.
Chondroblasts	Are young, immature cartilage cells that eventually form chondrocytes via a process of chondrogenesis.

Creep relaxation	Is a measurement of how much a particular gasket material spreads out when force is applied.
Diabetes mellitus	A metabolic disorder in which the body has high sugar levels for prolonged periods of time.
Diaphyseal	The shaft of a long bone.
Dual energy X-ray absorptiometry	(DEXA) is a procedure that measures bone mineral density (BMD) using two X-ray beams with different energy levels.
Embryologic	The branch of biology and medicine concerned with the study of embryos and their development.
Encapsulation	The action of enclosing something in or as if in a capsule.
Endosteum	Is a thin vascular membrane of connective tissue that lines the inner surface of the bony tissue that forms the medullary cavity of long bones.
Epiphyseal	The end part of a long bone, initially growing separately from the shaft.
Erupt	Tooth eruption is the movement of the developing tooth from its non-functional position in the alveolar bone to its final functional position in the oral cavity.
Estrogen	Any of a group of steroid hormones which promote the development and maintenance of female characteristics of the body.
Extracellular matrix	A complex meshwork of proteins and carbohydrates.
Fibroblasts	A cell in connective tissue which produces collagen and other fibers.
Foreign body giant cells	Is a collection of fused macrophages (giant cell) which are generated in response to the presence of a large foreign body.
Growth factors	A substance, such as a vitamin or hormone, which is required for the stimulation of growth in living cells.

Growth spurt	Is an occurrence of growing quickly and suddenly in a short period of time.
Haversian systems	Also called an osteon, is a cylindrical-shaped structural unit of compact bone. It consists of a haversian canal, which is a small channel that contains blood vessels and nerves, and concentric laminae or lamellae, which are layers of bone tissue that surround the canal.
Hematoma	Is a localized collection of blood outside of a blood vessel.
Homogenous	Having the same relation, relative position, or structure.
Howship's lacunae	Tiny depressions, pits, or irregular grooves in bone that are being resorbed by osteoclasts.
Hyalin cartilage	A translucent bluish-white type of cartilage present in the joints, the respiratory tract, and the immature skeleton.
Hydroxyapatite	A mineral related to apatite which is the main inorganic constituent of tooth enamel and bone, although it is rare in rocks.
Ibandronate	Is a bisphosphonate medicine used to prevent and treat osteoporosis in women who have undergone menopause.
Immunologic response	Is a bodily defense reaction that recognizes an invading substance (an antigen) and produces antibodies and lymphocytes specific against that antigen.
Infrazygomatic crest	Is a palpable bony ridge running between the alveolar ridge and the zygomatic process of maxilla.
Intermaxillary fixation	Fixation of fractures of mandible or maxilla by applying elastic bands or stainless-steel wire between the maxillary and mandibular arch bars or other types of splints.
Lymphoid tissues	Is a tissue responsible for the production of lymphocytes and antibodies. It is part of the

	lymphatic system, which helps the body fight infections and diseases.
Macrophages	A large phagocytic cell found in stationary form in the tissues or as a mobile white blood cell, especially at sites of infection.
Mandibular buccal shelf	Is the area between the buccal frenum and anterior border of masseter muscle. It extends medially from the crest of the ridge, laterally to the external oblique ridge and distally up to the retromolar pad.
Maxillary sinus membrane	Is the membranous lining of the maxillary sinus cavity.
Maxillomandibular fixation	Is a procedure that involves binding or connecting the upper and lower jaw by wires, elastic bands, or metal splints.
Menarche	The first occurrence of menstruation.
Mesenchyme	A loosely organized, mainly mesodermal embryonic tissue which develops into connective and skeletal tissues, including blood and lymph.
Metaphyseal	Means of or relating to the metaphysis, the portion of a developing long bone between the shaft and the end.
Monocytes	A large phagocytic white blood cell with a simple oval nucleus and clear, greyish cytoplasm.
Mucopolysaccharides	Any of a group of compounds occurring chiefly as components of connective tissue. They are complex polysaccharides containing amino groups.
Neovascularization	Is the natural formation of new blood vessels usually in the form of functional microvascular networks, capable of perfusion by red blood cells, that form to serve as collateral circulation in response to local poor perfusion or ischemia.
Neutrophils	A neutrophilic white blood cell.
Olecranon	A bony prominence at the elbow, on the upper end of the ulna, attachment of the muscle triceps.

Orthodontics	The treatment of irregularities in the teeth and jaws.
Orthodontic anchorage	Anchorage in orthodontics is defined as a way of resisting movement of a tooth or number of teeth by using different techniques.
Ossification center	Is a site in bones where calcification begins, and bone replaces fibrous connective tissue or cartilage.
Osteoblast	A cell which secretes the substance of bone.
Osteocyte	A bone cell formed when an osteoblast becomes embedded in the material it has secreted.
Osteoclast	A large multinucleate bone cell which absorbs bone tissue during growth and healing.
Osteoconduction	Is a physical effect by which the matrix of the graft forms a scaffold that favors outside cells to penetrate the graft and form new bone.
Osteogenesis	Formation or development of new bone by cells contained in the graft.
Osteogenic	Relating to the formation of bone.
Osteoinduction	Is a chemical process by which bone morphogenetic proteins (BMP) contained in the graft converting the neighboring cells into osteoblasts, which in turn form bone.
Osteons	Osteons are cylindrical structures that are characteristic of mature bone.
Osteoprotegerin	Is a cytokine receptor of the tumor necrosis factor receptor superfamily.
Osteotomy	The surgical cutting of a bone, especially to allow realignment.
Palate	The roof of the mouth, separating the cavities of the mouth and nose in vertebrates.
Parathyroid hormone	A hormone that regulates calcium levels in a person's body.

Periosteum	A dense layer of vascular connective tissue enveloping the bones except at the surfaces of the joints.
Phagocytosis	Is a process by which a cell engulfs a particle and digests it.
Primum Non Nocere	Is a Latin phrase that means "first, do no harm".
Progenitor stem cells	Is a biological cell that can differentiate into a specific cell type.
Prostheses	An artificial body part, such as a limb, a heart, or a dental implant.
Rheumatoid arthritis	A chronic progressive disease causing inflammation in the joints and resulting in painful deformity and immobility, especially in the fingers, wrists, feet, and ankles.
Sinus lift	A sinus lift is a surgical procedure that increases the amount of bone in the maxilla, in the posterior teeth, by lifting the sinus membrane and placing a bone graft.
Sharpey’s fibers	Are a matrix of connective tissue consisting of bundles of strong predominantly type I collagen fibers connecting periosteum to bone.
Sphenomandibular ligament	Is a flat, thin band that connects the spine of the sphenoid bone to the lingula of the mandibular foramen.
Stress relaxation	Decrease in stress in response to the same amount of strain in a structure over time.
Testosterone	A steroid hormone that stimulates development of male secondary sexual characteristics, produced mainly in the testes, but also in the ovaries and adrenal cortex.
Trabeculae	Each of a series or group of partitions formed by bands or columns of connective tissue, especially a plate of the calcareous tissue forming cancellous bone.
Transplant	Take (living tissue or an organ) and implant it in another part of the body or in another body.

Trephine	A hole saw used in surgery to remove a circle of tissue or bone.
Tribology	The study of friction, wear, lubrication, and the design of bearings; the science of interacting surfaces in relative motion.
Tuberosity	Is a rounded prominence or projection of a bone, usually serving for the attachment of muscles or ligaments.
Ultimate stress	The maximum amount of stress that a material can withstand before breaking.
Yield stress	The value of stress at a yield point or at the yield strength.
Young's modulus	A measure of elasticity, equal to the ratio of the stress acting on a substance to the strain produced.